S.I.S.S.A. **I.S.A.S.**

SCUOLA INTERNAZIONALE SUPERIORE DI STUDI AVANZATI

-

INTERNATIONAL SCHOOL FOR ADVANCED STUDIES

Intracellularly selected recombinant antibodies targeting β Amyloid Oligomers

Thesis submitted for the degree of

"Doctor Philosophiæ"

Candidate

Giovanni Antonio Meli

Supervisor

Prof. Antonino Cattaneo

Co-*supervisor*

Dr. Michela Visintin

INDEX

Materials and methods

Results

Discussion

Abstract

Targeting beta Amyloid (Aβ) peptide, in relation to the degenerative processes of Alzheimer Disease (AD), and studying the mechanisms of Aβ misfolding, oligomerization and aggregation are currently two hot-topics in AD research. Both these aspects can be preferentially approached by the use of anti-Aβ antibodies, in particular of those which are conformation specific, as demonstrated by *in vitro* studies and by *in vivo* immunotherapy.

Here, we describe the generation of a large panel of anti-Aβ scFvs recombinant antibodies, exploiting a novel *in vivo*, yeast two hybrid-based, approach developed in our laboratory: the "Intracellular Antibody Capture Technology" (IACT). In this way, we have selected and characterized a panel of 18 different anti-Aβ scFvs, which show interesting features *in vitro* and in cells.

IACT-selected anti-Aβ scFvs are conformation specific versus Aβ oligomers and show peculiar immunoreactivity pattern versus the *in vivo* produced Aβ deposits in human AD brains. Moreover, our anti-Aβ scFvs, being *in vivo* selected in the yeast cytoplasm, can be readily expressed as intracellular antibodies in mammalian cells, targeted to different cellular compartments, allowing new promising strategies to study the emerging role of intracellular Aβ processing and oligomerization in AD pathology.

The panel of IACT-selected scFvs under study represents a new tool in the survey of existing anti-Aβ antibodies, and the unique characteristics of the selection strategy used for their isolation appear to be particularly suited for the selection of oligomeric specific anti-Aβ antibodies. Furthermore, the recombinant nature of the antibodies makes them ideally suited for extracellular and for intracellular delivery, *in vitro* as well as *in vivo*.

INTRODUCTION

1. Alzheimer's Disease and Beta Amyolid peptide

1.1 Alzheimer's Disease: a Protein Misfolding Disorder

In several neurological and systemic disorders, specific proteins can accumulate within cells and tissues as a result of changes in protein conformation (misfolding) that render the molecules prone to self-aggregation and resistant to clearance. These conformational diseases, or Protein Misfolding Disorders (PMDs), comprise systemic amyloidoses, in addition to neurodegenerative conditions that are marked by the buildup of characteristic proteins in the brain, such as Alzheimer's disease (AD), Parkinson's disease (PD), Huntington's disease (HD), and prion diseases. (Walker, 2006)

Although the proteins involved in different PMDs do not share sequence or structural identity, all of them can adopt at least two different conformations without requiring changes in their amino acid sequence. The misfolded form of the protein usually contains stacks of β sheets organized in a polymeric arrangement known as a 'cross-β' structure. Because β-sheets can be stabilized by intermolecular interactions, misfolded proteins have a high tendency to form oligomers and larger polymers.

Two main mechanisms of AD pathology are based on the involvement of two aggregation-prone proteins: amyloid-β (Aβ) and tau. Aβ is the main constituent of senile plaques, one of the key pathological characteristics of AD. Tau, a microtubule-associated protein, is the main component of neurofibrillary tangles, the other hallmark lesion of AD.

Plaques and tangles in AD pathology are present mainly in brain regions involved in learning and memory and emotional behaviours such as the entorhinal cortex,

hippocampus, basal forebrain and amygdala. Brain regions with plaques typically exhibit reduced numbers of synapses, and damaged neurites of cholinergic and glutamatergic neurons.

The accumulation of misfolded proteins is also a hallmark of ageing; as cells age they lose their ability to correct the misfolding through chaperone proteins and the "stress response" machinery. So neurodegenerative diseases, such as AD and PD, may be considered a manifestation of ageing, with mutations in particular gene products accelerating the process. In addition, as with other age-related diseases, there are likely to be behavioural, dietary and other environmental factors that may affect the risk of AD. Currently, it is estimated that 50% of people older than age 85 years are afflicted with AD. The risk of AD, the most common cause of dementia today, dramatically increases in individuals beyond the age of 70 and it is predicted that the incidence of AD will increase threefold within the next 50 years.

The vast majority of cases of AD are sporadic - they do not run in families. Nevertheless, molecular genetic analyses suggest that there are likely to be many genes that influence one's susceptibility to AD; these genes are primarily related to the 'metabolism' of Aβ peptide, as, for instance, the genes coding for Amyloid Precursor Protein, Presenilin1 and 2, Apolipoprotein E (Mattson, 2004).

1.2 Beta Amyloid in Alzheimer's Disease

In the 1980s, biochemists focused on the isolation of the amyloid deposits from AD brains to identify its principal component. Glenner and Wong purified microvascular amyloid deposits from the meninges of AD brains and provided a partial sequence of a

protein of ~4-kDa that they named amyloid β-protein (Aβ). Shortly thereafter, Masters, Beyreuther and co-workers identified the same protein as the subunit of amyloid plaque cores that were isolated from post-mortem AD cortices.

Numerous pieces of evidence indicate that Aβ is the principal misfolded protein involved in AD pathogenesis, leading to the formulation of the following 'Aβ hypothesis': a chronic imbalance between the production and clearance of this small hydrophobic peptide with a tendency to misfold and aggregate leads gradually to synaptic and neuritic compromise and glial activation (Selkoe 1991, Hardy 1992, Hardy & Selkoe 2002, Selkoe 2004).

1.3 Aβ generation: the processing of Amyloid Precursor Protein (APP)

Aβ is generated by proteolytic processing of β-amyloid precursor protein (APP), through sequential cleavages by β-secretase and γ-secretase.

APP is an extremely complex protein that may be a functionally important molecule in its full-length configuration, as well as being the source of numerous fragments with varying effects on neural function.

APP is a single transmembrane polypeptide that is cotranslationally translocated into the endoplasmic reticulum and then posttranslationally modified ("matured") through the secretory pathway. Both during and after the trafficking of APP through the secretory pathway, it can undergo a variety of proteolytic cleavages to release secreted derivatives into vesicle lumens and the extracellular space (Selkoe, 2001).

The processing of APP at the cell surface is one example of a general physiological mechanism now known as "regulated intramembrane proteolysis" (RIP). Aβ is released

from APP through sequential cleavages by β-secretase (also called BACE-1), a membrane-spanning aspartyl protease with its active site in the lumen, and γ-secretase, an unusual intramembrane aspartyl protease containing presenilin at its catalytic site complexed with three other membrane proteins, nicastrin, Aph-1 and Pen-2 (fig.1).

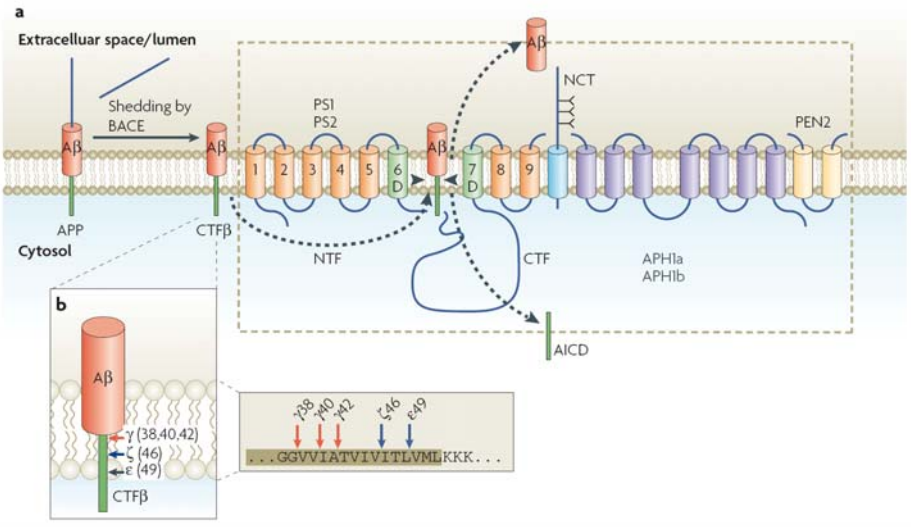

Fig. 1. Regulated Intramembrane Proteolisis (RIP) of APP (from Haass & Selkoe, 2007)

The γ-cleavage is variable and occurs after Aβ amino acids 38, 40 or 42 (Fig.1 and fig.2). The precise sites of these γ-cleavages have an important influence on the self-aggregating potential and resulting pathogenicity of Aβ, as the Aβ42 peptide has a strong propensity to oligomerize *in vivo*.

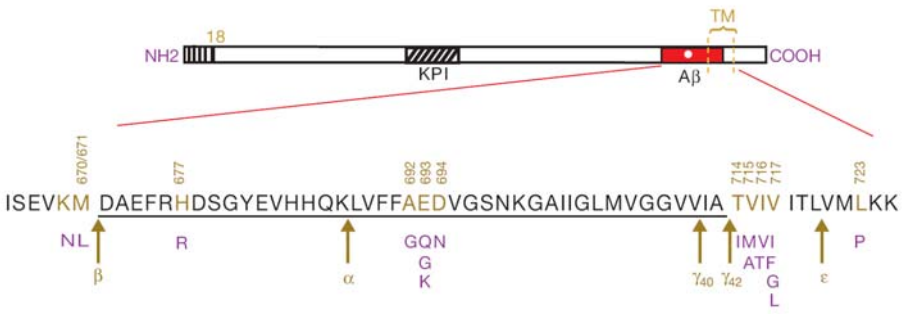

Fig.2 Cleavage sites on the 'Aβ-generating' region of APP (from Selkoe, *Nat Cell Biol* 2004)

As mentioned above, during its trafficking through the secretory pathway, APP can undergo proteolytic cleavages, and Aβ can be produced at multiple intracellular sites. In neurons, APP undergoes fast anterograde transport to nerve terminals (Koo et al., 1990; Ferreira et al., 1993; Buxbaum et al., 1998), and is metabolized within axonal or presynaptic vesicles into Aβ peptides that are released and deposited as amyloid plaques around nerve terminals (Lazarov et al., 2002; Sheng et al., 2002). Furthermore, synaptic activity increases Aβ secretion, indicating that the presynaptic terminal is an important regulatory site for Aβ generation (Kamenetz et al., 2003; Cirrito et al., 2005). Thus, the axonal/synaptic fractions of APP appear particularly important in the generation of Aβ species that are ultimately deposited in amyloid plaques. However, Lee E.B. and coworkers (2005) highlight the importance of perikaryal versus axonal APP proteolysis in the development of Aβ amyloid pathology in AD (Lee et al., 2005).

1.4 Interactions between the cholinergic system, neurotrophins and APP metabolism

The regulation of APP metabolism is a very complex process modulated by a lot of mechanisms, most of which are under investigation including cholinergic mechanisms and neurotrophin receptor signaling (Fig.3).

The deprivation of Neurotrophic Growth Factor (NGF) leads to the formation and deposition of Aβ in AD11 mice (Capsoni et al, 2000, 2002), as well as to the activation of the amyloidogenic pathway with overproduction and accumulation of Aβ in PC12 differentiated cells (Matrone et al, submitted paper), suggesting a direct link between NGF signaling and abnormal APP processing.

APP expression and processing have been shown to be under the direct regulatory control of NGF, via independent and potentially conflicting signaling through p75 and TrkA receptors (Roßner, et al., 1998). Thus, an imbalance in this two-receptor system (Chao and Hempstead, 1995), determined by a variety of different causes, may have direct effects on APP processing and on the homeostatic mechanisms regulating hippocampal and cortical NGF, APP, and cholinergic activity.

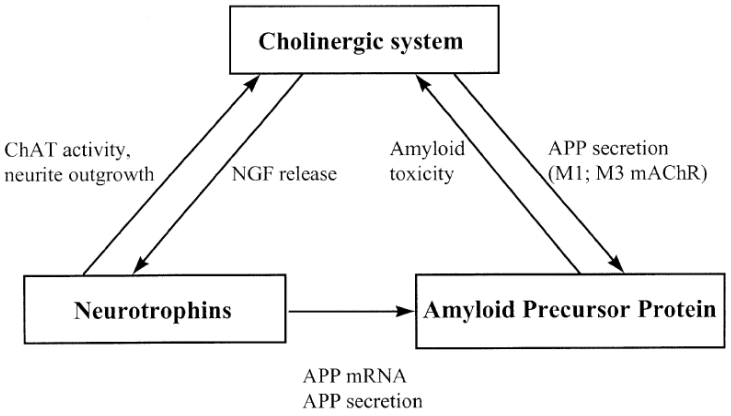

Fig.3 Interactions between the cholinergic system, neurotrophins and amyloid precursor protein metabolism.
Cholinergic neurons of the basal forebrain are vulnerable to amyloid toxicity. Lack of stimulation of M1/M3 mAChR in neocortical cholinoceptive target areas or impaired mAChR signaling may favor the amyloidogenic pathway of APP processing. NGF plays a role in maintaining cholinergic function, but also controls expression and processing of APP (from Roßner, et al., 1998).

1.5 Aβ aggregation

The misfolded Aβ usually contains stacks of β sheets organized in an arrangement known as a 'cross-β' structure. Because β-sheets can be stabilized by intermolecular interactions, Aβ have a high tendency to form oligomers and larger polymers (Soto, 2006).

It has been demonstrated by a number of studies that both synthetic Aβ and its analogs, and also isolated senile plaque proteins, spontaneously assemble into amyloid protofibrils and fibrils exhibiting a β-pleated sheet conformation consistent with native AD amyloid-β-proteins (Antzutkin, 2004).

The pathway of aggregation, extending from Aβ monomers, to Aβ oligomers and finally to Aβ fibrils, can be studied using several experimental methods: nuclear magnetic

resonance (NMR) spectroscopy, circular dichroism (CD) spectroscopy, transmission electron microscopy (TEM), Atomic Force Microscopy (AFM) (Antzutkin, 2004).

Petkova and coworkers (2002) showed a structural model for amyloid fibrils of Aβ1-40 peptide, based on a set of experimental constraints from solid state NMR spectroscopy (fig.4).

Approximately the first 10 residues of Aβ1–40 are structurally disordered in the fibrils. The monomer unit has a hairpin geometry with two anti-parallel β-strands. Residues 12–24 and 30–40 adopt β-strand conformations and form parallel β-sheets through intermolecular hydrogen bonding. Residues 25–29 contain a bend of the peptide backbone that brings the two β-sheets in contact through sidechain-sidechain interactions. A single cross-β unit is then a double-layered β-sheet structure with a hydrophobic core and one hydrophobic face. The only charged sidechains in the core are those of D23 and K28, which form salt bridges. Fibrils with minimum mass-per-length and diameter consist of two cross-β units with their hydrophobic faces juxtaposed.

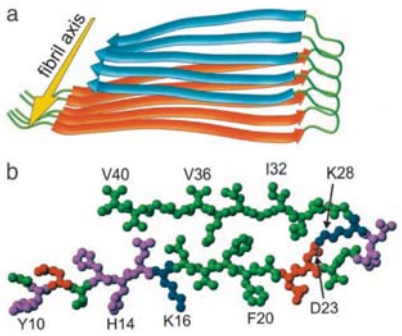

Fig.4 Structural model for Aβ1–40 fibrils, consistent with solid state NMR constraints on the molecular conformation and intermolecular distances and incorporating the cross-β motif common to all amyloid fibrils (a). Detail of the monomeric unit (b). Residues 1–8 are considered fully disordered and are omitted. Residues are color-coded according to their sidechains as hydrophobic (green), polar (magenta), positive (blue), or negative (red). (from Petkova et al., 2002)

Recently, Mastrangelo and coworkers (2006) investigating the formation and structure of earliest formed oligomers of Aβ42 using the high resolution AFM, suggest different possible structures (fig.5), sharing with other models the hairpin structure of monomeric unit.

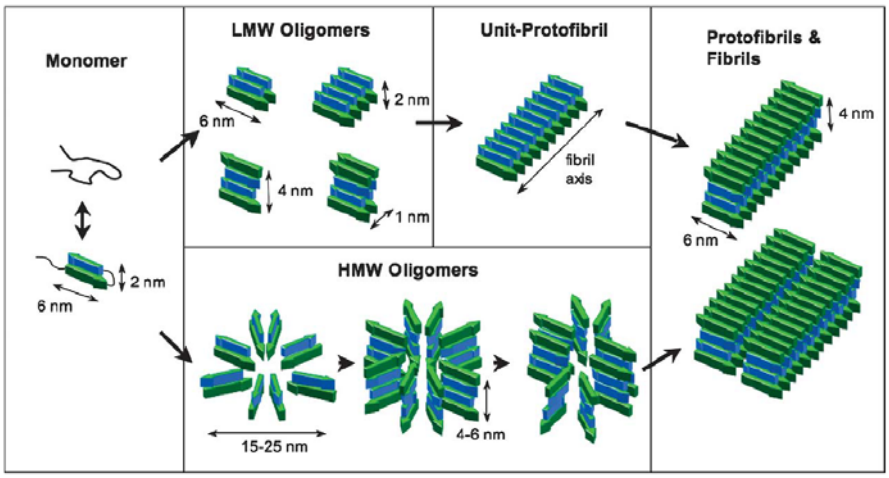

Fig.5 A model showing the sequence of assembly and possible structures of Aβ42 monomers, low molecular weight (LMM) oligomers, high molecular weight (HMM) oligomers, unit-protofibrils, and protofibrils/fibrils (from Mastrangelo et al., 2006)

It is evident that Aβ40 and Aβ42 peptides form *in vitro*, but reasonably also *in vivo*, a variety of structures, including multiple monomer conformers, different types of oligomers, protofibrils and fibrils.

1.6 Aβ oligomers

A large and confusing body of literature describes many types of intermediate oligomeric forms of synthetic and natural Aβ, including protofibrils (PFs), annular structures, paranuclei, Aβ-derived diffusible ligands (ADDLs), globulomers (Haass & Selkoe, 2007).

Some different types of recognized Aβ oligomers are summarized in the following table:

Oligomeric assembly	Characteristics
Protofibril (PF)	Intermediates of synthetic Aβ fibrillization; up to 150 nm in length and ~5 nm in width; β-sheet structure: bind Congo red and Thioflavin T
Annular assemblies	Doughnut-like structures of synthetic Aβ; outer diameter of ~8–12 nm; inner diameter of ~2.0–2.5 nm
Aβ-derived diffusible ligands (ADDLs)	Synthetic Aβ oligomers smaller than annuli; might affect neural signal-transduction pathways
Aβ*56	Apparent dodecamer of endogenous brain Aβ; detected in the brains of an APP transgenic mouse line and might correlate with memory loss
Secreted soluble Aβ dimers and trimers	Produced by cultured cells; resistant to SDS; resistant to the Aβ-degrading protease IDE; alter synaptic structure and function

Aβ, amyloid β-protein; APP, β-amyloid precursor protein; IDE, insulin-degrading enzyme.

from Haass & Selkoe, *Nat. Mol.Cell Biol.* 2007

A critical question is whether soluble oligomers are transient or relative stable structures, and if they represent only intermediate building blocks in the assembly of the mature fibrils. Stable oligomeric aggregates of Aβ can exist *in vivo*, as demonstrated by the isolation of Aβ*56 (probably a dodecamer of Aβ) from brains of APP transgenic mice Tg2576 (Lesnè et al., 2006). Moreover, Stine and coworkers (2003) have characterized chemical-physical conditions *in vitro* (time, concentration, temperature, pH, ionic strength) able to influence selectivily the aggregation of Aβ monomers in oligomers or fibrils. Finally, the oligomeric and mature fibrillar structures are distinct on the basis of

their mutually exclusive reactivity towards antibodies specific for generic fibrils and oligomer conformations (Kayed et al., 2003; Glabe, 2004).

1.7 Soluble oligomers in AD pathogenesis

Prior to the last decade, insoluble Aβ fibrils were considered the aggregated species with a significant role in the pathogenesis of AD. Over the last years, an increasing body of evidence has been produced, that supports a fundamental shift in our view of the pathogenic mechanism of AD. The original 'Aβ hypothesis' shifted essentially in 'Aβ synaptic hypothesis', attaching importance to soluble oligomers targeting the synapses.

Synaptic dysfunction occurs early in Alzheimer's Disease (AD) and is considered the best pathological correlate of cognitive decline (Masliah et al., 2001). Recent studies suggest that Aβ oligomers are the most synaptotoxic Aβ species in the human brain (Gong et al., 2003), and in transgenic mice AD models (Klyubin et al, 2005; Lesnè et al, 2006). Soluble oligomers correlate much better with the presence and degree of cognitive deficits than do simple plaque counts. However, it must also be pointed out that the large plaques areas of fibrillar Aβ, often intimately surrounded by a number of smaller assemblies (probably oligomers), in AD brains typically show dystrophic neurites, indicating that insoluble aggregates might contribute to neuronal injury. At the current stage of research, one should not conclude that either large, insoluble deposits or small, soluble oligomers represent the sole neurotoxic entity; indeed, a continuous dynamic exchange between these forms might well be detrimental (Haass & Selkoe, 2007).

In vitro studies have demonstrated differential mechanisms of toxicity mediated by Aβ fibrils or by Aβ oligomers. The latter (in a concentration range of nM) cause a fast and

massive toxic effect, whereas Aβ fibrils (in a range of μM) induce progressive dystrophy and modest cell death in human cortical neurons (Desphande et al, 2006).

Several lines of evidence suggest that Aβ oligomers (both natural and synthetic) can inhibit the maintenance of hippocampal Long Term Potentiation (LTP), altering memory function, by both *in vivo* microinjection in living rats (Walsh et al., 2002) and by treatment of hippocampal slices (Towsend et al., 2006). In addition, the effects of the natural oligomers on LTP are specifically neutralized by anti-Aβ antibodies *in vivo*, either through active vaccination or passive infusion (Klyubin et al., 2005).

The biochemical mechanism by which soluble oligomers bind to synaptic plasma-membranes and interfere with the complex system of receptor and/or channel proteins and signalling pathways that are required for synaptic plasticity is under intensive study.

Recent studies show that Aβ oligomers bind to NMDA receptors triggering reactive oxygen species (ROS) production (De Felice et al., 2007) and spine density reduction (Lacor et al., 2007). Shankar and coworkers (2007) have observed also the involvement of NMDA receptors in the induction of reversible synapse loss mediated by natural oligomers.

Other evidences suggest that Aβ oligomers can physically intercalate into and penetrate membranes, leading to permeabilization; the concomitant increase in intracellular calcium may be the proximate initiator of several pathogenic pathways, including reactive oxygen species (ROS) production, altered signaling pathways and mitochondrial dysfunction (Glabe et al., 2006).

In conclusion, the involvement of Aβ oligomers in AD pathogenesis is under intense investigation suggesting that early-stages of the disease might be due to specific impact

on the signaling biochemistry required for synaptic plasticity. If so, new treatments such as oligomers-targeting drugs may not only stop AD's inexorable course, but may actually reverse the dysfunction in mild cognitive impairment and early-stage AD.

1.8 Intracellular oligomerization

As discussed above, Aβ peptide can be produced intracellularly in different sites. Increasing evidence supports also the role of intracellular Aβ oligomerization and accumulation as an early event in AD pathogenesis in humans and in transgenic mice.

Accumulation of Aβ42, occurs intracellularly in AD (Gouras et al., 2000; D'Andrea et al., 2001) and in transgenic mice that develop Aβ plaques (Oddo et al., 2003; Sheng et al., 2003). In Tg2576 (mice harboring the Swedish mutant human APP (Hsiao et al.,1996)) and human AD brain, but also in aged cultured Tg2576 primary neurons, accumulation of Aβ42 oligomers within neuronal processes and synaptic profiles is associated with pathological alterations and with synaptic degeneration (Takahashi et al., 2004).

Finally, the reduction of intracellular Aβ in triple transgenic mice by passive immunization (Oddo et al., 2004) was the best correlate of their cognitive improvement (Billings et al., 2004).

To conclude, synaptic alterations can be induced by extracellular as well as by intracellular Aβ oligomers. Increasing evidence supports an as yet poorly understood dynamic relationship between extracellular and intracellular Aβ, modulation of which might be especially important also in Aβ antibody induced therapeutic effects (Oddo et al, Am J Pathol 2006).

2. Targeting Beta Amyloid through antibodies

2.1 Targeting Aβ pathological assemblies through antibodies: from *in vitro* studies to *in vivo* applications

Antibodies (Abs) are an important tool for analyzing protein misfolding and aggregation, as well as for targeting degenerative processes that are caused by protein misfolding.

Several *in vitro* studies showed that monoclonal antibodies (MAbs), raised against the N-terminal of Aβ, can inhibit synthetic Aβ fibrillogenesis and can even disrupt pre-existing fibrils. In addition, the disassembly of fibrils is accompanied by strongly reduced neurotoxicity in culture (Solomon, 1996, 1997; Frenkel, 1998, 1999). Moreover, also several anti-Aβ single-chain Fv (scFv) antibody fragments, developed from phage display libraries (Liu et al., 2004) or from MAbs, exhibit anti-aggregating properties and prevent the toxic effect of Aβ fibrillar aggregates (Frenkel et al., 2000).

The anti-Aβ MAb 'm266.2' directed against amino acid residues 13–28 has been shown to act as an Aβ "sink" in an *in vitro* dialysis system; when administered peripherally into PDAPP transgenic mice, 'm266.2' promotes clearance of Aβ via the plasma and prevents Aβ plaque accumulation, acting also *in vivo* as a "peripheral sink" (DeMattos et al., 2001, 2002). Another MAb directed against the N terminus (amino acid residues 1–5) of Aβ, 'm3D6', has also been shown to decrease Aβ deposition when administered parenterally (Bard et al., 2000).

Recent *in vitro* studies suggested a new mechanism of action of anti-Aβ antibodies (N-terminal and mid-domain specific) through cell membrane surface binding, at the

extracellular Aβ-domain of APP, reducing intracellular Aβ and protecting against synaptic alterations in APP mutant (Tg2576) neurons (Tampellini et al., 2007).

The identification of conformational epitopes in Aβ fibrils and in Aβ oligomers in recent studies gives uniqueness to the antibody-approach in Aβ targeting studies. Early experiments with rabbit polyclonal sera suggested that amyloid fibrils possess a non-native structure and that antibodies can be generated that are specific for the amyloidogenic conformation (Linke et al., 1973). Recently, a new class of antibodies associated with a fundamental amyloid-folding motif recognizing common conformational epitopes independently of aminoacid sequence, has been specifically elaborated against fibrils (O'Nuallain & Wetzel, 2002) and against oligomers (Kayed et al, 2003). Subsequently, both monoclonal (Lambert et al., 2006) and polyclonal (Lambert et al., 2003; Barghorn et al., 2005) anti-Aβ oligomer antibodies have been specifically developed.

Significantly, anti-oligomer antibodies have been found to block the toxicity when tested *in vitro* (Kayed et al., 2003; Lambert et al., 2003, 2006) but also *in vivo* (Barghorn et al., 2005). Oddo and colleagues found that passive immunization prevented tau pathology but did not affect phosphorylated tau aggregates that existed prior to antibody treatment (Oddo et al., 2006 a, b).

In conclusion, *in vitro* and *in vivo* studies show that the relevance of the antibody-approach to target Aβ pathological assemblies, in particular Aβ oligomers.

2.2 Immunotherapy

Immunotherapy is a new and promising approach for AD treatment, through either active Aβ-peptide vaccination or passive infusion of anti-Aβ monoclonal antibodies, attempting to target the toxic forms of Aβ directly without perturbing the enzymatic activities of the secretases (classic targets of actual pharmacological therapy, through secretases inhibitors), which process many important substrates.

Active immunization

Improvements in pathology and cognition in mouse models of AD after treatment with Aβ1–42 (Schenk et al., 1999) and Aβ1–40 (Lemere et al., 2000; Weiner et al., 2000), together with the observed safety characteristics in a broad range of animal species, led to the initiation of Phase 1 and Phase 2 clinical studies in AD patients. Unfortunately, the Phase 2 clinical trial of an Aβ1–42 vaccine (using aggregated Aβ1–42 (AN1792) in combination with QS21 adjuvant) in AD patients was associated with the development of a T-cell-mediated (Nicoll et al., 2003; Ferrer et al., 2004), autoimmune meningoencephalitis in 6% of patients, leading to cessation of dosing. Despite this self-limited reaction, patients who subsequently developed anti-Aβ antibodies had reduced cerebrospinal levels of tau and showed a slower cognitive decline (Gilman et al., 2005; Masliah et al., 2005).

T-cell infiltrates were present in the brains of two patients with encephalitis, suggesting a T-cell-mediated immune response as a reason for the adverse events (Nicoll et al., 2003; Ferrer et al., 2004).

Active immunization induces both a humoral (antibody mediated) and cellular immune response (via T lymphocytes). After immunization with Aβ, the peptide is processed by

antigen-presenting cells in the periphery and then presented to T and B cells. Epitope mapping of these events following Aβ immunization in AD patients indicates that the predominant T-cell epitopes are in the carboxyl terminus of Aβ. By contrast, most of the B-cell or antibody producing epitopes detected from immunized patients reside in the amino-terminal region of the peptide (Schenk, 2004).

Also in mice (Lemere et al., 2000; Town et al., 2001; McLaurin et al., 2002; Cribbs et al., 2003) and in monkeys (Lemere et al., 2004), the majority of anti-Aβ antibodies generated, from active Aβ immunization, recognize an epitope located within the amino terminus of Aβ protein (e.g., Aβ1–15).

These observations have been used to design alternative immunogens, which encompass the N-terminal antibody epitope of Aβ but lack the more C-terminal T-cell reactive sites for immunization in AD animal models. Such shorter Aβ fragments have been shown to lead to an immune response when conjugated to T-helper (Th) cell epitopes (Monsonego et al., 2001) and/or have been used on a branched peptide framework (Agadjanyan et al., 2005). Recently, Maier and coworkers (2006) demonstrated that four alternative Aβ 1–15-containing immunogens reduce cerebral Aβ load and learning deficits in J20 mouse, an AD model ($hAPP_{FAD}$), in the absence of an Aβ-specific cellular immune response.

Interestingly, Moretto and coworkers (2007) found that conformation-sensitive antibodies against Aβ (recognizing preferentially oligomers and fibrils, but not monomers) are elicited by immunization with a thioredoxin-constrained-Aβ1-15.

Passive immunization

Passive immunization eliminate a cellular response to Aβ. In AD mouse models, peripheral injection of Aβ-specific antibodies reduced cerebral Aβ levels (Bard et al., 2000; DeMattos et al., 2001) and improved cognitive function (Dodart et al., 2002); anti-Aβ antibodies are also in clinical trial in humans (Schenk, 2004; Morgan, 2006). Proposed mechanisms of action for anti-Aβ immunotherapy include local microglia-mediated plaque phagocytosis (through an Fc receptor-mediated mechanism), systemic sequestration of Aβ in plasma that results in its efflux from the brain (peripheral sink) and/or the inhibition of Aβ oligomerization and cytotoxicity.

Interestingly, Bacskai and coworkers (2002) found a plaque clearance by a direct administration to the brains of APP transgenic mice, not only of anti-Aβ antibodies but also of Fab fragments, raising questions as to whether Fc receptor-mediated phagocytosis was required for plaque clearance, as originally reported. Wilcock and coworkers (2003), have demonstrated a two-phase mechanism of anti-Aβ antibody-mediated plaque clearance: the first phase is fairly rapid and involves clearance of diffuse Aβ without microglial activation; the second is slower, involving clearance of compact Aβ through activation of microglial Fc receptors and phagocytosis of pre-existing plaques.

Fukuchi (2006) and Levites (2006) have recently tested a novel gene therapy modality where adeno-associated virus (AAV) encoding anti-Aβ single-chain antibodies (scFvs) are intracranial injected of AD mouse models. AD mouse models subjected to AAV injection showed a significant reduction of amyloid deposits. Because the scFv lacks the Fc portion of the immunoglobulin molecule, this modality may be a feasible solution for

AD without eliciting inflammation, and possibly confirming the mechanism non-Fc receptor mediated.

3. From recombinant antibodies to their *in vivo* selection

3.1 Recombinant antibodies

Recombinant DNA technology and antibody engineering have supplemented, and in some instances, replaced hybridoma technology in the production of antibodies (Hudson and Souriau, 2001). Antibody genes from animals can be amplified by PCR and expressed in different expression systems in various formats, such as the Fab, Fv, single domain (VH), single chain Fv (scFv) and the variable fragment (V_{HH}) of single-domain heavy chain antibodies (HCAb) from camelids (fig.6). Different recombinant antibody fragments, e.g. Fab, scFv and V_{HH} have been synthesized and found to possess binding characteristics comparable to their respective parent polyclonal and/or monoclonal antibodies (Yau et al, 2003).

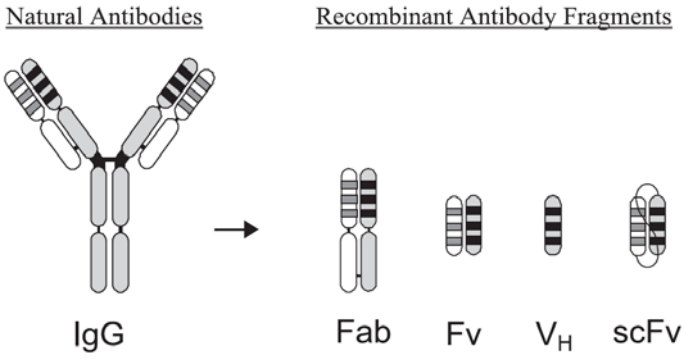

Fig.6 Schematic diagram illustrating the structures of conventional antibody molecule (IgG) and its different recombinant formats.

The major advantage of these antibody fragments is that they are smaller in size and therefore easier to manipulate genetically and express in bacterial systems. Furthermore, these antibody fragments can be expressed and anchored on bacteriophage surfaces as fusion proteins. Displayed antibody fragments remain functional for the purpose of affinity selection. As a result, specific antibody fragments and their coding sequences can be selected simultaneously from a diverse library of displayed antibodies. Antibody fragments can either be displayed on the surfaces of a bacterium or yeast, or as a fusion to viral coat proteins. The common feature among the various display technologies is that a direct link is created between the genotype and phenotype of the antibody being displayed. By having easy access to the genotype, display technologies allow antibodies to be rapidly evolved to suit specific applications by protein engineering methods (Hoogenboom et al, 1992; Winter and Milstein, 1991; Winter et al, 1994).

The format of recombinant antibodies discussed in this thesis is the single-chain Fv (scFv) fragment, which comprises H- and L-chain variable (VH and VL) segments held together by a short, flexible, linker sequence (Fig.7) (Bird et al., 1988). ScFv carry the variability inherent in the antibody combining site, namely the three hypervariable complementarity-determining regions (CDRs) of each V region (Fig.7), which together constitute the antigen-binding region of the antibody. A single domain alone can also serve for antigen recognition. The CDRs are close to each other in the tertiary structure, forming an antigen-binding pocket (Fig.7). However, the scFv and single-domain formats do not carry any effector functions, because the variable V regions are normally associated with the constant (C) region of the antibody.

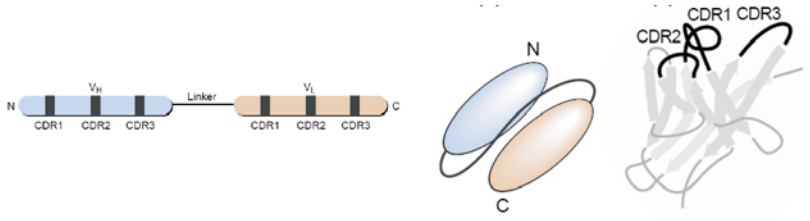

Fig.7 The single-chain Fv (scFv) antibody fragment consists of a VH (blue) and a VL (pink) domain, connected by a flexible linker peptide (total weight, ~30 kDa). The N-terminal (N) parts of both domains are responsible for binding antigen. Tertiary structure of a single VH or VL domain of scFv, showing the three complementarity-determining regions (CDRs) that form the antibody combining site. VL–VH might also be a suitable format, the one used in our system. (modified from Lobato & Rabbitts, 2003).

The availability of recombinant antibodies and the possibility to express them in different formats is the prerequisite for the use of antibodies as genes, rather than as proteins, which allows expressing them in different cells and in different compartments, an approach pioneered by our group (Biocca & Cattaneo, 1995; Cattaneo & Biocca, 1997; Piccioli et al., 1995).

3.2 From the principle of intracellular antibodies to the development of new strategies of antibody selection

On the basis of their pioneering studies, in the nineties, Cattaneo and coworkers developed the idea of intracellular immunization and its feasibility through the ectopic expression of recombinant single chain Fv fragments (scFvs) antibodies inside the cells (Biocca & Cattaneo, 1995). They demonstrated that intracellularly expressed scFvs can function in antigen recognition in eukaryotic cells and that this interaction can inhibit the function of proteins in the cytoplasm, the nucleus, or the secretory pathway (for a review, Cattaneo & Biocca 1997).

A major hindrance for this interesting approach was the paucity of scFvs antibodies, normally functioning "in vitro", that maintain this ability also "in vivo" in eukaryotic cells, presumably because not all antibodies fold correctly in the cytoplasm. To overcome this problem, in our group was developed an *in vivo* assay for functional intracellular antibodies using a two-hybrid approach (Visintin et al., 1999).

Visintin and coworkers (1999) adapted the eukaryotic two-hybrid assay to monitor the interaction of scFv fragments with their corresponding antigens, under conditions of intracellular expression. These studies were the 'proof of principle' of the following developments of yeast two hybrid-based selection strategies, for *de novo* selection of intracellular antibodies (Intracellular Antibody Capture Technology, IACT) (Visintin et al., 2002, 2004).

From the yeast two-hybrid to the intrabody selection

The yeast two-hybrid system was a logical extension of studies that demonstrated the modular nature of transcriptional activators. Site-specific transcription factors often have discrete, separable DNA-binding domains (DBDs) and transcriptional activation domains (ADs). In the original two-hybrid system, two putative interacting proteins X and Y are respectively fused to the DBD and AD of a yeast transcriptional activator. An interaction between X and Y can reconstitutes the activator (DBD-AD) and leads to transcription of 'reporter' genes, resulting in an easily detectable phenotype (Fields & Song, 1989).

Visintin and coworkers (1999) exploited the two-hybrid system to monitor intracellular antigen-antibody interactions via reporter gene activation.

Through the cotransfection of two specific expression vectors in yeast cells, the target antigen can be expressed as a (C-terminal) fusion of the DNA binding domain (DBD) of the *E. coli* protein LexA, and the specific scFv fragment can be expressed as a (N-terminal) fusion of the activation domain (AD) of the herpes virus 1 VP16 transcription factor (Fig.8).

The system exploited the L40 yeast strain, lacking histidine production (not growing in the absence of histidine) but that carry the *HIS3* gene and the *lacZ* gene under the control of a minimal promoter with LexA DNA recognition site (Fig.8). Thus, HIS3 and lacZ represents the two 'reporter genes'. If the scFv antibody fragment binds to the antigen target *in vivo*, a complex is formed that can bind to the *HIS3* and lacZ promoters and activate transcription, as above described in the classic two-hybrid system. This activity restore histidine independent growth of the yeast or the β-gal production (measured by activation of β-galactosidase and blue colonies) (Fig.8).

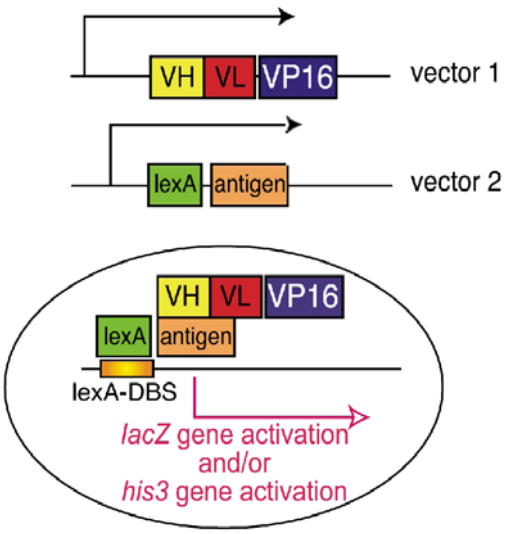

Fig.8 Scheme of antibody-antigen interaction in vivo, based on the two-hybrid system. (modified from Visintin et al., 1999)

The authors showed also that most scFvs selected from phage display libraries do not bind to antigen in the cytoplasm of yeast cells (Visintin et al., 1999), confirming that not all antibodies are able to bind antigens under conditions of intracellular expression. The low number of scFvs that can bind *in vivo* is probably the result of the lack of disulfide bonding in the reducing environment of the cell cytoplasm (Biocca et al, 1995). The folding stability of antibody domains is contributed by many residues in the frameworks (Proba et al., 1998), with different scFv fragments having different overall stabilities. Therefore, those scFv fragments that are intrinsically more stable will tolerate the loss of intrachain disulfide bond and remain folded, whereas others will not. In addition, good intracellular expression is related to additional parameters such as solubility versus propensity to aggregate, cellular half-life, and others (Visintin et al., 1999).

Intracellular Antibody Capture Technology (IACT)

The first studies performed in the field of antigen-antibody two-hybrid system provided a 'proof of principle' for the Intracellular Antibody Capture Technology (IACT), an *in vivo* selection strategy for functional intracellular antibodies (ICAbs) (Visintin et al., 2002). IACT is a procedure that allows the isolation of specific ICAbs from complex mixtures (i.e., libraries of recombinant antibodies). In a few words, the antigen fused to the DNA binding domain can be used as "bait" to screen a library of recombinant antibodies cDNA clones that are fused to an activation domain. The selected or 'captured' antibody represents the "prey".

Diverse scFv libraries, cloned in the two-hybrid Activation Domain vector, can be used for IACT selections, starting from different V repertoire sources: naïve or immunized phage display libraries, hybridomas, immunized splenocytes, and peripheral blood lymphocytes (PBLs) (Visintin et al., 2004b).

The first examples of IACT selections used phage display libraries of scFvs. In this way, in our laboratory, Visintin and coworkers demonstrated that IACT can be effectively applied to the *de novo* selection of panels of functional ICAbs against diverse protein antigens and report the full characterization of a set of ICAbs selected against the microtubule associated protein Tau, involved in Alzheimer's disease (Visintin et al., 2002).

The authors demonstrated that antibodies suitable for intracellular expression are present in natural repertoires, which have been incorporated into phage libraries and can be readily isolated with IACT, avoiding the need for any rational mutation strategy or molecular evolution approaches (Visintin et al., 2002).

They also demonstrated that a rapid preselection of phage antibody libraries may represent one possibility to provide an antigen specific enriched input library in yeast, allowing the subsequent selection of several functional antibodies readily suitable for intracellular expression.

However, the enrichment step of phage display scFv libraries requires the antigen as purified protein in coating, not exploiting one relevant and real potential of IACT: its ability to select recombinant antibodies directly from the gene sequence of the antigen (‘‘from gene to intrabody’’).

The use of libraries enriched at the source in ‘‘good intracellular antibodies’’, for instance ad hoc engineered libraries exploiting intracellular consensus sequences (ICS) (Visintin et al., 2002), would represent a solution to avoid the antigen-based enrichment step. Recently, we explored also the possibility of exploiting naïve repertoires of natural V regions, superseding the need for framework consensus engineering, with the development of Single Pot Libraries of INTrabodies (SPLINT) (Visintin et al., 2004a).

Single Pot Libraries of INTrabodies (SPLINT)

SPLINT libraries represented a significant improvement of the IACT genetic selection strategy (Visintin et al., 2004a).

In order to explore the probability of isolating intrabodies directly from primary (mouse) antibody repertoires, we have engineered a single pot antibody library in an activation domain vector and tested it in a two-hybrid selection strategy by using a wide panel of different antigens. The results obtained from all the different selections performed have indicated that the SPLINT library is a good source of antibody fragments, able to bind

proteins intracellularly. In fact, it was possible to select several scFv against each antigen challenged with the IAC technology. For most of the target antigens, it was possible to isolate several antibodies, thus indicating that, although this proof of principle SPLINT library has a complexity of ~10^7, the diversity obtained is still sufficient to isolate antibody binders that recognize particular antigens as, for example, proteins that are highly conserved between species. It is very well reported that the probability to find antibodies of a given affinity in a library has a direct relationship with the size of the library itself, in such a way that higher affinity antibodies can be selected from highly diverse libraries of greater complexity (Perelson and Oster, 1979). The required diversity for the selection of high affinity antigen-specific antibodies from an immune library is much lower than that required for such selection from a non-immune library. On the other hand, the conditions of intracellular expression allow antigen–antibody pairs to achieve higher local concentrations, making affinity as would be determined in vitro not the most important parameter for being a good, functional intrabody.

We have demonstrated that a relatively small library (with a diversity of 10^7) derived from a natural repertoire, contains functional ICAbs against all antigens against which it was challenged, and can therefore provide a good source of antibodies suitable, not only for intracellular expression (Visintin et al., 2004a), but also as conventional antibodies.

This certainly contrasts with the well-established observation (Visintin et al., 2002; Tse et al., 2002) that a very high proportion of ELISA-positive antigen-specific scFv fragments isolated from phage display libraries fail to pass the in vivo IACT selection against the same antigen. Several reasons may explain this finding.

First of all, it is possible (although unlikely) that phage display selects antibodies that are particularly unsuitable for intracellular expression, as opposed to antibodies that are directly derived from natural repertoires, with no intermediate selection.

Second, unfolded or aggregating antibodies certainly provide a growth disadvantage to cells, and this is likely to contribute a background of antigen independent selection that provides an enrichment for functional intrabodies in the SPLINT library, which are then selected in an antigen-dependent way.

Third, the relatively lower affinity requirement for intrabodies reduce the size of the library necessary to isolate intracellular binders.

Last but not least, it is possible that the effective diversity of the library is actually higher than the initial number of yeast transformants, if more than one scFv is expressed in any given yeast cell, and this may or may not result in further recombination events and in segregation of different scFvs in daughter cells.

3.3 IACT and SPLINT: novel approaches to select recombinant antibodies targeting Aβ oligomers

Antibodies, in particular the conformation specific ones, are important tools for analyzing Aβ misfolding and aggregation, as well as for targeting Aβ-related degenerative processes of Alzheimer Disease (AD). In addition, the precise intracellular targeting of recombinant antibodies to specific cellular locations (Cattaneo & Biocca, 1997, 1999), where post translationally modified pathological forms of proteins, such as Aβ oligomers, are formed is a promising strategy (the intrabody approach for protein knock-out) in AD studies.

In this work, we describe a novel generation of anti-Aβ scFvs recombinant antibodies, exploiting a revolutionary approach developed in our laboratory, called "Intracellular Antibody Capture Technology" (IACT) (Visintin et al., 1999, 2002, 2004a, 2004b). Current evidences obtained from the characterization of the IACT-selected anti-Aβ scFvs under study, demonstrated their interesting binding properties *in vitro*, with conformation specificity for Aβ oligomers; in addition, being *in vivo* selected in the yeast cytoplasm, scFvs are highly stable and readily folded to be intracellularly expressed also in mammalian cells.

Moreover, we discuss for the first time a comparative approach of selection from two different Single Pot Libraries of INTrabodies (SPLINT): one naïve and the other derived from Aβ-immunized mice. SPLINT are specialized libraries for subsequent IACT selection. We demonstrated that the SPLINT immune in comparison to that naïve, is a

source of scFv fragments with specific binding properties, biased towards N-terminal epitopes of Aβ.

The IACT-selected scFvs under study represent a new strategic tool in the survey of anti-Aβ antibodies, and for the peculiar characteristics of the selection strategy they can be used both for extracellular and for intracellular purposes, *in vitro* as well as *in vivo*.

Several anti-oligomer specific antibodies have been developed as monoclonal or polyclonal antibodies, but not as intrabodies. On the other hand, several single-chain Fv (scFv) fragments anti-Aβ, but not conformation specific, have been developed:

i) from phage display libraries (Manoutcharian K., et al., 2003, 2004; Liu et al., 2004),

ii) from monoclonal Abs (MAbs) (Frenkel et al., 2000).

These anti-Aβ scFvs exhibit anti-aggregating properties and prevent the toxic effect of Aβ fibrillar aggregates. Moreover, a recent experimental report showed that a scFv intrabody targeting the β-secretase cleavage site of APP can reduce the generation of Aβ (Paganetti et al., 2005), supporting our proposed intrabody-based approach to investigate intracellular Aβ processing and oligomerization.

For intracellular studies, scFvs intrabodies, targeted to specific intracellular compartments, can act as specific functional knock-out tools (Cattaneo & Biocca, 1997). This stage-specific, "protein interference" approach could not be pursued with the now standard RNA interference (RNAi) methods (Wall et al., 2003), because Aβ is a proteolitic fragment deriving from its APP (Amyloid Precursor Protein) precursor. RNAi based approaches could not be pursued to specifically target intracellular Aβ, or even more difficult, Aβ oligomers, as appeared to target the whole APP precursor. Even tough

targeting β-secretase BACE I with small interfering RNAs (siRNAs) reduce Aβ production and ameliorates neuropathology in an AD mouse model (Singer et al., 2005), the selective targeting versus oligomeric forms of Aβ peptide is only possible with antibody-based strategies and this is the peculiar and unique feature of our scFvs panel and of our experimental strategy.

In an *in vivo* perspective, anti-Aβ scFvs represent an attractive alternative to more conventional antibody-based therapeutics for AD, since they are smaller, and therefore have a facilitated access/diffusion in the brain parenchyma and since they do not contain the antibody Fc region, responsible for activating the complement response in brain inflammation. For gene or cell therapy purposes, scFv are ideal, since there is only one gene to be expressed, instead of the two antibody chains.

Recent studies showed that an anti-Aβ scFv based gene delivery, by intraventricular administration of adeno-associated virus in the brain of transgenic AD model mice, elicits a decrease in Aβ deposition and a rescue of pathological phenotype (Fukuchi et al., 2006; Levites et al., 2006). These data support the hypothesis to develop our Aβ conformation-specific scFvs as *in vivo* therapeutics in animal models, exploiting different approaches, from the passive immunization using scFvs as recombinant purified proteins, to gene-therapy approaches using specialized viral vectors, to an “ex vivo” cell therapy, in which genetically engineered cells can express and secrete our neutralizing the SPLINT-selected anti-Aβ scFvs.

Aim of the work

In this thesis, we discuss the selection of a panel of recombinant scFv antibodies against the 'neurologically relevant' antigen β-amyloid peptide, from a SPLINT naïve library and from an *ad hoc* created SPLINT Aβ-immune library.

The *in vivo* strategy of antibody selection here proposed was favorably supported by previous studies on Aβ-Aβ interaction (Hughes et al., 1996; Festy et al., 2001) and Aβ interactors selections (Yan et al., 1997; Hughes et al., 1998) performed in the yeast two hybrid systems.

The aim of the thesis work was:

- the creation of immune library
- the selection of anti-Aβ antibodies from the immune and the naïve SPLINT libraries and their sequence characterization
- the expression of selected antibodies for their subsequent characterization *in vitro* and *in vivo*
- the biochemical, immunohistochemical and cellular characterization of the panel of selected antibodies

MATERIALS AND METHODS

1. Immunization of mice

Three mice Balb-C (6-8 weeks old) were used for immunization.

Human Aβ1-42 peptide (Biosource) was diluted at 2 mg/ml in phosphate buffer saline (PBS). The aggregation status of Aβ peptide was not checked before immunization, but we can assume that it was mainly constituted of aggregated in forms of oligomers and protofibrils, because the antigen was incubated at 37°C before the administration.

Preimmune serum was taken on day 0. A total of four subcutaneous injections were performed (100μg antigen per animal per injection). For the first immunization, equal parts antigen and complete Freund's adjuvant were used, while for the subsequent 3 injections the antigen was mixed with incomplete Freund's adjuvant and injected at 3-week intervals. The mice were killed five days after the last injection.

The mice sera (diluted down to 1:10000) have been tested for antibodies titer by ELISA assay against Aβ peptide coating (mostly monomeric; 10μg/ml in PBS), and unrelated antigen Bovine Serum Albumin (BSA). As general procedure of ELISA assay, see the below-discussed section 7a.

Immunization of mice was entirely and kindly performed by Dr. M. Stebel (University of Trieste) in the Animal Facility of the University of Trieste.

2. Construction of the immune SPLINT library

Mouse spleens (extracted from freshly sacrificed immunized mice) were washed and cleaned in PBS and the lymphocytes released by pressing the spleen with a hypodermic needle and a sterile spatula. The cell suspension was then transferred to a sterile tube and left to deposit for 5 min. The supernatant was then removed and the cells washed twice in PBS and H_2O to remove the red blood cells. The cells were then immediately used for total RNA extraction.

The **total RNA** was extracted using a kit (Rneasy Mini Kit, Qiagen) according to the manufacturer's protocols.

2a. cDNA synthesis

After extraction, the RNA was quantified (about 30 µg from 10 mg of original tissue) and used for **cDNA synthesis** using random primers (GIBCO Brl). The synthesis of the DNA complementary to individual RNA filaments was obtained by using Superscript II Rnase H- Reverse Transcriptase enzyme (GIBCO Brl).

Random primers	1µl (100 ng);
RNA total	5µl;
dNTP mix (10mM each)	1µl;
H_2O DEPC	5µl.

The mix is heated to 65° C for 5 min, then rapidly cooled on ice. The content of the tube is collected after brief centrifugation and were added:

First-strand buffer 5 x	4 µl,
DTT 0.1M	2 µl

The tube content is mixed and then incubated for 2 min at 42° C, after which 1 µl (200U) of Superscript II is added and incubated for 50 min at 42° C. The reaction is inactivated at 70° C for 15 min. 1 µl (2U) of RNAseH is added to remove the residual RNA bound to

the formed DNA and is left for 20 min at 37° C. The cDNA can then be used to amplify the variable chains.

2b. VL and VH regions amplifications

To obtain cDNA from the immunoglobulin variable regions, the V regions were amplified by PCR using degenerated 5' and 3' primers that permit the amplification of a greater number of variable chains.

The immunoglobulin variable regions were amplified using V-region PCR (Orlandi et al., 1992), using the following degenerated primers:

VH mouse BACK:

TTA TCC TCG AGC GGT ACC GAK GTR MAG CTT CAG GAG TC	HB1
TTA TCC TCG AGC GGT ACC GAG GTB CAG CTB CAG CAG TC	HB2
TTA TCC TCG AGC GGT ACC CAG GTG CAG CTG AAG SAS TC	HB3
TTA TCC TCG AGC GGT ACC GAG GTC CAR CTG CAA CAR TC	HB4
TTA TCC TCG AGC GGT ACC CAG GTY CAG CTB CAG CAR TC	HB5
TTA TCC TCG AGC GGT ACC CAG GTY CAR CTG CAG CAG TC	HB6
TTA TCC TCG AGC GGT ACC CAG GTC CAC GTG AAG CAG	HB7
TTA TCC TCG AGC GGT ACC GAG GTG AAS STG GTG GAA T	HB8
TTA TCC TCG AGC GGT ACC GAV GTG AWG YTG GTG GAG TC	HB9
TTA TCC TCG AGC GGT ACC GAG GTG CAG SKG GTG GAG TC	HB10
TTA TCC TCG AGC GGT ACC GAK GTG CAM CTG GTG GAG TC	HB11
TTA TCC TCG AGC GGT ACC GAG GTG AAG CTG ATG GAR TC	HB12
TTA TCC TCG AGC GGT ACC GAG GTG CAR CTT GTT GAG TC	HB13
TTA TCC TCG AGC GGT ACC GAR GTR AAG CTT CTC GAG TC	HB14
TTA TCC TCG AGC GGT ACC GAA GTG AAR STT GAG GAG TC	HB15
TTA TCC TCG AGC GGT ACC CAG GTT ACT CTR AAA GWG TST G	HB16
TTA TCC TCG AGC GGT ACC CAG GTC CAA CTV CAG CAR CC	HB17
TTA TCC TCG AGC GGT ACC GAT GTG AAC TTG GAA GTG TC	HB18
TTA TCC TCG AGC GGT ACC GAG GTG AAG GTC ATC GAG TC	HB19

VH mouse FOR:

GAT TGG TTT GCC GCT AGC TGA GGA GAC GGT GAC CGT GGT	HF1
GAT TGG TTT GCC GCT AGC TGA GGA GAC TGT GAG AGT GGT	HF2
GAT TGG TTT GCC GCT AGC TGC AGA GAC AGT GAC CAG AGT	HF3
GAT TGG TTT GCC GCT AGC TGA GGA GAC GGT GAC TGA GGT	HF4

VL mouse BACK:

AGC AAG CGG CGC GCA TGC CGA YAT CCA GCT GAC TCA GCC	LB1
AGC AAG CGG CGC GCA TGC CGA YAT TGT TCT CWC CCA GTC	LB2
AGC AAG CGG CGC GCA TGC CGA YAT TKT GMT VAC TCA GTC	LB3
AGC AAG CGG CGC GCA TGC CGA YAT TGT GYT RAC ACA GTC	LB4
AGC AAG CGG CGC GCA TGC CGA YAT TGT RAT GAC MCA GTC	LB5
AGC AAG CGG CGC GCA TGC CGA YAT TMA GAT RAM CCA GTC	LB6
AGC AAG CGG CGC GCA TGC CGA YAT TCA GAT GAY DCA GTC	LB7
AGC AAG CGG CGC GCA TGC CGA YAT YCA GAT GAC ACA GA	LB8
AGC AAG CGG CGC GCA TGC CGA YAT TGT TCT CAW CCA GTC	LB9
AGC AAG CGG CGC GCA TGC CGA YAT TGW GCT SAC CCA ATC	LB10
AGC AAG CGG CGC GCA TGC CGA YAT TST RAT GAC CCA RTC	LB11
AGC AAG CGG CGC GCA TGC CGA YRT TKT GAT GAC CCA RAC	LB12
AGC AAG CGG CGC GCA TGC CGA YAT TGT GAT GAC BCA GKC	LB13
AGC AAG CGG CGC GCA TGC CGA YAT TGT GAT AAC YCA GGA	LB14
AGC AAG CGG CGC GCA TGC CGA YAT TGT GAT GAC CCA GWT	LB15
AGC AAG CGG CGC GCA TGC CGA YAT TGT GAT GAC ACA ACC	LB16
AGC AAG CGG CGC GCA TGC CGA CAG GCT GTT GTG ACT CAG GAA TC	LBL

VL mouse FOR:

GAA GTT ATG GTC GAC CCT CCG GAA CGT TTK ATT TCC AGC TTG G	LF1/2
GAA GTT ATG GTC GAC CCT CCG GAA CGT TTT ATT TCC AAC TTT G	LF4
GAA GTT ATG GTC GAC CCT CCG GAA CGT TTC AGC TCC AGC TTG G	LF5
GAA GTT ATG GTC GAC CCT CCG GAA CCT AGG ACA GTC AGT TTG G	LFL

The primers were kindly provided by Dr. Visintin (LayLineGenomics, Trieste)

To create the library that is as representative as possible, single amplifications were performed using each oligonucleotide described above according to the following schemes:

	HB1	HB2	HB3	HB4	HB5	HB6	HB7	HB8	HB9	HB10	HB11	HB12	HB13	HB14
HF1	x	X	x	x	x	x	x	x	x	x	x	x	x	x
HF2	x	X	x	x	x	x	x	x	x	x	x	x	x	x
HF3	x	X	x	x	x	x	x	x	x	x	x	x	x	x
HF4	x	X	x	x	x	x	x	x	x	x	x	x	x	x

	HB15	HB16	HB17	HB18	HB19
HF1	X	x	x	x	x
HF2	X	x	x	x	x
HF3	X	x	x	x	x
HF4	X	x	x	x	x

	LB1	LB2	LB3	LB4	LB5	LB6	LB7	LB8	LB9	LB10	LB11	LB12	LB13	LB14	LB15	LB16	LBL
LF1/2	x	x	x	x	x	x	x	x	x	x	x	x	x	x	x	x	
HF3	x	x	x	x	x	x	x	x	x	x	x	x	x	x	x	x	
HF4	x	x	x	x	x	x	x	x	x	x	x	x	x	x	x	x	
HF5	x	x	x	x	x	x	x	x	x	x	x	x	x	x	x	x	
LFL																	x

This procedure allows verification of the library quality, without having to introduce a prevalence of determinate variable regions that are more easily amplified than others. In this specific case, 141 individual amplifications are carried out, starting from the cDNA obtained from the total RNA extracted from the immunized mouse spleen. The conditions used to amplify the variable chains were:

PCR reaction mix

cDNA 0.5 µl;

H_2O 30.5µl;

10X PCR buffer 5µl;

dNTP 2.5mM each 5µl;

$MgCl_2$ 25mM 3 µl;

Oligo1 (10pmol/µl) 2.5µl;

Oligo 2 (10pmol/µl); 2.5µl

Taq polymerase 1µl

Mineral oil (50-100µl) is added to prevent evaporation in the test tube containing the reaction mixture. The tube is then placed in a thermocycler programmed as follows:

PCR amplification cycles

94°C, 5',

(94°C, 1' 60°C , 1' 72°C, 1') for 30 cycles;

72°C, 10';

4°C

After the variable regions have been amplified, they are analyzed on a 1.5% agarose gel and quantified. The same quantity of DNA for each amplified products is then used for cloning. A total of 10μg of a variable chain is then used for each cloning.

2c. PULL THROUGH

After all the VL and the VH variable regions have been amplified from the cDNA, they are reamplified to increase the quantity of DNA for cloning and to add extra sites to each terminus of the variable region previously amplified with the degenerated primers. After the variable chains (PTVL and PTVH) have undergone pull through, the amplified products are purified with gels. After purification, the PTVL and the PTVH are used for in vitro assembly. The pull through is used to insert a small polypeptide chain (called linker) that, after in vitro assembly, is in turn needed to reconstruct the single chain sequence. The assembly was done in a single step.

The primers used for pull through were:

VH PTL 220 BACK

GGA GGG TCG ACC AGC GGT TCT GGG AAA CCA GGT TCC GGT GAA GGC TCG AGC GGTA

VH PTMIC FOR

CCA GGC CCA GCA GTG GGT TTG GGA TTG GTT TGC CGC TA

VL PTL 220 FOR

ACC GCT CGA GCC TTC ACC GGA ACC TGG TTT CCC AGA ACC GCT GGT CGA CCC TCC

VL PTMIC BACK

CGC TGG ATT GTT ATT ACT CGC AGC AAG CGG CGC GCA TGC C

The pull-through protocol was:

VL 5µl (~100 ng);

VL PTL 220 FOR 5 µl;

VL PTMIC BACK 5 µl;

$MgCl_2$ 2 µl;

dNTPs 10 µl;

buffer 10X 10 µl;

Taq polymerase 2 µl;

H_2O 61 µl;

VH 5 µl (~100 ng);

VH PTL 220 BACK 5 µl;

VH PTMIC FOR 5 µl;

$MgCl_2$ 2 µl;

dNTPs 10 µl;

buffer 10X 10 µl;

Taq polymerase 2 µl;

H_2O 61 µl.

Mineral oil (50-100µl) is added to prevent evaporation in the test tube containing the reaction mixture.

The tube is then placed in a thermocycler programmed as follows:

94°C –5’; (94°C –30”, 60°C –30”, 72°C –30”) for 20 cycles; 72°C –10’;

4°C –24h.

2d. ASSEMBLY

After the pull-though band for the VH and VL is isolated, the chains are purified with gel and the amplified products are used for in vitro **assembly**. In all, about 200 ng of DNA is used for the reaction (100 ng of PTVL and 100 ng of PTVH).

The assembly reaction primers are:

VH PT2 FOR

TGG TGA TGG TGA GTA CTA TCC AGG CCC AGC AGT GGG TTT G

VL PT2 BACK

TAC CTA TTG CCT ACG GCA GCC GCT GGA TTG TTA TTA CTC

The reaction is:

PTVL 100 ng;
PTVH 100 ng;
VL PT2 BACK (100µM) 0.5 µl;
VH PT2 FOR (100µM) 0.5 µl;
dNTPs 10 µl;
Buffer 10X 10 µl;
$MgCl_2$ 2 µl;
Taq polymerase2 µl;
H_20 to 100 µl.

Mineral oil (50-100µl) is added to prevent evaporation in the test tube containing the reaction mixture. The tube is then placed in a thermocycler programmed as follows: 94°C –5'; (94°C –30", 68°C –30", 72°C –30") for 8 cycles without primers and 12 cycles with primers; 72°C –10'; 4°C –24h.

After assembly of the VH and the VL, the assembled scFv library is purified with gel as described above.

After purification, the DNA is digested with enzymes NheI and BssH2 in the following way:

DNA mix 10µg;

NheI (NEB 20 U/µl) 1.5µl;

Buffer 2 (NEB)10µl

BSA (10mg/ml)1µl;

H_2O Q.S. (final V=100µl) ,

and left to digest for 4 h at 37°C.

After digestion and purification with gel, the DNA is cut with BssHII:

DNA mix 10µg

BssHII (NEB 20 U/µl) 1.5µl;

Buffer 3 (NEB) 10µl;

H_2O Q.S. (final V=100µl).

The reaction mixture is incubated at 50°C for 4 h.

The digested chains are then purified with 1.5% gel using a purification kit (Gel extraction kit, Qiagen). After purification, the DNA is quantified on 1.5% agarose using spectrophotometry at a wavelength of 260 nm.

2e. LARGE SCALE LIGATION FOR LIBRARY

The library is then ligated in the vector pMV1: about 300ng of vector were used for this step; ligation was performed in gradient to optimize the reaction. The reaction mix is:

pMV1: 80 µl (320ng);

VL-VH assembly: 20 µl (200 ng);

Ligase:10µl (400U/µl);

Buffer: 40µl;

H_2O: 240µl;

The reaction mixture is placed in 8 Eppendorf tubes and incubated overnight at 16° C, in PCR thermocycler. The next day, the reaction is inactivated at 65° C for 10 min. After

incubation, the reaction mix is purified with QIAGEN PCR purification columns, eluited in final 45 µl of EB buffer QIAGEN, and then electroporated in DH5αF'.

For each electroporation, 30 µl of bacteria plus 1 µl of ligase mix is used (max. 100 ng per electroporation). After transformation, the bacteria are resuspended in 1 ml of SOC medium + 10 nM MgCl2 and incubated for 1 h at 37° C, after which they are seeded on LB+ ampicillin plates. The next day, the efficiency of the transformation is evaluated. The library thus obtained was estimated to be about $1.7X10^6$ CFU.

At this point, the SPLINT library was used for the control test such as PCR-fingerprinting to test library diversity, antibody sequences taken randomly, western blot analysis to check the expression of the individual chains in yeast and screening on a panel of known antigens.

3. Aβ BAITS CONSTRUCTS

All DNA encoding Aβ baits were cloned into pMICBD1, *kindly provided by Dr. Visintin, (LayLineGenomics, Trieste)* (see the "Results section" for the description of the vector) in the same reading frame of LexA, between BamHI-PstI restriction sites of the polylinker.

lexA MIC sense

CTT CGT CAG *CAG AGC TTC ACC ATT GAA* GGG CTG GCG GTT GGG GTT ATT CGC AAC GGC GAC

polylinker MIC antisense

TGG CTG **GAA TTC CCG GGG ATC CGT CGA CCT GCA G**CC AAG CT*A ATT CCG GGC GAA TTT C*TT

EcoRI SmaI **BamHI** SalI **PstI**

Aβ baits inserts preparation:

DNA coding for human and murine Aβ42 were obtained by PCR amplification using two overlapping oligonucleotides. The DNA of all the other baits were obtained by annealing of complementary oligonucleotides.

Human Aβ42

Oligonucleotides

hAβ (1-42) BamHI sense

5' GAA TTC CCG GGG ATC CTC GAT GCA GAA TTC CGA CAT GAC TCA GGA TAT GAA GTT CAT CAT CAA AAA **TTG GTG TTC TTT GCA GAA GAT GTG GGT TCA 3'**

hAβ (1-42) PstI antisense

5' TAG GCA TTA CTG CAG CTA CGC TAT GAC AAC ACC GCC CAC CAT GAG TCC AAT GAT TGC ACC TTT GTT **TGA ACC CAC ATC TTC TGC AAA GAA CAC CAA 3'**

Obtained amplimer

hAβ42 (BamHI-PstI)

GAATTCCCGGGGATCCTC**GATGCAGAATTCCGACATGACTCAGGATATGAAGTTCATCATC AAAAATTGGTGTTCTTTGCAGAAGATGTGGGTTCAAACAAAGGTGCAATCATTGGACTC ATGGTGGGCGGTGTTGTCATAGCG**TAGCTGCAGTAATGCCTA

Note: in bold highlighted the coding sequence of hAβ42; underlined restriction sites BamHI and PstI .

PCR reaction mix for hAβ42 amplification

Oligo BamHI sense	3µl (1µg)
Oligo PstI antisense	3µl (1µg)
dNTPs 2.5mM each	0.5µl
Buffer 10X	5 µl
Pfu Polymerase	1µl
H2O	35.5µl

PCR reaction cycles

95°C , 5min

(95°C, 1 min; 65°C, 30 sec; 72°C, 1min) x 15 cycles

72°C, 10min

4°C

Mouse Aβ42

Oligonucleotides

Aβ(1-42) mouse BamHI sense

GAA TTC CCG GGG ATC CTC GAT GCA GAA TTC GGA CAT GAT TCA GGA TTT GAA GTC CGC CAT CAA AAA **CTG GTG TTC TTT GCT GAA GAT GTG GGT TCG**

Aβ (1-42) mouse PstI antisense

TAG GCA TTA CTG CAG CTA CGC TAT GAC AAC GCC GCC CAC CAT GAG TCC GAT GAT GGC GCC TTT GTT **CGA ACC CAC ATC TTC AGC AAA GAA CAC CAG**

Obtained amplimer

Mouse Aβ42 (BamHI-PstI)

GAA TTC CCG GGG ATC CTC **GAT GCA GAA TTC GGA CAT GAT TCA GGA TTT GAA GTC CGC CAT CAA AAA CTG GTG TTC TTT GCT GAA GAT GTG GGT TCG AAC AAA GGC GCC ATC ATC GGA CTC ATG GTG GGC GGC GTT GTC ATA GC**TAGCTGCAGTAATGCCTA

Notes: highlighted in yellow only coding mutations in comparison to human sequence. PCR reaction similar to human Aβ42 (see above).

DNA sequences of Aβ baits inserts (BamHI-PstI)

1. human Aβ42

GAATTCCCGGGGATCCTC**GATGCAGAATTCCGACATGACTCAGGATATGAAGTTCATC ATCAAAAATTGGTGTTCTTTGCAGAAGATGTGGGTTCAAACAAAGGTGCAATCATTG GACTCATGGTGGGCGGTGTTGTCATAGCG**TAGCTGCAGTAATGCCT

2. human Aβ40

GAATTCCCGGGGATCCTC**GATGCAGAATTCCGACATGACTCAGGATATGAAGTTCATC ATCAAAAATTGGTGTTCTTTGCAGAAGATGTGGGTTCAAACAAAGGTGCAATCATTG GACTCATGGTGGGCGGTGTTGTC**TAGCTGCAGTAATGCCT

3. mouse Aβ42

GAATTCCCGGGGATCCTC**GATGCAGAATTCGGACATGATTCAGGATTTGAAGTCCGCC ATCAAAAACTGGTGTTCTTTGCTGAAGATGTGGGTTCGAACAAAGGCGCCATCATCG GACTCATGGTGGGCGGCGTTGTCATAGC**TAGCTGCAGTAATGCCTA

4. human Aβ28

GAATTCCCGGGGATCCTC**GATGCAGAATTCCGACATGACTCAGGATATGAAGTTCATC ATCAAAAATTGGTGTTCTTTGCAGAAGATGTGGGTTCAAACAAA**TAGCTGCAGTAATG CCTA

5. mouse Aβ28

GAATTCCCGGGGATCCTC**GATGCAGAATTCGGACATGATTCAGGATTTGAAGTCCGCC ATCAAAAACTGGTGTTCTTTGCTGAAGATGTGGGTTCGATAGCG**TAGCTGCAGTAATG CCTA

6. human Aβ17

GAATTCCCGGGGATCCTC**GATGCAGAATTCCGACATGACTCAGGATATGAAGTTCATC ATCAAAAATTG**TAGCTGCAGTAATGCCTA

7. mouse Aβ17

GAATTCCCGGGGATCCTC**GATGCAGAATTCGGACATGATTCAGGATTTGAAGTCCGCC ATCAAAAACTG**TAGCTGCAGTAATGCCTA

8. human Aβ10

GAATTCCCGGGGATCCTC**GATGCAGAATTCCGACATGACTCAGGATAT**TAGCTGCAGTA ATGCCTA

9. mouse Aβ10

GAATTCCCGGGGATCCTC**GATGCAGAATTCGGACATGATTCAGGATTT**TAGCTGCAGTA ATGCCTA

DNA inserts and pMICBD1 vector were digested BamHI-PstI (in Buffer3 NEB +BSA, 37°C, 1h)

The digested vector was dephoshorylated with CIAP prior to ligating to the insert DNA.

For ligation, the ideal ratio of insert-to-vector DNA is variable; however, a reasonable starting point is 1:3 (vector-to-insert molar ratio), measured in available picomole ends. This is calculated as follows:

$$\text{Picomole ends/microgram of DNA} = \frac{2 \times 10^6}{\text{n.of base pairs} \times 650}$$

MW of a double-stranded DNA molecule=(#of base pairs) x (650daltons/base pair)
Average weight of a DNA basepair (sodium salt)= 650 daltons

	pMICBD1 + insert 1:3	pMICBD1 + insert 1:5	pMICBD1 + ligase	pMICBD1 prepared vector
Prepared pMICBD1 vector	1 µl	1µl	1µl	1µl
Prepared insert	3X	5X	/	/
T4 DNA ligase	1U	1U	1U	/
10X ligase buffer	1	1	1	1µl
H_2O MQ	to 10 µl	to 10 µl	to 10 µl	to 10 µl

Ligate overnight at 16°C.

Performed a standard transformation of the vector construct into *E.coli* competent cells.

4. IACT selection method using SPLINT libraries

List of abbreviations

Two-Hybrid Terminology

AD vector	Plasmid encoding the VP16 activation domain (AD)
DNA-BD vector	Plasmid encoding the lexA DNA-binding domain (DNA-BD)
scFv-VP16	A hybrid protein comprised of the single chain fv fragment (scFv) previously cloned to the VP16 activation domain
SPLINT	Mouse scFv library naïve or immune (iperimmune anti-Aβ) constructed in AD vector such that the scFv is fused to the VP16 activation domain
DNA-BD/target protein	A hybrid protein (the "bait") comprised of the lexA DNA-BD fused with your target protein
DNA-BD/target plasmid	Plasmid encoding the "bait" (i.e., the DNA-BD/target protein)

Yeast Phenotypes

Trp$^-$	Requires tryptophan (Trp = W) in the medium to grow, i.e., is a Trp auxotroph
Leu$^-$	Requires leucine (Leu = L) in the medium to grow, i.e., is a Leu auxotroph
His$^-$	Requires histidine (His = H) in the medium to grow, i.e., is a His auxotroph
LacZ$^+$	Express the *lacZ* reporter gene, i.e., is positive for β galactosidase activity
His$^+$	Express the *HIS3* reporter gene, i.e., does not require HIS in the medium to grow

Yeast Selection Media

YC	Synthetical minimal medium

MATERIALS

vectors

pMICBD1 vector (bait plasmid)

pVP16 vector (negative control)

plexA-lamin (negative control)

plinker220 and pMV1 (prey plasmids) represented by SPLINT libraries

primers

MIC sense 5' CAg AgC TTC ACC ATT gAA 3'
MIC antisense 5' gAA ATT CgC CCg gAA TT 3'
BssH2 sense 5' gTg gCC CAg CCg AgC gCg CAT gCC 3'
NheI antisense 5' CCg CTT CTT CTT ggg TgC CAT ggC 3'
SalI antisense 5' TTT CCC AgA ACC gCT ggT CgA CCC 3'
linker 220 sense 5' AAA CCA ggT TCC ggT gAA ggC TCg 3'
linker 220 antisense 5' gCT CgA gCC TTC ACC ggA ACC Tgg 3'
VP16 antisense 5' TCg AgC TCg gTA CAC CTg gg 3'

Host strain

L40 *S.cerevisiae* strain (Invitrogen, # C830-00)
Mata *his*3Δ200 *trp*1-901*leu*2-3,112*ade*2LYS2::(lexAop)$_4$-HIS3 URA3::(lexAop)$_8$-*lac*Z GAL4

Antibodies

Anti-lexA polyclonal antibody (Invitrogen, #R990-25)
Anti-VP16 polyclonal antibody (BD-Clontech, #3844-1)

All the materials were kindly provided by Dr. Visintin (LayLineGenomics, Trieste)

REAGENTS AND SOLUTIONS

- Yeast Nitrogen Base without amino acids and ammonium sulfate (SIGMA #Y-1251)
- Bacto Agar (BD # 214010)
- NaOH (Riedel-deHaen #30620)
- Adenine hemisulfate salts (SIGMA #A-9126)
- L-arginine HCl (SIGMA #A-5131)
- L-cysteine (SIGMA #C-6852)
- L-threonine (SIGMA #T-8652)
- L-aspartic acid (SIGMA #A-4534)
- L-isoleucine (SIGMA #I-2752)
- L-methionine (SIGMA #M-9625)
- L-phenylalanine (SIGMA #P-2126)
- L-proline (SIGMA #P-0380)
- L-serine (SIGMA #S-4500)
- L-tyrosine (SIGMA #T-3754)
- L-histidine (SIGMA #H-8125)
- Uracil (SIGMA #U-0750)
- L-leucine (SIGMA #L-8912)
- L-lysine HCl (SIGMA #L-5626)
- L-tryptophan (SIGMA #T-0254)
- Ammonium sulfate (Fluka #09980)
- Polyethylene glycol 4'000 (Fluka #95904)
- D-(+) Glucose anhydrous (SIGMA #G-7021)
- Lithium Acetate dihydrate (SIGMA #L-6883)
- Succinic acid (SIGMA #S-7501)
- Dimethyl sulfoxide –DMSO (Fluka #41639)
- Glass beads 425-600 microns acid washed (SIGMA #G-8772)
- Yeast extract (BD # 211931)
- Bacto peptone (BD #211840)
- Colony lifts, Protran BA85 (Schleicher & Schuell #10 401116)
- 3-amino-1,2,4-triazole (SIGMA #8056)
- 5-bromo-4-chloro-3 indolyl-β -D-galactosidase –X-gal (Eppendorf #0032006.400)
- N-N-dimethylformamide (Fluka #34903)

4a. Preparation of the Yeast host strain

The interaction system that we have used requires the yeast strain L40 (Hollenberg et al., 1995) which contains lexA operator-responsive reporters chromosomally integrated; the genotype of L40 is:

Mata *his*3Δ200 *trp*1-901 *leu*2-3,112 *ade*2 LYS2::$(lexAop)_4$-HIS3 URA3::$(lexAop)_8$-*lac*Z GAL4

The expression of HIS3 gives a growth selection for interaction while the expression of lacZ, which encodes the enzyme β-galactosidase, can be monitored using a colorimetric assay based on the activity of β -galactosidase: the $lacZ^+$ yeasts form blue colonies in the presence of the chromogenic substrate 5-bromo-4-chloro-3-indolyl- β -D galactoside (X-gal).

This strain is deficient for TRP and LEU (auxotrophic phenotype) and cannot grow on minimal medium lacking those nutrients unless functional TRP1 and LEU2 genes are introduced. Moreover, this strain carries the ade2 mutation, which confers a red color (due to a red pigment accumulation) on medium containing limiting amounts of adenine that turns darker as the colony age.

Yeast Strain Maintenance

1. Yeast strain can be maintained as stock in YPD medium with 30% glycerol and can be stored indefinitely at -80°C.
2. To recover frozen strains and prepare working stock plates:

a) streak a small portion of the frozen stock onto YPD agar plate.
b) Incubate the plate at 30°C until yeast colonies reach ~ 2mm in Ø (this takes ~3 days)
c) Seal plates with Parafilm and store at 4°C for up to 2 weeks

Preparation of stock cultures of new yeast strain

1. Use a sterile inoculation loop to scrape an isolated colony from the agar plate
2. Thoroughly resuspend the cells in 200 µl of YPD medium. Add sterile 50% glycerol to a final concentration of 30%.
3. Tightly close the cap. Vortex the vial before freezing at -80°C.

Phenotype Verification

Yeast colonies should appear slightly pink or red (because of the *ade2-101*) mutation and grow to > 2 mm in Ø. However, small white colonies will form at the rate of 1-2% due to spontaneous mutations that eliminate mitochondrial function. The strain turns darker as the colony ages.

Test of the strain

L40 yeast strain should not grow in these media:

Yeast strain	**YC selection media**	**phenotype**
L40	-W	No growth
L40	-L	No growth
L40	-H	No growth
L40	-U	Growth
L40	-K	Growth

L40 strain is deficient for TRP and LEU and cannot grow on minimal medium lacking those nutrients unless functional TRP1 and LEU2 genes are introduced.
L40 can grow onto –U and –K media because the lexA operator is integrated into URA and LYS markers. Using media with Ura and Lys dropped out, results in minimal background.

4b. Preparation of Media and Reagents

Yeast strains, which employ auxotrophic mutations as markers, are grown on nutrient-rich media at 30°C to minimize selections for revertants.

Strains to be preserved are grown to logarithmic phase on YPD plates; the yeast is then scraped up with sterile inoculation loop and suspended in a 15-30% (v/v) glycerol-YPD medium; yeast can be stored now indefinitely at -70°C (the vials should be vortex briefly before freezing at -70°C to avoid cells settling to the bottom of the tube).

When needed, the yeast strain can be revived by transferring a small portion of the frozen sample onto YPD plates (yeast L40 colonies should appear slightly pink onto YPD plates and grow to >2 mm in diameter); yeast can be also stored at 4°C on YPD plates for up to 2 months. To verify the phenotype of the yeast strain provided, the streaking of few colonies from the working stock onto separate YC plates is performed (see table); phenotype will appear after 3-4 days of incubation at 30°C.

YPD medium

10 g yeast extract (BD # 211931)

20 g bacto peptone (BD # 211840)

20 g bacto-agar (BD # 214010)

2% glucose (SIGMA # G-7021)

Add H_2O to 950 ml. Adjust **pH to 5.8** then adjust to 1 liter. Autoclave 121°C for 15 min.

YPA medium

10 g yeast extract (BD # 211931)

20 g bacto peptone (BD # 211840)

20g bacto-agar (BD # 214010)

0.1g Adenine hemisulfate salt (SIGMA # A-9126)

Add H_2O to 950 ml. Adjust **pH to 5.8** then adjust to 1 liter. Autoclave 121°C for 15 min.

YC medium

1. **YNB w/o aa & $(NH_4)_2SO_4$:**

1.2 g yeast nitrogen base, w/o amino acids and ammonium sulfate (SIGMA # Y-1251)

20 g bacto-agar (BD # 214010)

Add H_2O to 800 ml. Autoclave 121°C for 15 min.

2. SALTS:
5.4g NaOH (Riedel-de Haen #30620)
10g succinic acid (SIGMA # S-7501)
5g ammonium sulfate (Fluka # 09980)

3. Glucose:
22g D-glucose
(SIGMA # G-7021)
Dissolve in 16 ml H_2O

Add H_2O to 100 ml and dissolve all components one by one. Add glucose (3.) and H_2O to solution 2. to obtain a final volume of 150 ml.

4. amino acids MIX:

5.8 g NaOH (Riedel-de Haen #30620)

1 g Adenine hemisulfate salts (SIGMA#A-9126)
1 g L-Arginine HCl (SIGMA # A-5131)
1 g L-Cysteine (SIGMA # C-6852)
1 g L-Threonine (SIGMA # T-8625)
0.5 g L-Aspartic acid (SIGMA # A-4534)
0.5 g L-Isoleucine (SIGMA # I-2752)
0.5 g L-Methionine (SIGMA # M-9625)
0.5 g L-Phenylalanine (SIGMA # P-2126)
0.5 g L-Proline (SIGMA # P-0380)
0.5 g L-Serine (SIGMA # S-4500)

Dissolve in 80 ml H_2O

5. L-Tyrosine:

0.5 g L-Tyrosine (Sigma # T-3754)

0.2 g NaOH (Riedel-de Haen #30620)
Dissolve in 10 ml by heating
Add to aa MIX (4.) the L-Tyrosine solution (5.) and H_2O to make a final volume of 100 ml. Filter –sterilize, aliquot and store at -20°C for up to 1 year.

6. Omitted aminoacid solutions:

L-Histidine (SIGMA # H-8125)**:**

- 5 g/l H_2O

Uracil (SIGMA # U-0750) **:**

- 10 g/l H_2O (+2 pellets NaOH)

L-Leucine (SIGMA # L-8912)**:**

- 10 g/l H_2O

L-Lysine HCl (SIGMA # L-5626)**:**

- 10 g/l H_2O

L-Tryptophan (SIGMA # T-0254)**:**

- 10g/lH_2O

Filter-sterilize and aliquot individually omitted amino acids (aa) solutions (H, W, L, K, U) and store at -20°C for up to 1 year.

Before preparing YC plates or media by mixing appropriate solutions, media must be adjusted to pH 5.8 and sterilized by filtering salts + aa final mix. All the components must be mixed as suggested in the following Table :

	YNB w/o aa & $(NH_4)_2SO_4$	**Salts**	**aaMIX**	**W**	**H**	**U**	**L**	**K**	**H_2O**
-UKW	800	150	10		10		10		20
-UKL	800	150	10	10	10				20
-UKWL	800	150	10		10				30
-WHUK	800	150	10				10		30
-WHULK	800	150	10						40

Table: mix of salts and aa to prepare selective media

Note: All the suggested volumes are expressed in ml.

4c. LiAc transformation (small-scale)

A number of specialized media and reagents are required for the protocols in this section. This protocol is a modification of published methods (Gietz et al., 1992), (Hill et al., 1991), (Schiestl and Gietz, 1989), made by Clontech laboratories. The expected transformation efficiency is 10^3-10^4 / μg plasmid DNA.

Materials

- 10X LiAc buffer: 1M LiAc, pH 7.5 adjusted with diluted glacial acetic acid autoclave-sterilized (lithium acetate dehydrate –SIGMA # L-6883)
- 50% (w/v) autoclave-sterilized PEG 4000: polyethylene glycol, avg. mol. wt.=3350-Fluka # 95904. (Solution must be kept in a tightly sealed glass bottle to avoid evaporation)
- 10X TE buffer: 100mM Tris, 10mM EDTA, pH7.5, autoclave-sterilized
- 100% DMSO: dimethyl sulfoxide (Fluka #41639)
- 10 mg/ml denatured carrier DNA from fish sperm (Roche # 1467140)

Procedure

Day 1: Inoculate few colonies of L40 in 50 ml of YPD and incubate for 16-18 hr with shaking at 250 rpm at 30°C to place the culture at mid log phase the next day (OD_{600} > 1.5). **Note.** Use only glass flasks carefully washed with ultra pure, pyrogen-free water and sterilized by autoclaving 15 min at 121°C.

Day 2:

1) Dilute the overnight culture to OD_{600} 0.2-0.3 in 300 ml of YPD prewarmed to 30°C. Grow at 30°C for 3 hours with shaking (230 rpm)

2) Pellet the cells by centrifugation (1000 X g for 5 min) at room temperature, discard the supernatant and resuspend the pellet in 50 ml of H_2O.

3) Centrifuge the cells again as in 2), decant the supernatant

4) Resuspend the pellet in 1.5 ml of freshly prepared 1X TE/LiAc (10mM TE, 0.1M LiAc)

5) Prepare in a tube a mixture of:

- ✓ 0.1 µg lexA-Ag vector construct
- ✓ 0.1 µg scFv-VP16 vector construct (if you need to test specific antigen-antibody partners)
- ✓ 0.1 mg denatured carrier DNA from fish sperm
- ✓ 100 µl freshly prepared yeast cells

6) Add 0.6 ml of a sterile PEG/LiAc (0.1 M LiAc, 10mM TE, PEG 4000 40%) to the tube and vortex to mix
7) Incubate 30 minutes at 30°C with shaking (230 rpm)
8) Add 70 µl of DMSO, mix gently by inversion and heat shock for 15 min in a 42°C water bath.
9) Chill cells on ice
10) Pellet cells by centrifugation (20 sec at maximum speed)
11) Remove supernatant and resuspend cells in 0.5 ml of sterile 1X TE; spread 100 µl for single transformation or 250 µl for a co-transformation on each 100 mm plate.

The competent cells can be stored at 4°C for 1 week without a significant reduction in competency.

4d. Characterization of the "Aβ baits"

A series of control experiments must be performed to establish whether the fusion proteins LexA-Aβ were suitable as such or whether it must be modified; the verifications of well-behaved bait are:

a) testing for activity
b) testing for expression
c) testing for toxicity

a) activity

A well-behaved bait should not transactivate in a non-specific way the reporter genes in the L40 strain and should not interact with either the nuclear localization signals or with the VP16 activation domain. Therefore, the L40 strain transformed with the bait alone or together with VP16 plasmid should not grow in the absence of histidine and should not contain any detectable β-galactosidase activity. Note: the bait must be modified by using a particular domain or a deletion mutant of the same protein in frame to lexA if it does not fulfill all the proposed features.

Test the extent of non specific activation of the reporter construct by the bait plasmid with the following protocol:

1) transform the bait plasmid into L40 strain using the small-scale yeast transformation protocol
2) select for transformants on appropriate YC plates as described in Table 2.2
3) assay the bait construct for activation of HIS3 reporter gene as described in Table 2.2 and for activation of the lacZ reporter gene using the β-galactosidase colony-filter assay as described below

Growth of the bait Ag **MUST** be kept low.

If growth on –H plates occurs background growth can be suppressed with 3AT: pick transformants from YC-UKW plates and restreak them in duplicate onto YC-UKWH plates with a range in 3AT concentrations from 0 to 150mM in 5mM increments.

Transformation controls for well-behaved "bait"

To test for the possibility of transactivation by the lexA fusion Ag the transformants must be plated onto diagnostic media (see the following Table.). It is very important that His gene does not switched on by intrinsic transactivation of the lexA fusion protein, as this would lead to growth on selective media.

„bait"	„AD"	YC selection medium	HIS3 phenotype	lacZ phenotype
lexA-Aβ		-UKW	+	white
lexA-Aβ		-WHUK	/	
lexA-Aβ	VP16	-UKWL	+	white
lexA-Aβ	VP16	-WHULK	/	

b) expression

- **Preparation of Crude Yeast Lysate for SDS-PAGE analysis**

To verify that the bait fusion protein is properly synthesized, an SDS-PAGE and immunoblot analysis on crude yeast lysate must be performed.

Materials

- ✓ master plate with bait-containing positive and control yeasts
- ✓ antibody to lexA (Invitrogen) or monoclonal/polyclonal to fusion protein
- ✓ Laemmli sample buffer 2x

Procedure

Day 1:

Incubate overnight at 30°C a 5-ml culture of the bait being tested and relative controls in the appropriate YC medium.

Day 2:

1) From each overnight culture start a new 5-ml culture at OD_{600}= 0.15. Incubate at 30°C until the culture has reached OD_{600}= 0.5-0.7.
2) Remove 1.5 ml from the tube and centrifuge cells 3 min at maximum speed
3) Remove the supernatant and working rapidly resuspend in 50 µl of 2x Laemmli sample buffer.
4) Vortex and place immediately the tube on dry ice.
5) Boil 5 min and centrifuge 1 min at maximum speed the sample before loading it on SDS-PAGE.

c) toxicity

A high level expression of the fusion protein could be toxic to the reporter strain and this could lead the transformant cells to be unable to grow. To alleviate this detrimental effect the truncation of the toxic protein or a conditional promoter on hybrid plasmid could be used.

After the scoring of His+ yeast colonies, a X-Gal lift assay is performed as described below (Visintin and Cattaneo, 2001).

β-galactosidase filter assay

(Breeden and Nasmyth, 1985)

Materials

- ✓ Nitrocellulose filter circles (Scheicher and Schuell BA85)
- ✓ Buffer Z (60 mM Na_2HPO_4, 40 mM NaH_2PO_4, 10 mM KCl, 1mM $MgSO_4$, pH 7.0. Store at room temperature for up 1 year)
- ✓ 50 mg/ml 5-bromo-4-chloro-3-indolyl-β-D-galactoside (Eppendorf # 0032006.400)
- ✓ Whatman filter circles
- ✓ Liquid nitrogen

Procedure

1) Prepare 5-bromo-4-chloro-3-indolyl-β-D-galactoside (Eppendorf # 0032006.400) in N,N-dimethylformamide (DMF) at a concentration of 50 mg/ml. Store in dark at -20°C.
2) Patch yeast colonies to a nitrocellulose filter circle
3) Lift filter and place colony side up on a pre-cooled aluminum boat floating upon a sea of liquid nitrogen
4) After 20 seconds, immerse boat and filter for 5 seconds
5) Allow the filter to come to room temperature and place on top of Whatman filter circle that had been prewet in 3 ml of Z buffer containing 30 µl of X-gal
6) Incubate the filter for up to 5 hours. Blue coloration is indicative of β-gal activity.

4e. SPLINT TRANSFORMATION AND SELECTION

When screening a SPLINT library the bait plasmid and the SPLINT library can be introduced sequentially into L40 strain. The flowchart of the SPLINT transformation and selection is below outlined.

Screening of SPLINT:

1) Construct the "Aβ bait": a fusion of the gene encoding the target protein and the sequences encoding the lexA DNA-BD in pMICBD1. The target gene should be inserted in the correct reading frame and orientation so that a hybrid consisting of the target protein fused to the lexA DNA-BD will be expressed from this vector.
2) Verify the bait construction by restriction digestion and sequencing. If sequencing, use the MIC back and MIC for junction primers
3) Test the lexA-Aβ target bait for transcriptional activation function in the L40 reporter strain before using it in a two-hybrid screening
4) Transform the hybrid construct into L40. Use the small-scale yeast transformation protocol. Plate transformants onto YC-UKW selection medium.
5) Assay transformants on YC-UKWH and for β-galactosidase activity using the colony-lift filter assay.
6) Introduce sequentially the lexA-Aβ and SPLINT library into L40 strain: use the SPLINT scale transformation protocol.
7) Screen the His^+, Trp^+, Leu^+, transformants for β-galactosidase activity using the colony-lift filter assay. Individual blue colonies are isolated by restreaking and again assayed for β-galactosidase activity.
8) Perform colony-PCR and BstNI fingerprinting analysis onto His^+ and $lacZ^+$ colonies. Use Lyse-N-Go PCR reagent (Pierce, # 78882) to lyse colonies prior to use them for PCR.
9) Select those His^+ , $lacZ^+$ and different fingerprinting pattern colonies and isolate the plasmid scFv-VP16 DNA.

10) Transform plasmid into E.coli and plate bacterial transformant onto LB + Amp.
11) Isolate plasmid DNA from bacteria and sequence insert in the putative true positive hybrid plasmids using the VP16 antisense primer. This is primarily to confirm that the sequence you have isolated encodes a scFv cDNA.
12) Verify positive interactions by a secondary screening and finally by an independent method, such as ELISA, immunoprecipitation, immunofluorescence etc.

SPLINT SCREENING

Transformation of lexA-Aβ construct into L40 yeast strain
↓
Select on YC-UKW plates at 30°C
3 days
↓
Grow the bait culture in a 10 ml YC-UKW media overnight at 30°C
↓
Inoculate 100 ml of YC-UKW overnight at 30°C
↓
SPLINT transformation
↓
Select on YC-WHULK plates at 30°C
3 days
↓
X-gal assay
↓
«positive» interaction clones selected
↓
PCR-BstNI fingerprinting analysis
↓
Isolate scFv-VP16 yeast target DNA
↓
Transform in E.coli
↓
Isolate scFv-VP16 bacterial target DNA
↓
Co-transform scFv-VP16 plasmid DNA with lexA-Aβ bait and controls
↓
Further analysis

4f. LiAc transformation (SPLINT-scale)

This protocol should allow a higher efficiency of transformation (≅ 10^6/μg DNA).

Materials

- ✓ 1 aliquot of SPLINT/carrier
- ✓ 150 ml YC-UKW
- ✓ 2 l YPAD
- ✓ 1 l YPA
- ✓ 1.5 l YC-UKWL + 10 YC-UKWL plates (100mm)
- ✓ 1.5 l YC-WHULK + 100 YC-WHULK plates (100mm)
- ✓ 100 ml 10X TE
- ✓ 20 ml 10X LiAc
- ✓ 150 ml 50% PEG 4000
- ✓ 20 ml DMSO

Procedure

1. **Day1**: grow L40 yeast containing bait plasmid in YC-UKW O/N
2. **Day2**: inoculate 100 ml of YC-UKW with an aliquot of the overnight culture in order to find a dilution that places the 100 ml culture to logarithmic phase the next day
3. **Day3**: transfer enough overnight culture in 1 L of prewarmed to 30°C YPAD to produce an $OD_{600} = 0.3$
4. Grow at 30°C for 3 hours
5. Centrifuge the cells at 1500 X g for 5 min at room temperature
6. Wash pellet in 500 ml of 1X TE then centrifuge again the cells at 1500 X g for 5 min at room temperature
7. Resuspend pellet in 20 ml 1X LiAc, 0.5X TE and transfer to a new flask
8. Add the pretowed and mixed SPLINT/carrier DNA aliquot
9. Add 140 ml of 1X LiAc, 40% PEG 3350, 1X TE; mix and incubate for 30 min at 30ºC with gently shaking
10. Add 17.6 ml of DMSO; swirl to mix

11. Heat shock for 15 minutes at 42ºC in a water bath swirl occasionally to mix
12. Rapidly cool at room temperature cells in a water bath diluting with 400 ml YPA
13. Pellet cells by centrifugation and wash with 500 ml YPA
14. After centrifugation resuspend pellet in 1 L of prewarmed YPAD
15. Incubate for 1 hour at 30°C with gently shaking
16. Pellet cells from 1 ml; resuspend in 1 ml YC-UKWL; spread 100 µl of a 1:1000, 1:100, 1: 10 dilutions for transformation efficiency controls.
17. Pellet cells from the remaining culture
18. Wash pellet with 500 ml YC-UKWL
19. Resuspend in 1L of prewarmed YC-UKWL and incubate O/N at 30°C with gently shaking
20. **Day4:** pellet cells and wash twice with 500 ml of YC-WHULK
21. Resuspend final pellet in 10 ml of YC-WHULK
22. Spread dilutions of the total on YC-UKWL plates to compare to the number of primary transformants. This allows to calculate the number of doublings and the number of his+ colonies which should be screened to roughly cover the number of primary transformants.
23. Spread part of the remaining transformation suspension on YC-WHULK plate. Store in 30% glycerol /YC-WHULK the cotransformed library at -80°C.

4g. Plasmid isolation from yeast

1) Inoculate single, well isolated yeast transformant colonies into 5 ml of appropriate selective media at 30°C, shaking at 250 rpm until the culture is saturated (16-24 hours)
2) Spin down the culture by centrifuging at 5000 x g and resuspend cells in 250 µl of Buffer 1 containing 0.1 mg/ml RNase A; transfer the cell suspension in a 1.5 ml microfuge tube
3) Add 0.3 g of acid-washed glass beads and vortex for 5 min at room temperature
4) Spin at maximum speed for 5 min and transfer the supernatant to a new 1.5 ml microfuge tube
5) Add 250 µl lysis buffer P2 to the supernatant and invert gently 4-6 times to mix. Incubate at room temperature for 5 min.
6) Add 350 µl neutralization buffer N3 to the tube and immediately invert 4-6 times the tube
7) Centrifuge at maximum speed for 10 min
8) Transfer the cleared lysate to QIAprep spin column placed in a 2 ml collection tube by pipetting
9) Centrifuge for 1 min at maximum speed; discard the flow-through
10) Wash QIAprep spin column by adding 0.75 ml of Buffer PE and centrifuging for 1 min
11) Discard the flow-through and centrifuge for an additional 1 min to remove residual ethanol from wash buffer
12) Place QIAprep spin column in a clean 1.5 ml microfuge tube.
13) Add 25 µl of H_2O to the center of each QIAprep spin column; let stand for 1 min, and centrifuge for 1 min at maximum speed

Then transform the 1µl of extracted DNA into bacteria using electroporation and plate on LB with 100µg/ml ampicillin.

Incubate the plate overnight at 37°C. Pick several bacterial colonies and inoculate individually into 5 ml of LB containing100µg/ml ampicillin. Grow overnight at 37°C with shaking. Extract plasmid DNA from each bacterial overnight culture using QIAprep Spin Miniprep Kit according to manufacturer's instruction. Elute DNA with 50µl of elution buffer. A quick comparison of the various scFv-VP16 clones can be achieved by a gel-DNA fingerprinting method of the product on 2% agarose gels.

4h. Fingerprinting PCR bands

Each individual V region of scFv gives an own "fingerprint". Fingerprinting carried out on V genes will give a number of discrete bands. They can be carried out on V regions amplified from cDNA from individual clones.

If the fingerprinting is performed onto E.coli clones, pick one clone with a toothpick and dissolve it in 100 µl ddH_2O. Use 1 µl in PCR reaction mix. Alternatively, if the fingerprinting is performed onto yeast clones, use Lyse-N-Go PCR reagent (Pierce, # 78882) to lyse colonies prior to use them for PCR.

DNA clone	1µl
PCR buffer	2µl
dNTP 2mM	2µl
Taq	1µl
BssH2 sense	1µl
NheI antisense	1µl
ddH_2O	12µl

94°C –1 min	|
58°C –1 min	| 30 cycles
72°C –1 min	|
72°C-10 min	
4°C-24h	

Check PCR amplifications on a 1.5% agarose gel, using 3 µl each PCR reaction mix. After verification, use the other 17 µl of reaction mix for digestion:

DNAmix	17µl
BstNI (20U/µl)	0.2µl
NEB buffer 2	4µl
BSA	0.4µl
ddH_2O	18.4µl

Incubate at 60°C for 2 hours. Add 5 µl 6X gel loading buffer to each tube and load on 4% Metaphor/Nusieve TBE gel. Run 60V-120 min. A definitive comparison of the isolated scFv is obtained from DNA sequence.

The isolated AD-fusion scFv plasmids must then undergo a secondary screening, for final validation, by cotransformation with the antigen bait and, in parallel, with a control unrelated antigen vector into L40 yeast strain (Visintin, 2002, 2004). The final validation for a positive interaction is assessed testing the co-transformed yeast colonies for His and lacZ gene activation.

4i. Verification of a positive Aβ-scFv two-hybrid interaction

SECONDARY SCREENING

The final validation for a positive interaction is assessed testing the co-transformed yeast colonies for His and lacZ gene activation.

LexA-lamin encodes a lexA DNA-BD/human Lamin C hybrid and provides a control for fortuitous interaction between an unrelated Ag hybrid protein and your own scFv-VP16 selected from SPLINT.

If a positive interaction occurs between your target protein Aβ and the scFv-VP16 selected from SPLINT the results you should obtain are shown in the table below:

„bait“	„scFv-VP16“	YC selection medium	HIS3 phenotype	lacZ phenotype
lexA-Aβ	scFv-VP16	-UKWL	+	blue
lexA-Aβ	scFv-VP16	-WHULK	+	blue
lexA-lamin	scFv-VP16	-UKWL	+	white
lexA-lamin	scFv-VP16	-WHULK	/	/

4j. Western blot analysis of scFv-VP16

In order to verify that your selected scFv-VP16 should not contain a stop codon or a deletion, a western blot analysis on protein extract must be performed.

Yeast protein extracts were prepared as described before; 20µl of sample are subjected to SDS-PAGE (12% acrylamide gels), in the presence of β-mercaptoethanol, and gels are subsequently blotted onto nitrocellulose membranes (Schleicher & Schuell). For immunodetection, the monoclonal antibody anti-VP16 (BD-Clontech, #3844-1) (in 2% MPBS) is used, followed by incubation with a polyclonal anti-mouse-peroxidase conjugate (DAKO) (1:2000 in 2% MPBS).

5. Expression of scFvs anti-Aβ in bacteria for protein preparation and purification

5a. Cloning and expression of scFvs anti-Aβ for periplasmic preparation

The anti-Aβ SPLINT-selected scFvs were cloned by restriction with the enzymes BssHII/NheI into the pDAN3 vector for periplasmic expression of proteins (kindly provided by prof. Sblattero, University of Trieste). The vector allows the expression with two tags at the C-terminus: an SV5 tag and a His tag. A specific suppressor strain HB2151 *E.coli* [K12, ara Δ(lac-pro), thi/F' proA+B+, lackI^q ZΔM15] (Invitrogen) was transformed with pDAN3-scFvs constructs, and positive clones were grown in the following conditions.

Periplasmic expression of scFvs anti-Aβ

400 mL of 2*YT medium + Ampicillin were inoculated with an overnight culture at 1:100 ratio. The cultures were grown at 37°C until an OD_{600}=0.5-0.6 and then induced with IPTG 1 mM for 4.5 hours at 30°C.

The cells were harvested at 5000 rpm (Beckman). The pellet was resuspended in 10 mL of cold PPB buffer (200mg/mL sucrose, 1mM EDTA, 30mM Tris-HCl pH8), and incubated on ice for 20 minutes. Then, the sample was centrifuged at 5000 rpm for 15 minutes and the supernatant was transferred in a new tube. The pellet was resuspended in 10 mL of 5 mM $MgSO_4$ buffer and incubated on ice for 20 minutes. Then, both preparation were centrifuged at 10000 rpm for 15 minutes, the supernatant was collected and dialyzed against PBS.

Purification of the scFv from periplasm

The purification of the scFv expressed in the periplasm of *E. coli* was achieved through affinity purification on the Ni-NTA resin (QIagen). The procedure was the one indicated by the manufacturer.

Purified scFv proteins were analyzed by SDS-PAGE and by the following Blue-Comassie staining.

For the SDS-PAGE, the discontinuous system was composed by a 6 % (w/v) stacking and a 12 % or 15 % running. The samples in Laemly sample buffer with reducing agents were boiled for 3 minutes and loaded, on the gel. The gel was run at 15 mA for 2 hours.

Gels were stained with Coomassie blue [solution: 40% (v/v) EtOH, 10% (v/v) CH_3COOH, 0.1% (w/v) Coomassie blue R250] for 2-3 hours and then destained for several hours [destaining solution for protein gels: 40% (v/v) EtOH, 10% (v/v) CH_3COOH].

All the analitical Superdex-75 gel filtration chromatographic analyses were performed in collaboration with Dr. Covaceuszach, (Lay Line Genomics, Trieste).

5b. Cloning and expression of the scFv in the cytoplasm of E. coli

Cloning of the scFv

The scFvs anti-Aβ selected from SPLINT were sub-cloned into the vector pGIO1 for cytoplasmic expression in BL21(DE3)pLysS *E.coli* (Novagen). The vector pGIO1 described in the "Results section" is derived from pETM13 kindly provided by Dr. Covaceuszach, (Lay Line Genomics, Trieste).

ScFvs were cloned by restriction with the enzymes BssHII/NheI into the pGIO1, and transformed in BL21(DE3)pLysS *E.coli*.

The following protocols were kindly provided by Dr. Paoletti (EBRI, Roma) and discussed in her PhD thesis (SISSA, 2006).

Experimental procedures of cytoplasmic expression and purification of scFvs anti-Aβ were kindly performed by Dr. Visintin (LayLineGenomics, Trieste).

Expression of the scFv in the cytoplasm of *E. coli*

400 mL of 2*YT medium + Kanamycin were inoculated with an overnight culture at 1:100 ratio. The cultures were grown at 37°C until an OD_{600}=0.7-0.8 and then induced with IPTG 0.5 mM for 4.5 hours at 37°C.

The cells were harvested at 5000 rpm (Beckman) and the pellets were saved at -80°C.

Extraction, purification and refolding of scFvs anti-Aβ from cytoplasmic inclusion bodies

Buffers composition

- IB-resuspension buffer: 100 mM Tris/HCl, pH 7; 1 mM EDTA
- IB-washing buffer (Triton-IB): 60 mM EDTA; 6% (v/v) Triton X-100; 1.5 M NaCl
- IB-washing buffer: 100 mM Tris/HCl, pH 7,0; 20 mM EDTA
- IB-solubilization buffer: 100 mM Tris/HCl, pH 8; 6 M GdmCl; 10 mM EDTA; 100 mM DTT

- IB-dialysis buffer: 6 M GdmCl, pH 4; 10 mM EDTA
- refolding buffer: Tris 100mM pH 8.5, 400mM Arg, 375uM GSSG, 5mM EDTA.

The cell pellet was resuspended with resuspension buffer at 5 mL/g. Then, lysozyme was added at 1.5 mg/g, together with 3mM MgCl2 and DNaseI 50µg/mL and the sample was incubated at 4°C for 30 minutes. Finally, the cell disruption was performed *via* sonication (three pulses of 45 seconds each at 13000 micron, followed by 1 minute incubation on ice). Then, 0.5 times the volume of buffer Triton-IB was added, and the sample was incubated at room temperature for 30 minutes on a stirring plate, to disrupt the membrane elements.

The IB were then centrifuged for 10 minutes at 4°C at 10000 rpm, resuspended in 20 mL of resuspension buffer + 10 mL of Buffer Triton-IB and incubated at room temperature for 30 minutes on a stirring plate.

The IB were then centrifuged for 10 minutes at 4°C at 10000 rpm and subsequently washed three other times, each one with 40 mL of washing buffer IB. The IB pellet was then stored at -20°C or immediately solubilized.

IB solubilization

The IB pellet was resuspended with solubilization buffer at a ratio of 5 mL/g and incubated for 2 h at RT on rocking platform. Then, the pH was lowered to 3-4 by dropwise addition of HCl 1M or concentrated CH_3COOH, to avoid the oxidation of Cysteins to disulfide bridges in denaturing conditions.

The insoluble cellular elements were then removed by centrifugation at 10000 rpm and 4°C for 30 minutes.

Subsequently, the DTT was removed through a triple dialysis each one against 300 mL of Buffer Dialysis IB, each for twelve hours at 4°C.

The protein concentration was estimated with the Protein Assay from BIO-RAD (Lowry system). The solute was immediately used for renaturation or stored at -80°C.

Refolding of scFvs anti-Aβ

The pulsed renaturation was performed in 1 L of refolding buffer, at 6°C at a protein concentration of 50 μg/mL. Every hour 35 μg/mL of new protein were added to the buffer under vigorous stirring and then the stirrer was switched off. The maximum sustainable concentration of GdmHCl was of 500 mM, to avoid loss of product. After 16-48 hours after the last addition, the sample was concentrated to a volume of approximately 200-300 mL, using a cross-flow filtration system or, alternatively, with an ultrafiltration device. Finally, the sample was dialyzed for 16 hours at 4°C against Tris 20mM pH8 buffer. Smaller volumes were dialyzed, covered with PEG 35000 and left at 6°C until the desired volume was reached.

Purification of refolded scFvs anti-Aβ

The purification of the refolded scFvs anti-Aβ were achieved through two subsequent steps: an anion exchange chromatography and a size-exclusion chromatography.

The anion exchange chromatography was performed on a HiTrap Q column (5 mL – Amersham Pharmacia), equilibrated with 20 mM Tris, pH 8 as A buffer. The elution of the sample was achieved with a linear gradient from 0 to 70 % of B buffer (A buffer + 1 M NaCl).

The sample was then dialyzed against PBS and purified on a size exclusion chromatography column, a Superdex 75 (Amersham Pharmacia), equilibrated with PBS.

The purification of the refolded scFvs were achieved through a ion exchange chromatography.

The cation exchange chromatography for A13 was performed on HiTrap SP column (5 mL – Amersham Pharmacia), equilibrated with 20mM sodium phosphate buffer, pH 7 as A buffer. The elution of the sample was achieved with a linear gradient from 0 to 70 % of B buffer (A buffer + 1 M NaCl).

The cation exchange chromatography for scFvs A1, A18, Im8, B2, A19 was performed on HiTrap SP column (5 mL – Amersham Pharmacia), equilibrated with 20mM sodium phosphate buffer, pH 6.5 as A buffer. The elution of the sample was achieved with a linear gradient from 0 to 70 % of B buffer (A buffer + 1 M NaCl).

The anion exchange chromatography for Im1 was performed on HiTrap Q column (5 mL – Amersham Pharmacia), equilibrated with 20 mM Tris, pH 8.5 as A buffer. The elution of the sample was achieved with a linear gradient from 0 to 70 % of B buffer (A buffer + 1 M NaCl). The sample was then dialyzed against PBS.

The anion exchange chromatography for Im47 was performed on HiTrap Q column (5 mL – Amersham Pharmacia), equilibrated with 20 mM Tris, pH 8.5 as A buffer. The elution of the sample was achieved with a linear gradient from 0 to 70 % of B buffer (A buffer + 1 M NaCl). The sample was then dialyzed against PBS.

The cation exchange chromatography for scFvs Im3 and Im18 was performed on HiTrap SP column (5 mL – Amersham Pharmacia), equilibrated with 20mM sodium phosphate buffer, pH 6.5 as A buffer. The elution of the sample was achieved with a linear gradient from 0 to 70 % of B buffer (A buffer + 1 M NaCl).

The anion exchange chromatography for Im32 was performed on HiTrap Q column (5 mL – Amersham Pharmacia), equilibrated with 20 mM Tris, pH 8.5 as A buffer. The elution of the sample was achieved with a linear gradient from 0 to 70 % of B buffer (A buffer + 1 M NaCl). The sample was then dialyzed against PBS.

Purified scFv proteins were also analyzed by SDS-PAGE and by the following Blue-Comassie staining, as indicated for periplasmic purified proteins (see above).

6. Cloning of scFvs anti-Aβ into scFv-cyto-SV5 vector and expression in mammalian cells

The cDNA of the scFvs anti-Aβ were subcloned by restriction with enzymes BssHII/NheI into the vector scFv-cyto-SV5 (kindly provided by Dr. Visintin, LayLineGenomics, Trieste) for mammalian cells transfection, cut with the same enzymes.

The subsequent transfection of the NIH 3T3 cells was performed with standards methods, using FuGene 6 (Roche) to transfect the cells, according to manufacturers instructions.

Immunofluorescence

3T3 cells were grown in D-MEM complete 10% FBS. For immunofluorescence purposes were grown on coverslips. The cells were fixed in 4 % paraformaldheyde for 20 minutes at room temperature and then washed 3-4 times with PBS. Then, they were permeabilized for 5 minutes in 0.1 % NP40 in PBS and washed three times with PBS. A blocking step in 10 % Fetal Calf Serum (FCS) was then performed for 20 minutes at room temperature. Then, the primary antibody anti-V5 (MAb Invitrogen) was applied, at a 1:1000 dilution in 10 % FCS, for 60 minutes at room temperature. After rinsing three times with 5 % FCS, the secondary antibody, anti-mouse AlexaFluor 488 conjugated was applied, at a 1:500 dilution in 10 % FCS for 30 minutes at room temperature. Then, the cells were washed and the DAPI (Boehringer) was applied at 1:1000 in PBS (from a stock solution of 2 mg/mL) for 5 minutes at room temperature. Finally, the cells were rinsed in PBS and the coverslips mounted in Vecta-shield (Vector laboratories). The Immunofluorescence was observed with a Zeiss Axioplan microscope. Images were acquired with Nikon Coolpix 990 digital camera.

7. IN VITRO ASSAYS

7a. ELISA with coating of different aggregated forms of synthetic Aβ peptide

Wells of PVC (Corning) were coated with monomeric, fibrillar and oligomeric forms (see below note 1) of human Aβ42 peptide (Biosource) in Phosphate-buffered saline (PBS) buffer (pH 7.4) and incubated at 10μg/ml over night at 4°C.

After removing the coating solution, the wells were incubated with the primary antibodies: MAb 4G8 (1μg/ml=~6.7nM) (Signet), immune sera of mice (1:10000), scFvs anti-Aβ (25μg/ml=0.8μM) or unrelated scFv (25μg/ml=0.8μM) in 2% non-fat dry milk/PBS, for 2hrs at room temperature. Recombinant purified scFvs present a C-terminal SV5 tag, that allows to detect them using a MAb anti-SV5 (1μg/ml) (Invitrogen). Anti-mouse HRP-conjugated secondary antibody (Dako) was incubated in 2% non-fat dry milk/PBS, for 1hrs at room temperature.

Between all the incubations steps the plate was washed with T-PBS (a PBS solution containing 0.05 % of Tween-20 detergent) and PBS for three times each.

The colorimetric reaction was detected using Tetramethylbenzidine (TMB) (Pierce) after stopping with H_2SO_4 1M. The intensity of the colorimetric signals were analysed with a spectrophotometer at 450 nm using an ELISA Reader.

Notes.

1) Monomeric and fibrillar Aβ42 were prepared as described (Stine et al., 2003); Aβ42 oligomers in format of ADDLs were kindly provided by Dr. Westlind-Danielsson (University of Stockholm) and prepared following the above-mentioned protocol (Stine et al.,2003).

All the Aβ species were checked by **Western Blot analysis**, using NuPAGE bis-tris 4-12% (Invitrogen) or Criterion XT bis-tris 4-12% (BioRad). Electrophoresis was performed in MES buffer (Invitrogen, BioRad), at 200V for ~30min. Samples, in non-

reducing LDS sample buffer, were not boiled before loading. Semi-dry blotting was then performed using appropriate transfer buffer on nitrocellulose membrane 0.2µm, for ~1h.
After blotting, the membrane was incubated for 1 hour at room temperature in 5 % blocking solution of non-fat dry milk in TBS-T (0.05 % of Tween-20). Then, the membrane was incubated with the primary antibody MAb 4G8 (Signet) (1:1000) in 3 % M-TBST, for 16 hours at 4°C. After washing with TBS-T and TBS, the membrane was incubated with the secondary antibody anti-mouse HRP-conjugated (Dako).
After washing again with TBS-T and TBS, the developing was carried out with the ECL chemiluminescent system. The membrane was briefly dried and incubated for 1 minute with the developing solution (mix solution A and B of the Amersham kit) and the films were exposed for different time frames.

7b. ELISA Protocol using NeutrAvidin™ Coated Plates (Pierce)

A. Materials

- Wash Buffer: PBS-T (PBS, 0.05% Tween®-20)
- Incubation Buffer: PBS, 0.05% Tween®-20, 0.1% BSA,
- Biotinylated Aβ40/42 (Bachem) (see below, note 1) diluted in Incubation Buffer
- Primary antibodies (see below, note 2) diluted in Incubation Buffer
- HRP-labeled secondary antibody
- TMB Substrate Kit (pierce) for horseradish peroxidase

B. Method

1. Wash each well three times with 200 µl of Wash Buffer.
2. Add 100 µl of the biotinylated Aβ to each well and incubate for 2 hours at room temperature.
3. Wash each well three times with 200 µl of Wash Buffer.
4. Add 100 µl of the primary antibody to each well and incubate plate for 2 hours at room temperature.
5. Wash each well three times with 200 µl of Wash Buffer.
6. Add 100 µl of the HRP-labeled secondary antibody to each well. Incubate plate for 1hour at room temperature.
7. Wash each well three times with 200 µl of Wash Buffer.
8. The colorimetric reaction was detected using 70 µl of Tetramethylbenzidine (TMB) (Pierce) after stopping with 70µl of H_2SO_4 1M. The intensity of the colorimetric signals were analysed with a spectrophotometer at 450 nm using an ELISA reader

Notes

1) Lyophilized amyloid peptides hAβ40-biot and hAβ42-biot (Bachem) according to the manufacturer's instructions were solubilized 1mg/ml in NH_4OH 2%. For standard NeutrAvidin assays were diluted in Incubation Buffer (see above) at different concentrations (see "Results section"). For Oligomerization Assay in NeutrAvidin plates hAβ42was solubilized in Ham F12 (without phenol red) (Biosource): details of this assay are in the "Results section".

2) Anti-Aβ scFvs SPLINT selected were tested at different concentrations. For details of these and other primary antibodies, see the "Results section".

7c. IMMUNOPRECIPITATION (IP)

Materials

- RIPA buffer for immunoprecipitation: 50 mM Tris, pH 7.4, 150 mM NaCl, 1 % Triton X-100, 1 % Deoxycholate, 10 mM EDTA
- PBS: 173 mM NaCl, 27 mM KCl, 4.3 mM Na_2HPO_4, 1.4 mM KH_2PO_4
- Protein G Sepharose (Amersham)
- PAb anti-V5 (Sigma)
- MAb anti-V5 (Invitrogen)
- MAb anti-Aβ 4G8 (Signet)
- PAb anti-Aβ42 (Chemicon)
- humanAβ42 monomer (Biosource) and hAβ42 ADDLs (kindly provided by Dr. Westlind-Danielsson, University of Stockholm) (see materials in "ELISA section")

Methods

IP scFv A1+hADDLs (protocol n.1)

scFv A1:

- concentration 160ng/µl ≈ 5µM = 5 pmoles/µl
- volume 80µl =12.8µg = 400pmoles

hADDLs:

- concentration: 0.45 µg/µl = 100µM monomer Aβ = 100pmoles/µl
- volume 10µl=4.5µg= 1000pmoles

Protocol:
- coincubation A1+ADDLs for 2hrs 30min 4ºC;
- coincubation ProtG (30µl) + PAb antiV5(1µl=4µg) for 1h;
- centrifuge protG, eliminate supernatant, and resuspend in 800µl RIPA
- add to protG in RIPA, in two different eppendorf: 1) (A1+ADDLs); 2) (ADDLs)
- coincubation for1h 30 min 4ºC;
- centrifuge at 6000rpm
- wash 3 times with 500µl RIPA buffer
- Western Blot with final pellets and first supernatant (primary antibody MAb anti-Aβ 4G8)

IP scFv B2+hAβ monomer (protocol n.1)
IP scFv B2+hADDLs (protocol n.1)

scFv B2:

- concentration 160ng/µl ≈ 5µM = 5 pmoles/µl
- volume 70µl =11.2µg = 350pmoles

hAβ monomer

- concentration: 0.45 µg/µl = 100µM of monomer Aβ = 100pmoles/µl
- volume 10µl=4.5µg= 1000pmoles

hADDLs:

- concentration: 0.45 µg/µl = 100µM of monomer Aβ = 100pmoles/µl
- volume 1µl=0.45µg= 100pmoles

Protocol:
- coincubation (B2+hAβ monomer) and (B2+ADDLs) for 3hrs 4ºC;
- coincubation ProtG (30µl) + PAb antiV5(1µl=4µg) in 500µlfor 1h 30min;
- centrifuge protG, elimin sup, and resusp in 800µl RIPA
- add to protG in RIPA, in four different eppendorf: 1) (B2+ Aβ monom); 2) (Aβ monom); 3) (B2+ADDLs); 4) (ADDLs)
- coincubation for1h 30 min 4ºC;
- centrifuge at 6000rpm
- wash 5 times with 500µl RIPA buffer
- Western Blot with final pellets and first supernatant (primary antibody MAb anti-Aβ 4G8)

IP scFvB2+hADDLs (protocol n.2)

scFv B2:

- concentration 160ng/µl ≈ 5µM = 5 pmoles/µl
- volume 60µl =11.2µg = 350pmoles

MAb anti-V5

- concentration 1.3µg/µl ≈ 100µM = 100 pmoles/µl
- volume 2.5µl =3.25µg = 250 pmoles (bivalent → binding: 1Ig:2scFvs)

hADDLs:

- concentration: 0.45 µg/µl = 100µM of monomer Aβ = 100pmoles/µl
- volume 1µl=0.45µg= 100pmoles

Protocol:
- coincubation (B2+MAb antiV5) for 1h30min 4ºC;
- add protG in 400µl RIPA, incubation for 4h 4ºC;

- wash (1x), resuspend in 400µl RIPA
- incubation 1h ice;
- add ADDLs 1µl (100pmoles)
- coincubation for1h 4ºC;
- centrifuge at 6000rpm
- wash 6 times with 400µl RIPA buffer
- Western Blot with final pellets and first supernatant (primary antibody PAb anti-Aβ42)

Note: for Western Blot analysis, see details above on 7a. section of "Materials and Methods", and also on the 'Results section'.

7d. IMMUNOHISTOCHEMISTRY (IHC) on human brains

Sections of 40μm were prepared from Temporal Cortex of post-mortem human AD brains (Braak stage V-VI) and control (Braak 0-I), fixed for 24 h in 4% paraformaldehyde, then cryoprotected in sucrose 30%.

Anatomical pieces were available in SISSA laboratories at -80°C, coming from the 'Netherland Human Brain Bank'. Free-floating sections were obtained using a microtome system and stored in 0.02% sodium azide in phosphate-buffered saline. The endogenous peroxidase activity was quenched for 30 min in 3% H_2O_2. Slices were incubated in blocking-permeabilization buffer (TBS, 0.3%TritonX100, 10%FBS) for 30 min. The appropriate primary antibody (in blocking solution) was applied overnight at 4 °C, at the following concentrations: MAb 4G8 (Signet): ~2μg/ml, (dilution 1:500 of initial stock 1μg/μl); PAb anti-Aβ42 (Chemicon): ~8μg/ml (dilution 1:150 of initial stock ~1μg/μl); scFvs anti-Aβ ~50μg/ml.

Sections were washed with PBS and incubated with the appropriate secondary antibody for 1 h.

When scFvs were used as primary antibodies, the signal were detected via a sandwich of antibodies using an intermediate MAb anti-V5 (Invitrogen, 1.3μg/μl, 1:1500), or PAb anti-V5 (Sigma, 4μg/μl, 1:800) and after the appropriate secondary for IHC.

Staining was revealed with the Vector ABC peroxidase standard kit and diaminobenzidine (DAB) (0.05% or 1:500 in Tris buffer for 2 min) (kit ELITE pK6100 Vector Laboratories).

7e. IMMUNOFLUORESCENCE (IF) on human brains

For fluorescence microscopy, sections were incubated in 90% formic acid for 7 min to expose the Aβ epitope. The steps of blocking-permeabilization are similar to the IHC protocol; the sections were then incubated in the appropriate primary antibody (see IHC for concentrations) overnight at 4 °C. After the incubation (~2h) with MAb or PAb anti-V5 only for scFvs (see IHC), suitable Alexa Fluor secondary antibody (Molecular

Probes) was applied. The reduction of autofluorescence was performed by treatment with Sudan Black solution 0.8% in EtOH70%. Subsequently, sections were washed in H_2O and phosphate buffered saline, mounted on slide and coverslip with Vectashield (Vector Laboratories).

8. CELL BIOLOGY ASSAYS

8a. SHSY5Y cell cultures: neuroprotection assay

Cell Culture and Treatments

Human neuroblastoma SHSY5Y cells were maintained in Dulbecco's modified Eagles medium (DMEM) (GIBCO) supplemented with 2 mM L-glutamine and 10% (v/v) fetal bovine serum (FBS). Cells were plated at low density and grown to 80% confluency on 96-well plates at 37ºC in a humidified 5% CO_2 atmosphere incubator.

Before treatment with anti-Aβ scFvs (*E.coli* purified proteins), cells were rinsed once with serum-free DMEM media (without phenol red).

In the chronic toxicity neutralization protocol scFvs anti-Aβ, (1.5nM to 600nM), and serum-free DMEM media (without phenol red) were added to cells simultaneously for 2 hrs, followed by addition of 600 nM Aβ oligomers hADDLs directly to cells and incubation for up to 46 hr at 37ºC.

In the acute toxicity neutralization protocol, Aβ oligomers hADDLs (2.5μM) were preincubated or not with scFvs anti-Aβ (550nM) in serum-free DMEM media (without phenol red) for 2 hrs with gentle shaking at 37ºC, followed by their addition to cells simultaneously and incubation for up to 16 hr at 37ºC.

In both protocols, cells were also treated with "vehicle solutions" and with scFvs alone as internal controls.

Cell viability assays

Cell viability was determined by DNA-binding fluorochrome Hoechst 33342 (5μg/ml) (Molecular probes); cells were incubated with the dye for 10min at 37ºC in the dark, rinsed with PBS and examined with Nikon Diaphot inverted epifluorescence microscope with 20X and 40X objectives. Cells showing condensed nuclei were identified from an average of ~300 cells per treatment and cell bacht. We evaluated 1500-2100 cells per treatment. See other details in the "Results section".

Cell viability was also measured by the MTT tetrazolium salt assay (Mosmann, 1983); MTT (Sigma) solution was added to cell cultures (0.5mg/ml) and was incubated for 1-

2hrs. Medium was then removed and the cells were solubized with DMSO (Applichem). The intensity of the colorimetric signals were analysed with a spectrophotometer at 570 nm (with the subtraction of 650nm measured background) using an ELISA Reader (BioRad).

Statistical analysis

Values are expressed as mean ± SE. Statistical analysis was performed with Anova followed by Newman-Keuls test, using the software SigmaStat™. Statistical significance was accepted at the 95% confidence level ($P<0.05$).

8b. Synaptic binding assay

Cell Culture

Hippocampal cells were kindly prepared from embryonic day 18 (E18) rat pups by M.T. Ciotti (Institute of Neurobiology and Molecular Medicine, CNR, Roma), coated on poly-L-lysine (0.002%) coated coverslips, and maintained in Neurobasal with B27 supplements and L-glutamine (2.5 μM), at least 21 days *in vitro* (DIV).

When ADDLs were added, medium was changed to F12 medium (phenol-red free) with 300 nM synthetic ADDLs; in the synaptic binding blocking assay, ADDLs (300nM) were previously incubated with scFvs anti-Aβ (300-600nM), for 2hrs at 37ºC. ADDLs or ADDLs-scFvs solutions were incubated for 20min, and then gently rinsed with PBS.

Immunocytochemistry

Cells were fixed at room temperature in 1.88% formaldehyde for 5 min, followed by a post-fix for 10 min in 3.7% formaldehyde.

The coverslips were washed, permeabilized with 0.1% Triton X-100 in 10% normal goat serum and PBS (NGS:PBS) for 60 min at room temperature. Bound ADDLs were identified by incubation with the polyclonal anti-oligomer PAb A11 (Biosource) (1:1000); MAb anti-PSD95 (Chemicon) (1:700) was co-incubated overnight at 4°C. Alexa Fluor (molecular Probes) anti-rabbit and anti-mouse were used as secondary antibodies (incubation ~2 hrs at room temperature). The cells were rinsed, mounted with Vecta-Shield (Vector Laboratories) and analyzed by fluorescence microscopy (Nikon).

8c. PC12 model

Cell culture

PC_{12} cells were maintained in RPMI medium containing 10% horse serum and 5% foetal bovine serum (GIBCO). Differentiation was achieved by placing PC_{12} in Petri dishes in the presence of 10% horse serum and 5% foetal bovine serum (GIBCO) and NGF (50ng/ml) for 10-12 days. To ensure maximum bioavailability, NGF and serum were replaced every 2 days.

To induce apoptosis, cells were washed three times with PBS and one in serum free medium. Subsequently, cells were placed in serum-free media with NGF (50 ng/ml) (+*NGF*) or without NGF (-*NGF*).

Treatment with γ and β secretase inhibitors and anti-Aβ antibodies

γ (L-685,458, Calbiochem) and β-secretase (MBL) inhibitors, anti-Aβ antibodies MAb4G8 (Chemicon) and scFv A13 (*E.coli* purified recombinant protein) were tested in PC_{12} cells deprived of serum (+*NGF*) and in PC_{12} cells deprived of serum and NGF (-*NGF*) for 48 hrs with the aim of evaluating the highest non toxic concentration of each drug. γ inhibitor was used at concentrations ranging from 50 to 70nM, β-secretase inhibitor from 0,2 to 2,4 μM, Mab4G8 was used at 6.7 nM and scFv A13 in the range from 1nM to 2 nM

Treatment with TrK-a (K-252a)

A 2mM stock solution of K-252a (Calbiochem) was prepared in dimethylsulfoxide (Me_2SO) and stored in the dark at 4 °C, according to the manufacturer. For each experiment, PC_{12} cells were deprived of serum for 2 hrs using a serum free RPMI containing either the K-252a stock solution in appropriate dilution (ranging from 50nM to 200nM) or similar amounts of Me_2SO as control. In dose-response experiments, after a 2 hrs K-252a incubation, cells were washed three times and re-exposed to NGF (50ng/ml) for 48 hrs when the cell viability and extent of ThT binding release were measured.

Western blotting

Equal amounts (10-20μg) of proteins were separated on 4-12% Bis-Tris SDS-PAGE gels or 16% Tricine gels (Invitrogen), blotted onto PVDF membranes (Millipore) and incubated overnight with the appropriate primary antibody. The antibodies used was mouse monoclonal anti Aβ (6E10) from Chemicon, and anti-β-actin antibody from Sigma.

Fibrils purification procedure

Beta sheets aggregates were isolated from media of cultured cells deprived of serum and NGF for 48 hrs, following the methods previously described and adapted to the experimental conditions of this study (Matrone et al., submitted paper).
Briefly, the culture medium was centrifuged at 10.000xg for 30 min in order to remove cell debris and the supernatant was further centrifuged at 100000xg for 2h at 4°C. The resulting small pellet was first dissolved in 100 μl of 70% glass-distilled formic acid and the volume was reduced by a vacuum concentrator (speed vac) to 10μl. Finally, 90μl of Tris 2M, containing protease inhibitors, were added to the samples to a final volume of 100μl and 10μl of each sample was quantified by Bradford methods. Equal amounts of proteins were finally analysed for $A\beta_{1-42}$ by Elisa assay and by Western Blot.

ELISA

Wells of PVC were coated with Donkey anti-mouse IgG in carbonate buffer (pH 7.4) and incubated over night at 4°C. After removing the coating solution, the wells were incubated with the capture mouse anti-Aβ antibody 6E10, recognizing residues 1-17 of Aβ (Chemicon) in 5% non-fat dry milk/TBS 0.05% Tween, for 3hrs at room temperature and then exposed to 50μl of appropriately diluted samples. The quantification of Aβ was done with the polyclonal rabbit antibody $A\beta_{1-40}$ and $A\beta_{1-42}$ (Biosource) 0.5μg/ml and 1μg/ml, respectively. The values of samples were compared against those of standard curve which was generated from samples of known concentrations (0.040 to 2.0 ng/ml) of $A\beta_{1-40}$ or $A\beta_{1-42}$ and then expressed as pg/mg of total protein. To ensure accuracy,

standards (duplicate or triplicates), and blank were run with each plate The colorimetric reaction was detected using Tetramethylbenzidine (TMB) after stopping with HCl 1M.

Thioflavine T assay

Fluorescence measurements of thioflavine binding proteins were obtained, at the excitation and emission wavelength of 446 and 490nm, respectively, incubating 5 μM thioflavin T (ThT, Sigma) in 1 ml of culture medium obtained from PC_{12}. Controls were run under the same conditions with fresh, non incubated media and subtracted form experimental samples. In preliminary experiments the possible interference of phenol red on Th-T binding and absorbance were performed by incubating cells under identical experimental conditions with a culture medium devoid of phenol red. We found that optical readings did not show any significative difference both in absence and in presence of phenol red.

Statistical analysis

Values are expressed as mean ± SE. Statistical analysis was performed with Anova followed by Newman-Keuls test. Statistical significance was accepted at the 95% confidence level ($P<0.05$)

The experiments in the PC12 model were performed in collaboration with Dr. Matrone (Institute of Neurobiology and Molecular Medicine, CNR, Roma).

RESULTS

Construction of an Aβ immune SPLINT library

and IACT selections of scFvs anti- Aβ

Here we describe the design, construction, analysis and selection of a single pot library of intrabodies (SPLINT) (Visintin et al., 2004), a library of V regions assembled in the format of single chain variable Fragments (scFvs), derived from hyperimmune spleens of mice immunized with human Aβ1-42.

Moreover, we describe the first complete comparative analysis between the selection of scFvs from SPLINT immune and SPLINT naïve libraries against the same antigen (Aβ 1-42), using the Intracellular Antibody Capture Technology (IACT) (Visintin et al., 2002, 2004a, 2004b).

1. Construction of scFv library from Aβ1-42 immunized mice

1.1 Immunization of mice and screening of sera

Three mice Balb-C (6-8 weeks old) were used for immunization. Preimmune serum was taken on day 0. A total of four injections were administered (100μg antigen per animal per injection). The first injection on day 0 with equal parts (v/v) of complete Freund's adjuvant and human Aβ1-42 (2mg/ml in PBS) was performed to stimulate the production of high affinity antibodies against this antigen. The aggregation status of Aβ peptide was not checked before immunization, but we can assume that it was mainly constituted of aggregated in forms of oligomers and protofibrils, because the antigen was resuspended in PBS and incubated at 37°C before the administration. The following three boosts were carried out with equal parts (v/v) incomplete Freund's adjuvant and antigen on days 21 and 42 with an additional final boost prior to spleen removal.

The mice sera have been tested for antibodies titer by ELISA assay against Aβ peptide coating (mostly monomeric; 10μg/ml in PBS), and unrelated antigen Bovine Serum Albumin (BSA). Mice sera before immunization and sera after the first boost did not show specific immunoreactivity against human Aβ1-42: similar ELISA values were observed against Aβ and BSA (unrelated antingen) and only at low dilutions (1:1) of sera. After different boosts, mice sera have shown high increase of specific immunoreactivity against Aβ peptide. After third and fourth boost, the antibodies titer was highly significant also at 1:10000 dilutions of sera (fig.1); only one mouse did not show high immunoresponse to human Aβ and shows splenomegalic complications.

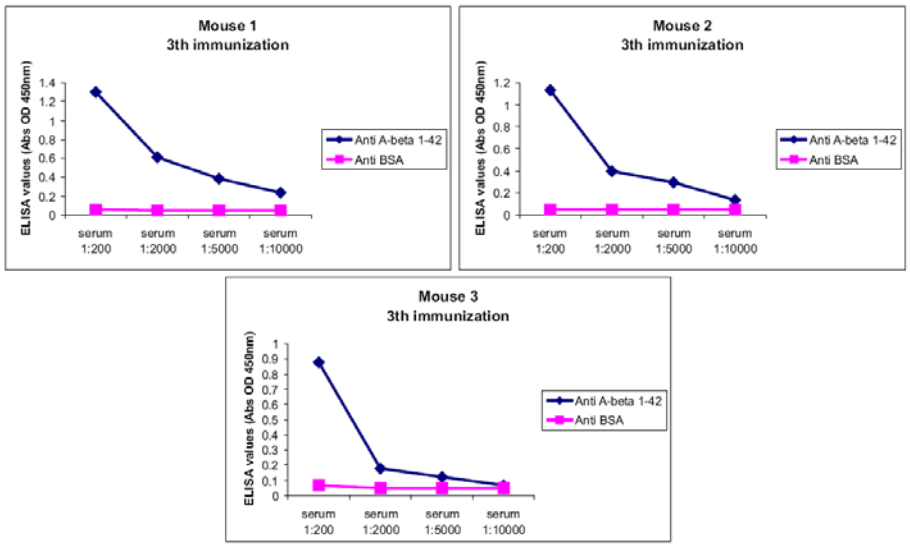

Fig.1 Titers of anti-Aβ Abs in the sera of immunized mice.

1.2 *Construction and evaluation of scFv repertoire*

The cloning scheme used to create the scFv library SPLINT immune is outlined in fig.2, and identical to scheme followed to create naïve library, described by Visintin and coworkers (2004a).

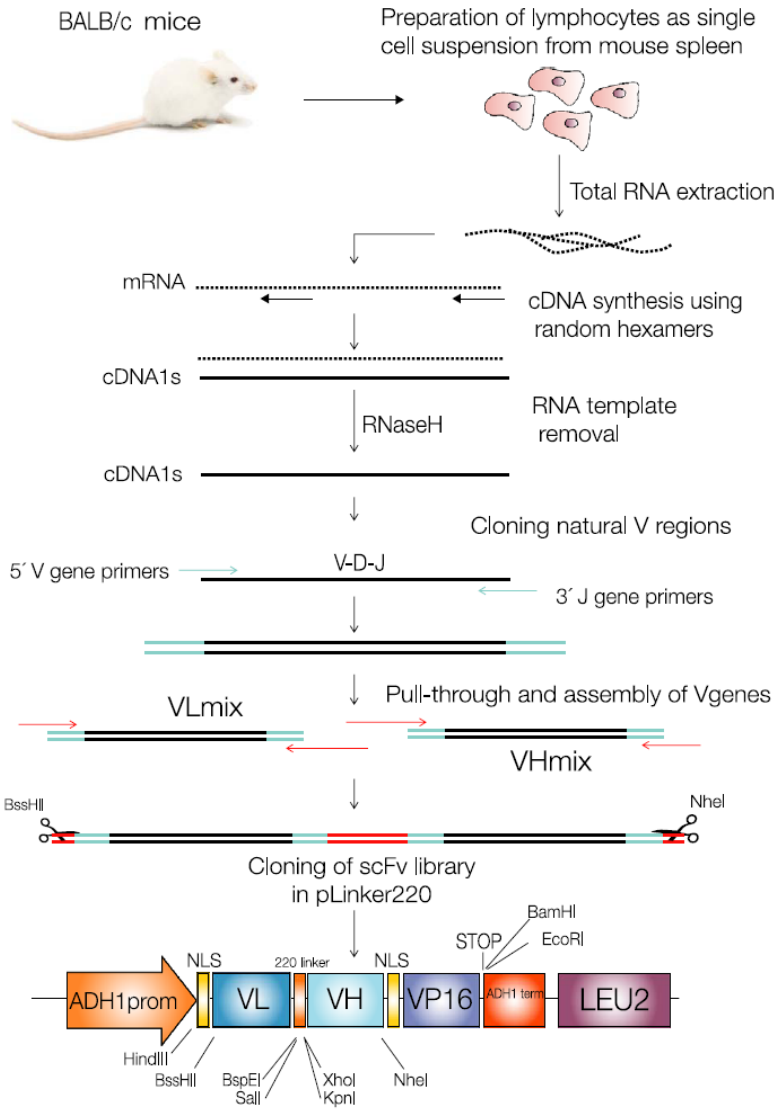

Fig.2 Construction of SPLINT library: from mice to cloning in two-hybrid vector (from Visintin et al, 2004a).

Natural V regions were cloned from total RNA extracted from lymphocytes pooled from three immunized mouse spleens.

After cDNA synthesis performed by random hexamer priming, mouse V regions were amplified (fig.3) by using a set of partially degenerated 5'and 3'mouse-specific primers (Orlandi et al., 1992), suitably re-designed (Sblattero and Bradbury, 2000).

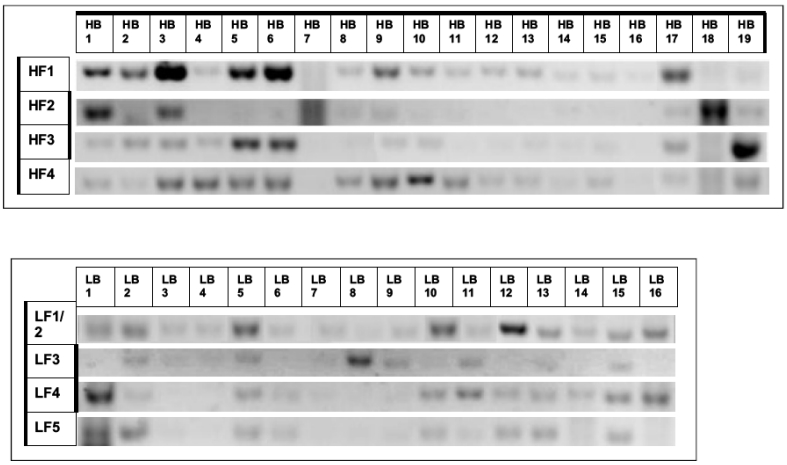

Fig.3 results of individual PCR amplifications of VH and VL regions.

V regions from cDNA were subsequently amplified, to add extra restriction sites for their assembly into scFv fragments. VH and VL gene mix were assembled together in the scFv format by overlap extension PCR (Sheets et al., 1998).

The scFv assembled library was then subcloned for expression as a VP16 fusion in pMV1 plasmid (modified version of pLinker220) kindly provided by Dr. Visintin (LayLineGenomics, Trieste) (fig.5). This cloning in pMV1 was obtained by large scale ligation and large scale transformation in electro-competent DH5αF' cells.

Large scale ligation was performed after several trials of small scale ligations in order to obtain the highest cloning efficiency: crucial was obtaining an excellent preparation of double-digested BssHII-NheI pMV1 vector, that produce the smallest number of false positive transformants carrying "empty" vector after transformation in *E.coli*. We performed large scale ligation following an optimized protocol mixing a total amount of ~400ng of pMV1 DNA and a total amount of ~250ng of "assembly scFv" cDNA. After a purification step of the ligation product, the ligated DNA was transformed in electro-competent DH5αF' cells (previously prepared and showing high efficiency of transformation: ~$6x10^9$ cfu / μg DNA). We obtained a large number of positive clones, estimated altogether in $1.7x10^6$. Cloning efficiency close to 99% was confirmed by PCR amplification of randomly isolated bacterial clones. The percentage of transformed cells with vector pMV1 lacking the insert (scFv) was less than 1%.

One hundred independent scFvs clones were randomly chosen and analyzed by separately amplifying VH and VL genes and fingerprinting them with the restriction enzyme BstNI (fig.4); the selected clones were also analyzed by sequencing. All the analyzed clones display a different sequence and fingerprinting pattern, confirming the diversity of the library. The "diversity" was estimated in 99% (percentage of different scFvs).

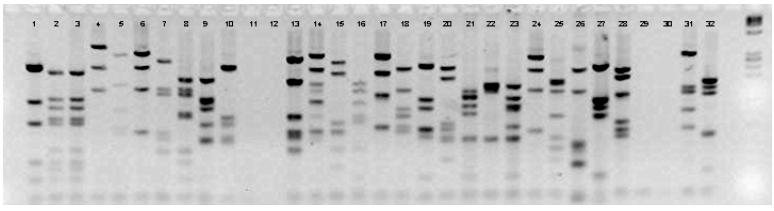

Fig.4 Evaluation of "diversity" of SPLINT Aβ immune library, by BstNI fingerprinting analysis.

Considering the high "diversity" of library, the total number of positive clones obtained from our large scale transformation in *E.coli*, estimated in $1.7x10^6$, corresponds approximately to the "complexity" of the library. The complexity of the library is the overall number of different VH and VL combinations that can obtained while constructing a scFv library.

Even if the complexity of SPLINT Aβ-immune library (~10^6 different scFvs clones per μg DNA of original non-amplified library) is lower than the complexity of SPLINT naïve library (~10^7) (Visintin et al., 2004a), it remains compatible with the efficiency of transformation threshold of yeast cells (~10^6 cfu/μg DNA). Moreover, the required diversity for selecting high affinity antigen-specific antibodies from an immune library is much lower than that required from an non-immune library.

As discussed by Visintin and coworkers (2004a), the real diversity of the library could be higher than the number of yeast transformants: this peculiarity could be achieved by yeast that express in any given cell more than one scFv. The final diversity may or may not result after further recombination events and after segregation of different scFvs in daughter cells. This latter event, could easily contribute to an increase of the real diversity by a factor ≥10 therefore, under the selective pressure of IACT, it may lead to the selective isolation of one antigen-specific scFv fragment.

Thus, we expect that immune SPLINT anti-Aβ library could be a good source of specific anti-Aβ scFvs.

The bulk DNA of the immune-library was transformed in L40 yeast cells to generate a population of scFvs-VP16 expressing yeast cells; the expression of scFv-VP16 fusion

protein and the diversity of the library were verified after selection of clones onto selective medium (–Leu = YC−UK**L**).

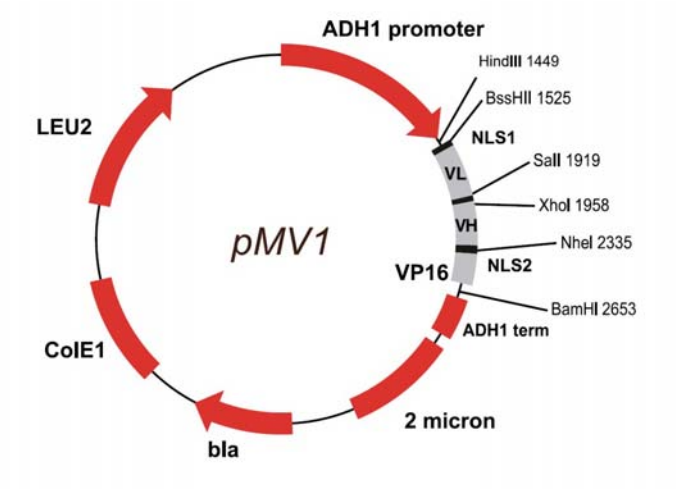

Fig. 5 pMV1, is used for expression of SPLINT library as fusion to the VP16 activation domain. The LEU2 gene allow the maintenance of the plasmid and the selection on media lacking leucine in yeast strain L40. The bla gene permits the selection of plasmid in *E.coli*. (from Visintin et al., 2004a)

2. IACT selections in yeast

2.1 Construction of human Aβ1-42 "bait"

DNA sequence coding for human Aβ1-42 was cloned (BamHI-PstI) into pMIC-BD1 (Visintin et al., 2004a, 2004b), specific vector for bait in IACT two-hybrid based system (kindly provided by Dr. Visintin, LayLineGenomics, Trieste).

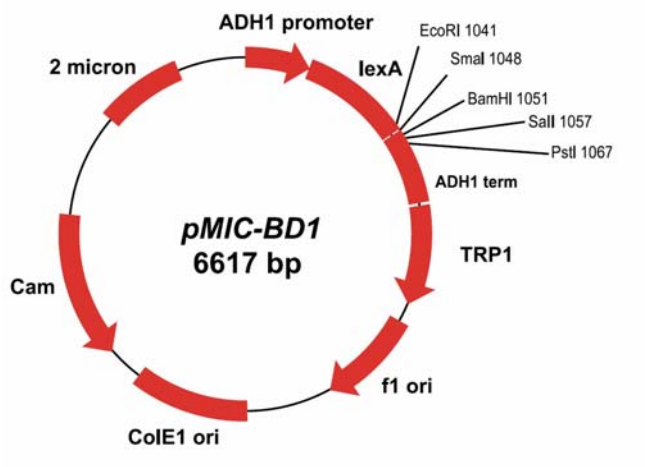

Fig.6 pMIC-BD1 uses the strong alcohol dehydrogenase promoter (ADH1) to express bait proteins as fusions to the DNA-binding protein lexA. The plasmid contains the TRP1 selectable marker and the 2μ origin of replication to allow propagation in yeast, and the chloramphenicol resistance gene (Cam) to allow the selection in *E. coli*.

We first check the expression level of the lexA fusion bait in L40 yeast cells (see Western Blot analysis in fig.7). Positive transformants carrying lexA-Aβ42 bait plasmid were selected by growth in medium lacking Trp (YC−**W**UK).

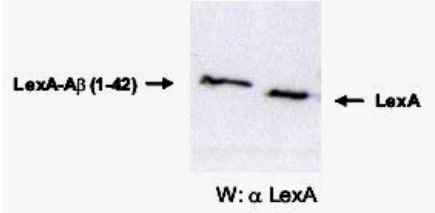

Fig.7 Western Blot analysis of LexA-Aβ42 fusion protein and LexA protein under denaturing conditions. Anti-LexA polyclonal antibody was used for the detection.

The toxicity of LexA-Aβ42 bait protein in terms of L40 viability was evaluated; Aβ42 bait showed a weak toxicity in L40 expressing cells, observing their growth and morphology in comparison with cells expressing only LexA. Finally, we have tested lexA-Aβ42 bait for unspecific trans-activation activity of the reporter genes. The Aβ42 bait plasmid was cotransformed with empty "prey" plasmid, carrying the VP16 activation domain (without any scFv). Auto-transactivation was not observed for His3 reporter gene: in fact, co-transformants can growth only in medium lacking Trp and Leu (YC −**W**UK**L**) that select for plasmids. Cotransformed yeast cells cannot growth in medium lacking Trp, Leu and His (YC −**WH**U**L**K) that select for specific protein-protein interaction, see table). Unspecific trans-activation activity was not observed for LacZ reporter gene too: in fact, Aβ42-bait and VP16-prey cotransformants that grown in medium lacking of Trp and Leu were not able to give a positive result in X-gal assay.

In conclusion, Aβ42 resulted a good bait because it is well expressed, slightly toxic and it does not transactivate reporter genes under basal conditions.

2.2 Large scale transformation of SPLINT libraries in L40

IACT primary and secondary screening

Two different screenings were performed: one using a naïve SPLINT library and the other using the above-discussed Aβ-immune SPLINT library.

The naïve SPLINT library was previously used in several selection strategies against a panel of different antigens (Visintin et al., 2004a). It shows a nominal complexity of ~10^7 different scFvs derived from V natural regions of non immunized mice.

Naïve and immune SPLINT libraries were separately introduced by maxi scale transformation into yeast cells expressing the LexA-Aβ1-42 "bait" and IACT selections were performed as described (Visintin et al., 2004a).

The transformed amount of each library was of ~500μg of plasmid DNA, a huge amount of DNA that fully represent the entire libraries (~10^7 clones for naïve library and ~10^6 clones for immune library).

Following table resumes the growth conditions for the selection of vectors and interaction of IACT-SPLINT technology using the yeast strain L40 (genotype: MATa his3D200 trp1-901 leu2-3112 ade2 LYS2::(4lexAop-HIS3) URA3::(8lexAop-lacZ) GAL4).

Table: selective media for plasmid transformation and for Aβ bait- scFv prey interaction

	Aβ bait	***scFv prey***	***Aβ bait + scFv prey***
Selection for plasmid transformation	YC −**W**UK	YC −UK**L**	YC −**W**U**L**K
Selection for interaction			YC −**WH**U**L**K

Note: L40 can grow onto –U and –K media because the lexA operator is integrated into URA and LYS markers. Using media with Ura and Lys dropped out, results in minimal background.

In the primary screening (fig.8), double transformants were selected for histidine prototropy (grown in selective medium YC −**WH**U**L**K) and lacZ activity. We have analyzed about 50 His+/lacZ+ different clones from the primary screening from naïve library and 50 different clones from the Aβ-immune library primary screening.

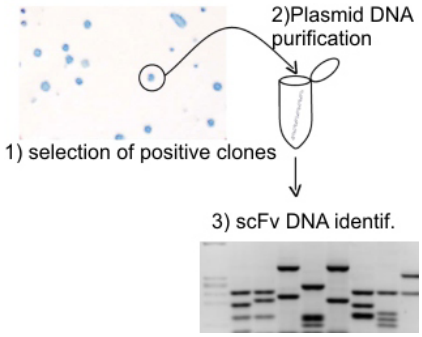

Fig.8 Primary screening: selection for histidine prototropy (in YC −**WH**U**L**K plates) and for lacZ activity of positive clones and characterization of their scFv DNA by PCR-fingerprinting.

Yeast clones selected from the primary screening were characterized for diversity (by PCR BstNI-fingerprinting) and for specificity against Aβ by a secondary screening. The secondary screening confirmed that true positives could be identified that interact specifically with the original bait, but not with other lexA fusions (lexA-lamin) (fig.9).

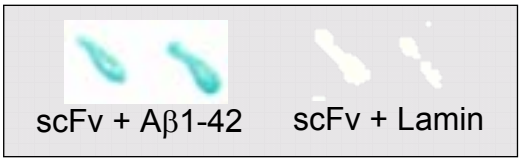

Fig.9 Secondary screening of one positive isolated clone selected from the primary screening. The plasmid coding the primarily selected scFv clone was co-transfected in L40 yeast with the plasmid coding the Aβ42 antigen (bait), or with the plasmid coding the unrelated antigen Lamin. Specific scFv clones are expected to interact only with Aβ bait.

The following tables 1 and 2, resume the results obtained from SPLINT transformations and from primary and secondary screenings of SPLINT selections.

Table 1. SPLINT selections with Aβ42 bait: efficiency of transformation of SPLINT naïve and immune libraries in L40 yeast and number of isolated positive clones from the primary screening selections (1/10 of total number of transformed yeast cells)

	cfu/μg SPLINT-DNA in L40	*No. of His3+/ lacZ+ rescued clones (I screening)*
Naïve Library	$1.2x10^6$	900
Immune Library	$1.3x10^6$	2400

Table 2. SPLINT selection with Aβ42 bait: primary and secondary screening results

	No. of His3+ / lacZ+ analyzed clones (I screening)	*No. of non specific clones (Lamin +) (II screening)*	*No. of true positive clones (Aβ+) His3+ / lacZ+ (II screening)*	*No. of uncertain positive clones (Aβ+) His3+ / lacZ− (II screening)*	*No. of different positive clones*
Naïve Library	50	15	**20**	15	**11**
Immune Library	50	1	**25**	24	**7**

Immediate interpretation of SPLINT selections results suggest that Immune Library in comparison to Naïve Library allows selection of a larger number of positive clones in primary screening.

ScFvs derived from immune library seems to be more specific because only 1/50 of the isolated scFv interacts with unrelated antigen Lamin in the secondary screening; moreover, these scFvs show stronger LacZ activation. However, the number of different

positive clones is higher from naïve SPLINT selection (11 naive scFvs versus 7 immune scFvs). In fact, a large number of true positive scFvs are highly redundant among the scFvs of the immune library screening: 3 different scFvs clones from the immune library (Im1, Im3 and Im47) represent more than 80% (Im3=10/25; Im1=5/25; Im47=5/25) of the total true positive clones.

From Naïve and Immune Libraries we have selected a panel of 18 different scFvs: 11 of them from naïve SPLINT library (A1, A2, A5, A7, A9, A13, A18, A19, B2, B15, B21) and 7 from immune SPLINT library (Im1, Im3, Im8, Im11, Im18, Im32, Im47).

Following tables (3 and 4) resume detailed properties of the selected anti-Aβ scFvs on differential modulation of reporter genes (His3 and LacZ).

Table 3: differential activation of reporter genes (His3 and LacZ) by naïve scFvs-Aβ bait interaction

	A1	***A2***	***A5***	***A7***	***A9***	***A13***	***A18***	***A19***	***B2***	***B15***	***B21***
-His selectivity	+	±	±	±	±	+++	++	±	+	+	++
-His growth	++	+	+	+	+	+++ +	++	+	+	+	++
LacZ activation	++	+	+	+	+	++	++	+	++	+	++

Table 4: differential activation of reporter genes (His3 and LacZ) by immune scFvs-Aβ bait interaction

	Im1	***Im3***	***Im8***	***Im11***	***Im18***	***Im32***	***Im47***
-His selectivity	++	+++	+++	++	+	+	±
-His growth	+++	++++	++	+	++	+++	+++
LacZ activation	+++	++++	+	+++	++	++	++

The stringency of histidine prototropy is lower than LacZ activation and a basal growth in –His is often possible also for unspecific interactors as scFv-lamin. In the table –His selectivity indicate the specificity of His3 reporter gene activation by scFv anti-Aβ interactors. Some scFvs, as A13, Im3 and Im8, are highly specific showing excellent selectivity for Aβ bait.

Normally, most of the clones that grow in the absence of histidine give a strong reaction in the X-Gal assay. ScFvs anti-Aβ determine a differential activation of the reporter genes; for instance, Im8 induce a strong and specific His growth activation but it is a weak activator of LacZ; in general, naïve scFvs gave a lower and slower reaction in the X-Gal assay respect to scFvs isolated from immune library. Further considerations are presented in the section regarding In Vivo Epitope Mapping (IVEM) characterization.

In conclusion, primary and secondary screenings of Naïve and Immune SPLINT Libraries allowed to select a panel of 18 different scFvs anti-Aβ42.

Preliminary observations suggested that there is a higher specificity and selectivity of the immune library in the *in vivo* selection against Aβ antigen. In order to obtain a complete

comparative analysis of scFvs from naïve and immune SPLINT libraries, further characterizations such as in vivo epitope mapping, sequence analysis, *in vitro* binding of synthetic and naturally produced antigen and *in vitro* modulation of Aβ-induced cell toxicity will be afterwards discussed in the next chapters.

3. In Vivo Epitope Mapping (IVEM)

For most practical purposes, an epitope is easy to define as part of an antigen involved in its recognition by an antibody. The term "epitope mapping" is usually applied to protein antigens, and is the process of locating the epitope on the protein surface or in the protein sequence. It is essential to distinguish between conformational ("discontinuous", "assembled") epitopes, in which amino acids far apart in the protein sequence are brought together by protein folding, and linear ("continuous", "sequential") epitopes, which can often be mimicked by simple peptide sequences. In order to determine the major sites recognized by selected antibodies on the Aβ1-42 surface, we applied the in vivo epitope mapping (IVEM) (Visintin et al., 2002). This method allows to produce in a very easy way an epitope map of the protein antigen used for the SPLINT selection applying the same IACT technology. To this aim we design a 'linear mapping' approach using baits that are C-terminal deletion mutants of human Aβ1-42: Aβ1-40, Aβ1-28, Aβ1-17 and Aβ1-10 (see fig.1).

$D_1AEFR_5HDSGY_{10}$

$D_1AEFR_5HDSGY_{10}EVHHQKL_{17}$

$D_1AEFR_5HDSGY_{10}EVHHQKLVFF_{20}AEDVGSNK_{28}$

$D_1AEFR_5HDSGY_{10}EVHHQKLVFF_{20}AEDVGSNKGA_{30}IIGLMVGGVV_{40}$

$D_1AEFR_5HDSGY_{10}EVHHQKLVFF_{20}AEDVGSNKGA_{30}IIGLMVGGVV_{40}IA_{42}$

Fig.1 sequences of the C-terminal deletion mutants of human Aβ42 used in IVEM

ScFvs are also tested by IVEM against deletion mutants of rodent baits (Aβ1-42, Aβ1-28, Aβ1-17, Aβ1-10): rodent Aβ has three different residues (5R>G, 10Y>F, 13H>R) in the

N-terminal portion of the peptide (fig.2); these changes are responsible for different biochemical and biophysical properties of the mouse Aβ peptide (Fung J. et al. 2004).

Fig.2 Sequence of human and murine Aβ42 with amino acid changes indicated.

Fig.3 Schematic colored representation of deletion mutants of human and rodent Aβ42 tested in IVEM with scFvs anti-human Aβ42.

The choice of the above-mentioned deletion mutants has been justified by the processing, folding and immunogenic properties of the Aβ peptide. In fact:

- Aβ1-10 represents the most unstructured portion and the most immunogenic part of Aβ peptide in immunizations; it is also involved in packaging and lateral aggregation.

- Aβ1-17 is naturally generated in the processing of APP by cleavage of α-secretase (C-term) and β-secretase (N-term);

-Aβ1-28 is the beginning of the second β-sheet (28-40/42), after the hairpin loop connecting with the first β-sheet (1-23) in the β- structured peptide model

-Aβ1-40 represents the most important alternative product of γ-secretase cleavage.

From the panel of the selected 18 scFvs, we have chosen five naïve scFvs (A1, A13, A18, A19, B2) and six immune scFvs (Im1, Im3, Im8, Im18, Im32, Im47), for the in vivo epitope mapping with the above-mentioned baits.

The results of IVEM are summarized in the following tables:

	human Aβ1-10	***human Aβ1-17***	***human Aβ1-28***	***human Aβ1-40***	***human Aβ1-42***
A1	−	−	±	+	+
A13	−	−	−	+	+
A18	−	−	−	±	+
A19	−	−	−	+	+
B2	+	+	+	+	+
Im1	+	+	+	+	+
Im3	+	+	+	+	+
Im8	−	−	−	+	+
Im18	−	−	−	±	+
Im32	+	+	+	+	+
Im47	+	+	+	+	+

	rodent Aβ1-10	***rodent Aβ1-17***	***rodent Aβ1-28***	***rodent Aβ1-42***
A1	−	−	−	+
A13	−	−	−	+
A18	−	−	−	+
A19	−	−	−	+
B2	+	+	+	+
Im1	+	+	+	+
Im3	+	+	+	+
Im8	−	−	−	+
Im18	−	−	−	+
Im32	+	+	+	+
Im47	+	+	+	+

SPLINT-selected anti-Aβ scFvs are able to recognize either human and murine Aβ deletion mutants in IVEM format, showing the same pattern of epitopes recognizition for both Aβ species.

From IVEM analysis, two family of non overlapping epitopes specific scFv can be distinguished:

1. scFvs recognizing Aβ1-10 N-terminal domain
2. scFvs recognizing Aβ1-40/42 C-terminal domain. The IVEM analysis shows that only A1 recognizes very weakly (in terms of LacZ activation) Aβ1-28, This is probably because it recognizes one epitope spanning partially this region.

In a simplistic way, we can consider the second category of scFvs as recognizing the C-terminal (28-42) part of Aβ; but, in the light of the complex folding of Aβ peptide, it is more correct to say that the portion 28-42 of Aβ is essential for anti-Aβ binding. The distribution of Aβ epitopes recognized surely is not casual, showing a clear enrichment in two clusters (fig.4). It is very interesting to note that scFvs derived from the naïve SPLINT library recognize in a higher proportion the C-terminal part of Aβ, while the pool of scFv from the immune SPLINT library are enriched in N-terminal binders (fig.4).

Fig.4 Scheme of two principal epitopes recognized by SPLINT-selected anti-Aβ scFvs.

The absence, or the lower overall representation of same epitope specificity might be due by different reasons:

1. Lack of scFvs, in naïve SPLINT libraries, recognizing particular epitopes, as notably the N-terminal epitope (*library hypothesis*);
2. Difficult exposure of non recognized epitopes on LexA-Aβ bait, motivated by its folding or by its aggregation into the yeast cytoplasm and nucleus (*conformational hypothesis*).

Probably both the hypotheses contribute to the observed epitope distribution.

The libraries naïve and immune are not equally representative in terms of epitope pattern recognition. In particular, as above-observed, a large part of immune scFvs recognizes N-term of Aβ: >90% of total, considering the high redundancy of this library. This result is in accordance with the immunization protocols performed in humans and in animals, and suggests that immunization with Aβ peptide provides a "directed evolution" of V regions, biasing their binding specificity toward N-terminal Aβ residues.

After immunization with Aβ peptide, most of the B-cells produce antibodies which recognized epitopes reside in the amino-terminal region of the peptide (Schenk D, et al, 2004).

"After immunization with Aβ, the peptide is processed by antigen-presenting cells in the periphery and then presented to T and B cells. Epitope mapping of these events following Aβ immunization in AD patients indicates that the predominance of T-cell epitopes lies in the central to carboxy-terminal region of the Aβ peptide. This agrees with the dominant Aβ T-cell epitope region identified in nontreated AD and control elderly individuals. By contrast, most of the B-cell or antibody producing epitopes detected from immunized patients reside in the amino-terminal region of the peptide. The latter point is reinforced by the observation that most anti-Aβ mouse monoclonal antibodies that have been produced are directed to the first 16 amino acids of the peptide. (Schenk D, et al, 2004)."

However, in the SPLINT libraries, because of the recombinant random assembly of VL and VH genes, do not reproduce the original VL-VH pairing observed *in vivo*, thus the particular combinations of VL and VH determine the binding properties of these SPLINT selected scFvs. Therefore, it is noteworthy that scFvs selected from immune SPLINT library show the observed and above-discussed epitope specificity.

In order to explain the non-random distribution of epitopes recognized by SPLINT-selected scFvs, we hypothesized also a conformational exclusion of some epitopes on the surface of the peptide ('conformational hypothesis'). A lot of structural data described models of Aβ42 peptide, in which its N-terminal part (Aβ1-10) is unstructured thus, the remaining portion of Aβ is crucial for the formation of β-structures (Petkova A., et al, 2002). Hypothesizing similar conformation for Aβ, as C-terminal portion of LexA-Aβ fusion protein, Aβ1-10 and Aβ28-42 could be the most exposed regions, available for interactions with scFvs.

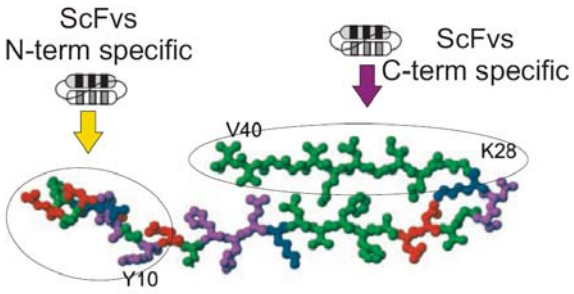

Fig.5 Structural model of Aβ40 monomer (modified from Petkova et al, 2002) and hypothesis of conformational epitopes exposure.

Aβ baits - scFv interactions: differential activation of reporter genes

As discussed above, different scFvs anti-Aβ determine distinct activation of the reporter systems (His3 and LacZ). In the light of IVEM results, we can observe that the best activators of the reporter LacZ gene for Aβ baits are scFvs Im1, Im3, Im32 and Im47 (specific for N-terminal epitope). Thus, scFvs specific for the C-terminal or recognizing conformations of whole peptide, gave a lower and slower reaction in the β-Gal assay; this is not a peculiarity of naïve scFvs because also Im8 and Im18 (C-terminal specific) show similar properties.

These observations could be in accordance with above-hypothesized conformations *in vivo* of Aβ42 bait (even if the peptide is fused with lexA as C-terminal fusion protein). β-structured (and probably aggregated) Aβ, interacting with the C-terminal specific scFvs, could interfere to the assembly of functional transcription machinery. Thus, the N-terminal specific scFvs, interacting with epitopes of Aβ baits not showing steric hindrance problems, could favour activation of reporter genes and give healthy phenotype in yeast cells.

4. Sequence analysis of scFvs clones

As above discussed, we have selected a panel of 18 different anti-Aβ scFv clones from naïve and immune SPLINT libraries. DNA sequence of each scFv clone shows the recombinant format VL-linker-VH. In particular, two Nuclear Localization Signals (NLS 1 and 2) are flanking the 5' and 3'of each scFv clone (5'_NLS1-VL-linker-VH-NLS2_3') in pLinker220 or in pMV1 plasmids used in IACT technology; moreover, scFv DNA is fused at 3' with the sequence of the Activation Domain (AD) VP16.

DNA clones were sequenced using specific sense and antisense primers for sequencing reactions.

For the analysis, scFv nucleotide sequences were translated and the conserved Variable regions (VL and VH) of antibodies were analyzed.

We performed multi-alignment analyses of scFvs aminoacidic sequences by ClustalW software.

The aim of this analysis was the following:

1. comparative analysis of the naïve variable regions versus the immune variable regions of the isolated scFvs
2. identification of "consensus sequences for the binding site", in the Complementary Determining Regions (CDRs)

Clustal W alignments allowed the identification of CDR regions in accordance to Kabat numbering scheme for variable regions of immunoglobulins superfamily.

ScFvs protein sequences were analyzed by ClustalW program version 1.83 (available online on the website of the European Bioinformatics Institute (EBI-EMBL): http://www.ebi.ac.uk/clustalw) that automatically align many sequences with a profile-based progressive alignment procedure.

ClustalW output files are:

1. score tables, obtained by pairwise alignments (all sequences are compared to each other);
2. multiple sequence alignments, showing aligned text of the sequences and their aminoacidic identities, similarities and gaps;
3. cladogram or phylogram tree, constructed describing the "progressive groupings" of the sequences by similarity.

In order to have a complete characterization of scFvs sequences we performed CLUSTAL W analysis on the following subgroups:

- all complete sequences: scFvs naïve and scFvs immune;
- only scFvs naïve;
- only scFvs immune;
- only VH of all scFvs;
- only VL of all scFvs.

Here we show exemplifying ClustalW analysis output files of 15 out of all 18 scFvs sequences, starting from the "score tables" obtained by pairwise alignments.

1. Score table

SeqA	Name	Len(aa)	SeqB	Name	Len(aa)	Score
1	Im1	252	2	Im3	253	79
1	Im1	252	3	Im8	254	62
1	Im1	252	4	Im47	252	96
1	Im1	252	5	Im18	253	78
1	Im1	252	6	Im32	253	84
1	Im1	252	7	A1	249	64
1	Im1	252	8	A2	252	55
1	Im1	252	9	A5	250	56
1	Im1	252	10	A7	254	76
1	Im1	252	11	A11	253	67
1	Im1	252	12	A13	238	63
1	Im1	252	13	A18	248	75
1	Im1	252	14	A19	237	66
1	Im1	252	15	B2	252	66

[...]

We show only exemplifying scores concerning the sequence of scFv Im1 compared with each other scFv sequence: for instance, the comparison between Im1 and Im3 (first row) gives the score of 79 (calculated on the basis of aminoacidic identities, similarities and gaps) that is a good score of similarity. The highest score of similarity, equal to 96, is obtained comparing Im1 and Im47: in fact, analyzing their sequences, they show only 6 different aminoacids.

The second output file generated by ClustalW is the multiple sequence alignment, showing aligned text of the sequences and their aminoacidic identities (indicated with *****), similarities (indicated with **:** and **.**) and gaps (indicated with −). In the fig.1 we show the exemplifying alignment of the first 55-60 residues of VL regions of the 15 analyzed scFvs.

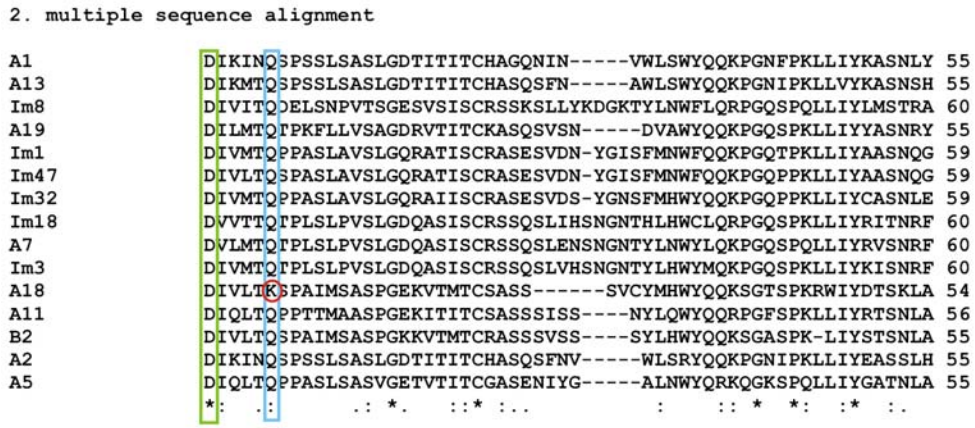

Fig.1 Multiple sequence alignment output file: the green box points out an example of identities (*****), the box points out (with only one aminoacid different between all scFvs) an example of strong similarity (**:**).

The Cladogram or Phylogram trees, at the end of the output file, are representations of a complex Guide Tree that lists all the distances between the sequences, the number of alignment positions used for each, the sequences joined at each alignment step and the branch lengths (data not shown).

We used the third output file generated by Clustal W analysis in the format of the Cladogram tree, only to have a validated representation of the distribution and the "derivation" of clusterized subgroups and individual scFvs.

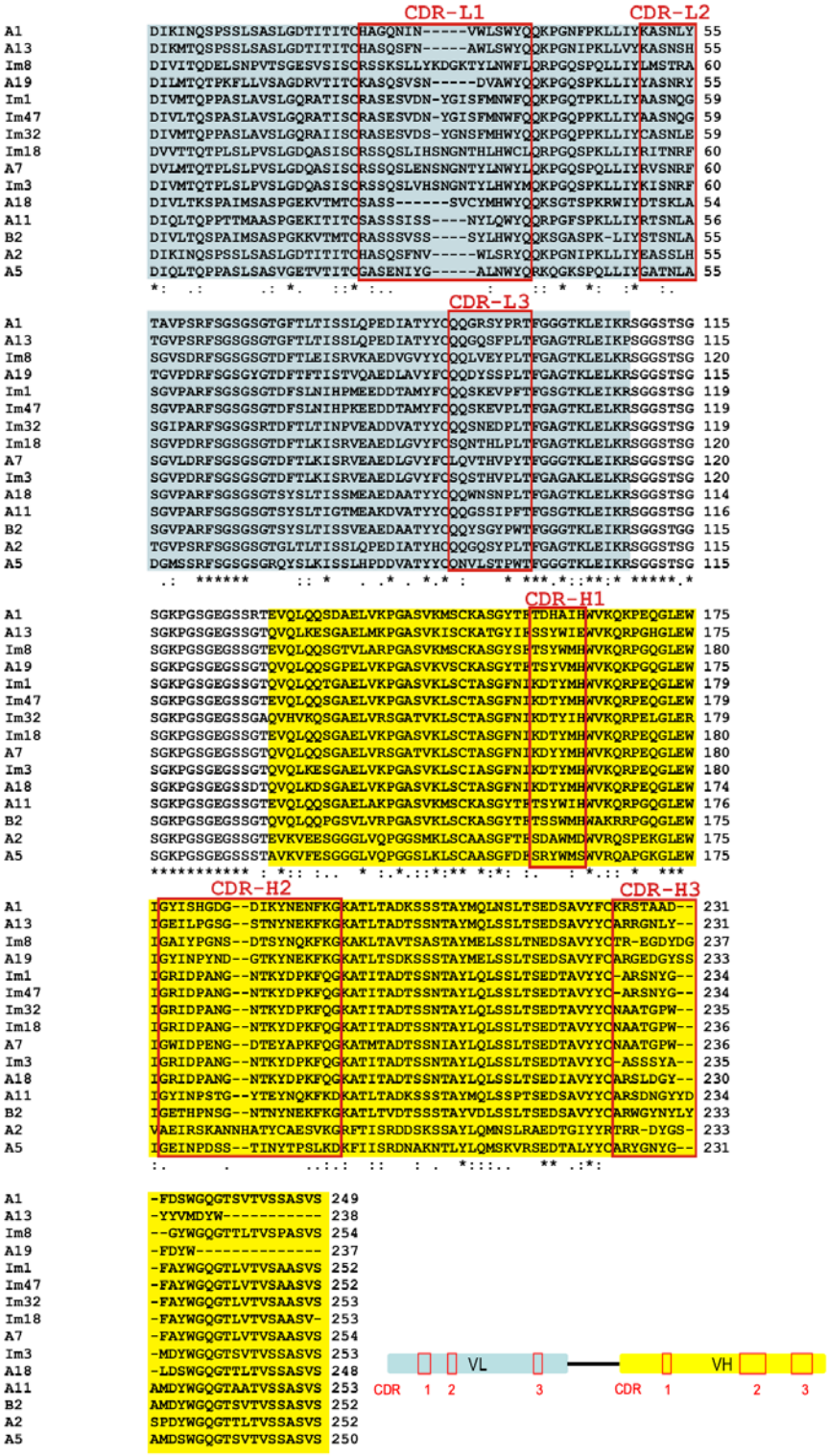

Fig.2 multiple alignment of 6 scFvs immune and 9 scFvs naïve; variable regions VL and VH are highlighted in blue and yellow respectively, CDRs are boxed in red.

The comparison of all sequences gives a first general overview on the diversity or similarity among the scFvs. Multiple alignments show critical residues that are highly conserved and the regions with the highest variability corresponding to the CDRs (see fig. 2).

Between Naïve and Immune subgroups, the latter shows the highest degree of identities (supplemented fig.1).

The Cladogram visualizes the distances between all sequences. All scFvs (except Im8) derived from immune SPLINT, clusterize in a subgroup that is highly conserved (fig.3). This result may be in accordance with an oligoclonal response obtained by the immunization.

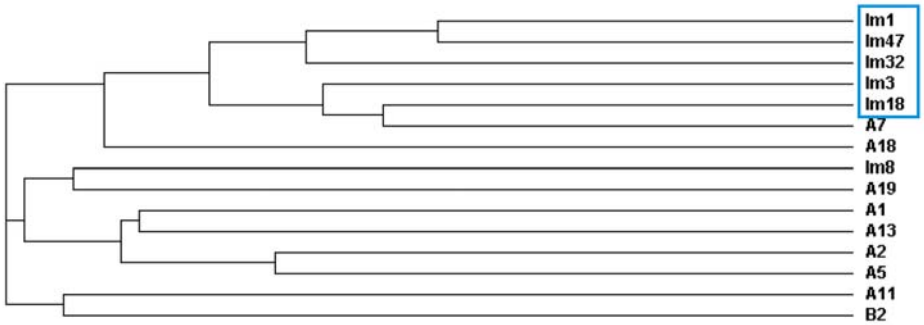

Fig.3 A large part of scFvs immune (blue box) clusterize in a subgroup highly conserved.

Differential analysis of VL and VH regions of the scFvs provides a further level of analysis. We focused on the analysis of the 11 scFvs (A1, A13, A18, A19, B2, Im1, Im3, Im8, Im18, Im32 and Im47) that were better characterized *in vitro* and by IVEM.

The highest variability in VL and VH regions is in CDRs, therefore their sequence analysis is highly relevant. All VH regions of the examined immune scFvs (except Im8)

are highly similar; CDRs-H2 are identical (GRIDPANGNTKYDPKFQG) and CDRs H1 are highly conserved (KDTYMH, except Im32 that has KDTYIH). Interestingly, the VH region of scFv A18, even though selected from the naïve SPLINT library, is very similar to an immune scFv, being its CDRs H1 and H2 identical to the above-mentioned sequences.

ScFvs Im1 and Im47 show identical CDR H3 (ARSNYGFAY) as well as Im18 and Im32 (NAATGPWFAY) explaining the sub-clusterization visualized in cladogram of VH regions (fig.5)

VH regions of naïve scFvs and their CDRs, except A18, show high variability in comparison to immune scFvs.

Table : CDRs of the VH regions of analyzed scFvs

ScFv	CDR H1	CDR H2	CDR H3
Im1	KDTYMH	GRIDPANGNTKYDPKFQG	ARSNYGFAY
Im47	KDTYMH	GRIDPANGNTKYDPKFQG	ARSNYGFAY
Im3	KDTYMH	GRIDPANGNTKYDPKFQG	ASSSYAMDY
Im32	KDTYIH	GRIDPANGNTKYDPKFQG	NAATGPWFAY
Im18	KDTYMH	GRIDPANGNTKYDPKFQG	NAATGPWFAY
Im8	TSYWMH	GAIYPGNSDTSYNQKFKG	TREGDYDGGY
B2	TSSWMH	GETHPNSGNTNYNEKFKG	ARWGYNYLYAMDY
A18	KDTYMH	GRIDPANGNTKYDPKFQG	ARSLDGYLDS
A13	SSYWIE	GEILPGSGSTNYNEKFKG	ARRGNLYYYVMDY
A19	TSYVMH	GYINPYNDGTKYNEKFKG	ARGEDGYSSFDY
A1	TDHAIH	GYISHGDGDIKYNENFKG	KRSTAADFDS

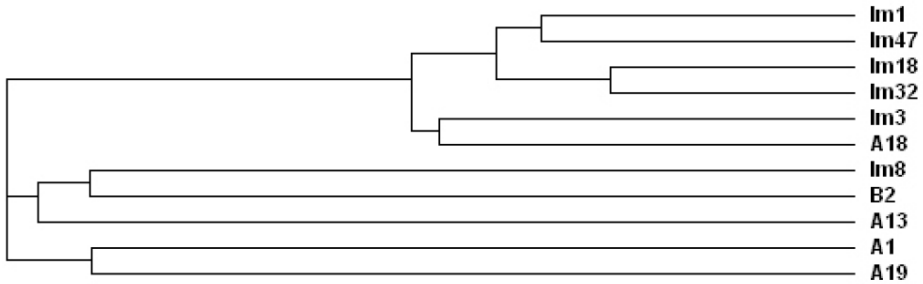

Fig.4 The Cladogram of the VH regions of 11 different analyzed scFvs.

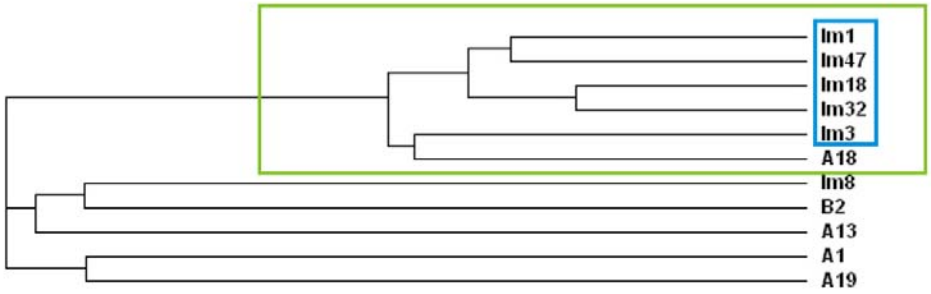

Fig.5 The VH regions from naïve scFv A18 and the VH regions from the scFvs isolated from the immune SPLINT (box blue) (except Im8), clusterize in one distinct subgroup (green box).

Cluster distribution of VL regions is different in comparison to cluster distribution of VH regions. VL of immune scFvs, for instance, clusterize in two different and distant subgroups: (Im1, 47, 32) and (Im3, 18, 8) (fig.7). VL region of Im8, similarly to its VH region, is the sequence less related to other immune scFvs.

Identities and similarities of CDRs sequences explain the distances of the branches of the cladogram tree. CDRs from Im1, Im47 and Im32 VL regions are highly related; in particular, CDRL1 (RASESVDNYGISFMN) and CDRL2 (YAASNQGS) are identical in Im1 and Im47 and their CDRL3 are highly conserved (QQSKEVPxT). CDRs L1-2-3 of Im32 are closely related to Im1 and Im47. CDRs from Im3 and Im18 VL regions are highly similar to a specific consensus (CDR L1: RSSQSLxHSNGNTxLH CDR L2: YxIxNRFS; CDR L3: SQxTHxPLT).

VL regions from naïve scFvs show a high diversity; A1, A13, A18 and B2 cluster appears to be derived from the same node generating the branch of Im1,47,32, confirming the different distribution of the VL regions comparing the VH regions (fig.7).

Table : CDRs of the VL regions of analyzed scFvs

ScFv	CDR L1	CDR L2	CDR L3
Im1	RASESVDNYGISFMN	YAASNQGS	QQSKEVPFT
Im47	RASESVDNYGISFMN	YAASNQGS	QQSKEVPLT
Im32	RASESVDSYGNSFMH	YCASNLES	QQSNEDPLT
Im3	RSSQSLVHSNGNTYLH	YKISNRFS	SQSTHVPLT
Im18	RSSQSLIHSNGNTHLH	YRITNRFS	SQNTHLPLT
Im8	RSSKSLLYKDGKTYLN	YLMSTRAS	QQLVEYPLT
B2	RASSSVSSSYLH	YSTSNLAS	QQYSGYPWT
A18	SASSSSVCYMH	YDTSKLAS	QQWNSNPLT
A13	HASQSFNAWLS	YKASNSHT	QQGQSFPLT
A19	KASQSVSNDVA	YYASNRYT	QQGQSYPLT
A1	HAGQNINVWLS	YKASNLYT	QQGRSYPRT

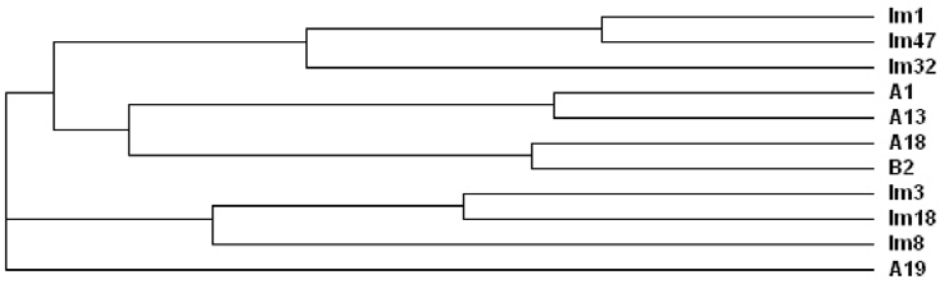

Fig.6 Cladogram of the VL regions of 11 different analyzed scFvs.

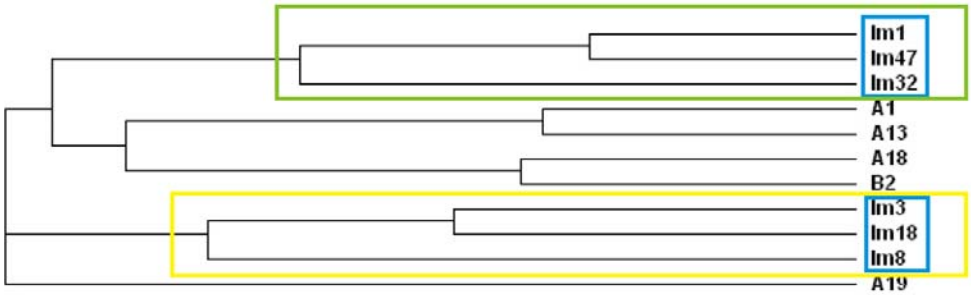

Fig.7 The VL regions from immune scFvs (blue boxes) clusterize in two different and distant subgroups: (Im1, 47, 32) (green box) and (Im3, 18, 8) (yellow box).

Detailed analysis of the CDRs confirms high similarities among the immune scFvs and the different cluster distribution of VL and VH regions.

Only scFvs Im1 and Im47 seem to derive from the same original paring of VL and VH regions; all the other scFvs, as expected, present different VL-VH pairing.

In the following figure, the cladogram generated by alignment of complete sequences of the above-mentioned 11 scFvs, allows to identify two functionally related subgroups, defined on the basis of the source of the library (immune scFvs) or of the binding properties of the isolated scFvs (C-terminal specific scFv).

We were unable to identify any consensus sequence in the analyzed scFv for the Aβ binding sites, not even linked to epitope specificity (C-terminal *versus* N-terminal). In fact, CDRs from C-terminal specific scFvs are highly diverse; moreover, B2, naïve scFv N-terminal specific, does not show a high similarity with Im1, Im3, Im32 and Im47 (that are also N-terminal specific); in addition, CDRs sequences of the immune scFv Im18 (C-terminal specific) are highly similar to that of immune N-terminal specific scFvs.

Further characterizations of the scFvs sequences will focus on the comparison between the available VL and VH sequences and other scFvs or anti-Aβ antibodies.

5. Production of scFvs as recombinant proteins in *E.coli*

ScFvs were expressed as recombinant proteins in *E.coli* using two different protocols optimized for periplasmic or for cytoplasmic expression. Periplasmic expression allows the purification of scFvs in native conditions from periplasmic space of *E.coli*; the production yields are very poor in comparison with the cytoplasmic production of recombinant proteins, especially that from inclusion bodies. SPLINT selected scFvs, are readily folded and stable in the yeast cytoplasm thus are good candidates for the cytoplasmic expression in *E.coli*.

ScFvs cDNAs were subcloned from yeast expression vector into prokaryotic expression vectors. In particular we used, for the expression in the *E.coli* periplasm, the plasmid pDAN3 (kindly provided by Prof. Sblattero, University of Trieste) and, for the expression in the *E.coli* cytoplasm, we modified the plasmid pETM13 (kindly provided by Dott. Covaceuszach, Lay Line Genomics, Trieste). One advantage of the latter system is that in many cases the target protein accumulates in the cytoplasm to such high levels that it constitutes a high percentage of the total cell protein. Therefore, it is relatively straightforward to isolate the protein in few chromatographic steps by conventional methods.

5.1 Periplasmic expression

The phagemid pDAN3 (fig.1) allows the expression of scFv under the control of a LacZ promoter inducible by IPTG (isopropyl β-D-thiogalactoside) with the secretion of the recombinant protein in the periplasmic space being directed through a PelB leader sequence at the N-terminus of the scFv; the expressed scFv carried also two peptide tags (SV5 and His6) at the C-terminus.

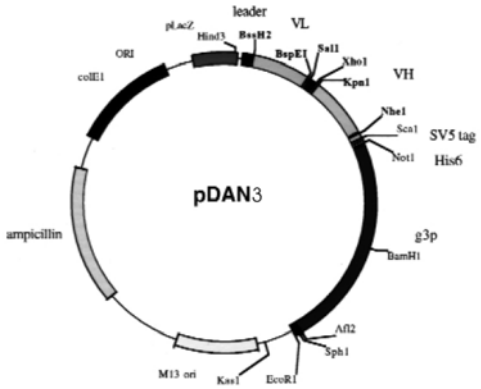

Fig.1 pDAN3 vector used for the periplasmic expression of scFvs in HB2151 *E.coli* strain.

A general protocol provides that transformed HB2151 *E.coli* were IPTG induced for 4h; the scFvs were purified from the isolated periplasmic fraction by affinity chromatography with NiNTA™ Agarose resin.

The yields of the purified scFvs are highly variable but generally are very low. The following table resumes the obtained final concentrations of purified scFvs and the total amount of protein per initial volume of culture. scFv αTL111 is a SPLINT derived unrelated scFv used as a control.

	Concentration of purified scFv	***Amount of scFv for ml of starting culture***
scFv A1	170 ng/µl	425 ng/ml
scFv A13	85 ng/µl	213 ng/ml
scFv A18	175 ng/µl	438 ng/ml
scFv A19	400 ng/µl	1000 ng/ml
scFv B2	170 ng/µl	425 ng/ml
scFv Im1	85 ng/µl	213 ng/ml
scFv Im3	500 ng/µl	1250 ng/ml
scFv Im8	85 ng/µl	213 ng/ml
scFv Im18	75 ng/µl	188 ng/ml
scFv Im32	80 ng/µl	200 ng/ml
scFv Im47	85 ng/µl	213 ng/ml
scFv αTL111	500 ng/µl	1250 ng/ml

A very common problem in the NiNTA preparations of heterologously expressed His-tagged proteins is the presence of *E.coli* SlyD, a prolyl isomerise that specifically binds divalent metal ions which can result in significant contamination of the purification step.

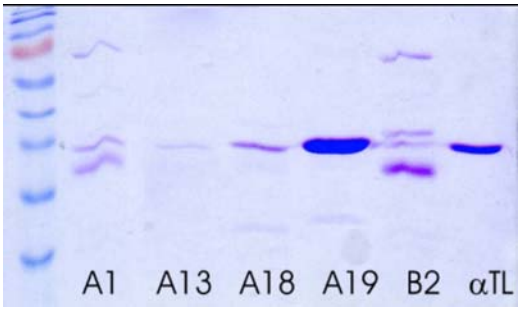

← ~30kDa

Fig.2. Analysis of the purified periplasmic preparation of scFvs by PAGE and Blue Comassie staining. It is noteworthy the different concentration of scFvs for the same loaded volume (αTL is used as reference), the presence of degradation products and high M.W. contaminants (correspondent to SlyD *E.coli* protein) in the scFvA1 and scFvB2 preparations.

The very low amounts of purified protein do not allow easily further steps of purification and analysis.

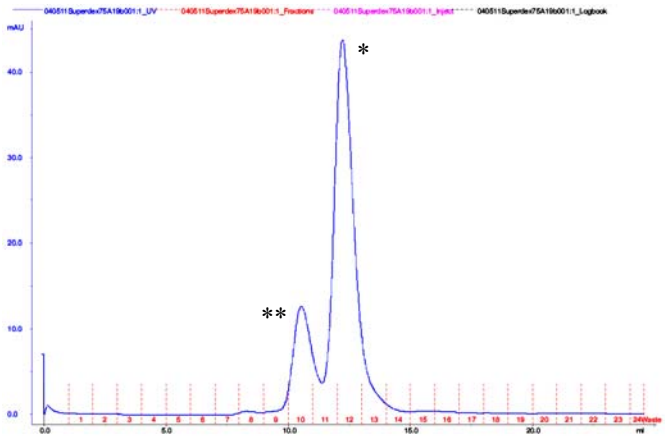

Fig.3 Representative analitical Superdex-75 gel filtration chromatograms of scFv A19, periplasmic purified, showing the prevalent peak (*) correspondent to the monomeric protein, and the secondary peak correspondent to the dimeric aggregated scFv (**). 100 µg/analysis of NiNTA purified scFv were used for this assay.

5.2 Cytoplasmic expression

The low yields of scFvs obtained from periplasmic expression system have induced us to optimize a cytoplasmic expression protocol, that was kindly provided by Dr. Paoletti (SISSA, Trieste).

In many cases and in several host systems, the recombinant proteins accumulate in cells as insoluble aggregates, so-called inclusion bodies. The proteins expressed as inclusion bodies are mostly inactive and denatured. The formation of inclusion bodies is a frequent consequence of high-level protein production in the cytoplasm. It is not possible to generalize or predict which proteins are produced as inclusion bodies.

Production of recombinant proteins as inclusion bodies has several advantages:

· The recombinant protein deposited as inclusion bodies can be 50% or more of the total cellular protein.

· Inclusion bodies often contain almost exclusively the over-expressed protein.

· In the form of inclusion bodies the protein is protected from proteolytic degradation resulting in higher yield.

· Expression as inclusion bodies will protect the cell against the toxicity of the recombinant protein since inclusion bodies have no biological activity.

· Inclusion bodies can be accumulated in the cytoplasm to a much higher level than when produced in soluble form.

For the expression of the scFv in the cytoplasm of *E.coli* we choose the largely used system vector-host pETM13 - BL21(DE3)pLysS *E.coli*. pETM13 uses the promoter of T7 bacteriophage and BL21(DE3)pLysS is an *E.coli* strain able to produce T7 RNA polymerase after IPTG induction.

The plasmid pETM13 was modified by site-specific mutagenesis (removing BssHII restriction site at the 2251nt of original pETM13, inside lacI gene) and by adaptation of the pDAN3 polylinker for scFv cloning (NotI-BssHII-**scFv**-NheI-NcoI) and a new vector named pGio1 was obtained (fig.4).

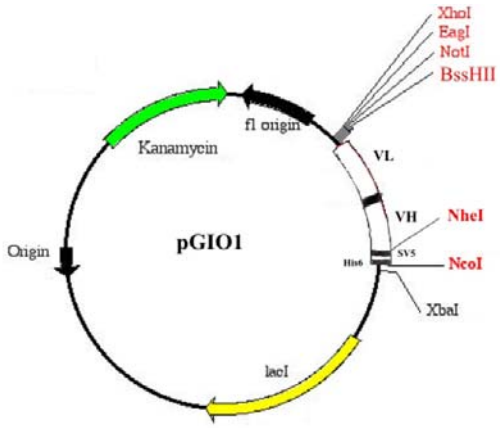

Fig.4 pGIO1, derivative of pETM13 vector was used for the cytoplamic expression of scFvs in BL21 *E.coli* strains.

Culture of BL21(DE3)pLysS carrying the scFv expressing plasmids pGio1 was induced with 1mM IPTG.

To obtain soluble scFv, the washed inclusion bodies are dissolved in denaturing agents and the released scFv is then refolded by gradual removal of the denaturing reagents by dialysis. Refolding is initiated by reducing concentration of denaturant used to solubilize inclusion bodies. Protein refolding is not a single reaction and competes with other reactions, such as misfolding and aggregation, leading to inactive proteins. Rate of refolding and other reactions is determined both by the procedure to reduce denaturant concentration and the solvent condition.

The procedure that has been used to solubilize inclusion bodies and to refold scFv was individually optimized for each anti-Aβ scFv, requiring a slightly different procedure which must be empirically determined. The cytoplasmic expression and purification of anti-Aβ scFvs were kindly performed by Dr. Michela Visintin (LayLineGenomics, Trieste).

The purification of the refolded scFvs was achieved through a ion exchange chromatography. Purified scFvs were also analyzed by Gel Filtration in Superdex75 columns, in order to recover only the fractions corresponding to the monomeric proteins.

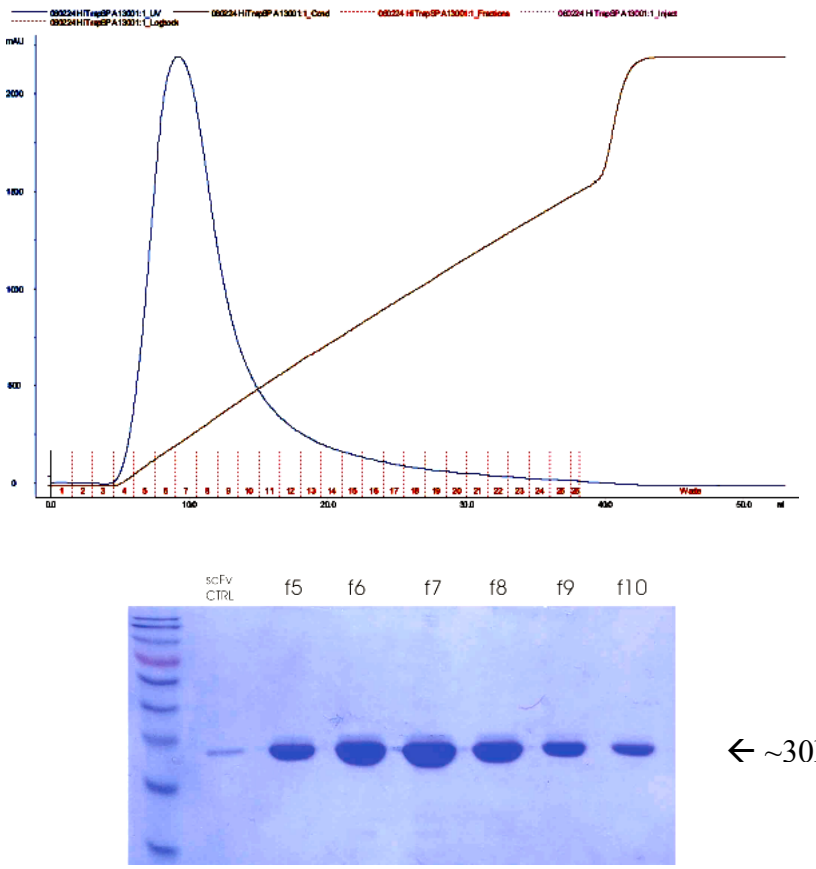

Fig.5 Representative cation exchange chromatography for refolded scFv A13 (performed on HiTrap SP column) from one cytoplasmic preparation, and analysis of scFv A13 (in the recovered fractions) by PAGE and Blue Comassie staining. This representative cytoplasmic preparation shows the high yield of production; the single peak high and tight, in the ion-exchange chromatography plot, indicates the pureness of preparation and the good rate of refolding.

The following table resumes the obtained final concentrations of purified scFvs, from inclusion bodies, and the total amount of protein per initial volume of culture.

	Concentration of purified scFv	***Amount of scFv for ml of starting culture***
scFv A1	8.7 µg/µl	8.8 µg/ml
scFv A13	4.5 µg/µl	3.3 µg/ml
scFv A18	0.6 µg/µl	0.3 µg/ml
scFv A19	4.0 µg/µl	3.0 µg/ml
scFv B2	0.16 µg/µl	0.17 µg/ml
scFv Im1	1.9 µg/µl	0.95 µg/ml
scFv Im3	5.45 µg/µl	2.72 µg/ml
scFv Im8	0.2 µg/µl	0.4 µg/ml
scFv Im18	2.1 µg/µl	1.58 µg/ml
scFv Im32	0.75 µg/µl	0.38 µg/ml
scFv Im47	3.38 µg/µl	4.5 µg/ml

The yields of purified scFvs by cytoplasmic expression were significantly higher (up to ~20 fold more for scFvs A1 and Im47) than those obtained by perisplamic expression, even though highly variable for different scFvs. Only scFv B2 resulted very difficult to purify by cytoplasmic expression, resulting very toxic for *E.coli*.

	PERIPLASMIC YIELDS ***Amount of scFv for ml of starting culture***	***CYTOPLASMIC YIELDS*** ***Amount of scFv for ml of starting culture***
scFv A1	425 ng/ml	8.8 µg/ml
scFv A13	213 ng/ml	3.3 µg/ml
scFv A18	438 ng/ml	0.3 µg/ml
scFv A19	1000 ng/ml	3.0 µg/ml
scFv B2	425 ng/ml	0.17 µg/ml
scFv Im1	213 ng/ml	0.95 µg/ml
scFv Im3	1250 ng/ml	2.72 µg/ml
scFv Im8	213 ng/ml	0.4 µg/ml
scFv Im18	188 ng/ml	1.58 µg/ml
scFv Im32	200 ng/ml	0.38 µg/ml
scFv Im47	213 ng/ml	4.5 µg/ml

6. Expression in mammalian cells as intrabodies

The selection of an antibody by IACT, on the basis of its ability to bind antigen in intracellular yeast enviroments, is a good and reliable predictor for the performance of an intrabody in mammalian cell lines (Visintin et al., 1999, 2002; Tse et al., 2002).

For intracellular studies, intrabodies targeted to specific sub-cellular compartments, can act as specific functional knock-out tools. The "protein interference" approach for knocking out Aβ function could not be pursued with the very well established RNA interference (RNAi) methodology (Wall et al., 2003) mainly because:

- Aβ peptide is a proteolitic fragment deriving from its APP (Amyloid Precursor Protein) precursor; RNAi can target only indirectly Aβ, through the modulation of APP or of β/γ secretases expression levels;
- RNAi based approaches could not allow to discriminate between Aβ monomers and Aβ oligomers.

Preliminary experiments of cytoplasmic expression in 3T3 fibroblast mouse cell line of SPLINT-selected scFvs anti-Aβ were performed. These experiments allow the evaluation of their solubility, stability and expression yeald in mammalian cell cytoplasm. Cells were transiently transfected with the vector scFvexcytoV5 (kindly provided by Dr. Visintin, Lay Line Genomics, Trieste) a modified version of scFvExpress-cyto vectors (Persic et al, 1997) expressing scFvs anti-Aβ (fig.1) in the cell cytoplasm.

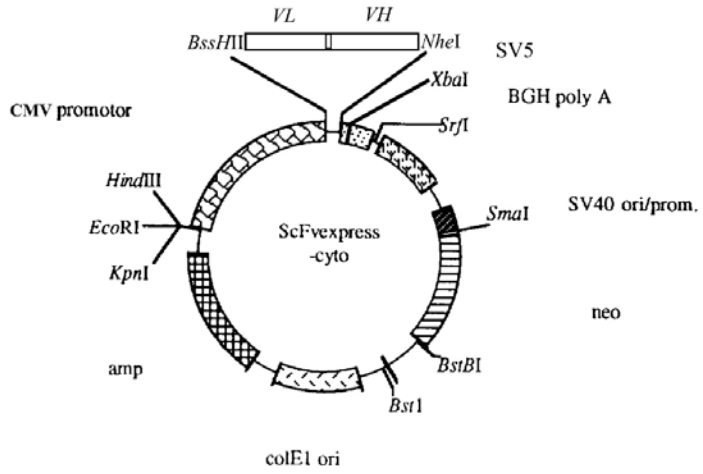

Fig.1 scFvexcyto-V5 vector used for the cytoplasmic expression of scFvs anti-Aβ. DNA sequence coding for each scFv were cloned (BssHII-NheI) into the vector backbone; scFv expression in mammalian cells in under the regulation of cytomegalovirus (CMV) promoter (modified from Persic et al., 1997).

Cytoplasmic expression of scFvs were detected with an anti-V5 antibody. The scFvs expression were tested by Western Blot analysis of cell extracts and by ImmunoFluorescence at 30 h post transfection.

A good level of expression for all scFvs tested were detected by Western Blot analysis. ImmunoFluorescence, indeed, demonstrated a differential distribution pattern of expressed recombinant proteins. Some scFvs, such as Im1, Im47, Im3 (see supplemented figure 2), show a diffuse expected intracellular staining, typical of soluble cytoplasmic proteins, but others (B2, A13, A18) display the greater the accumulation of the intracellular scFv in a puntiform or 'donut-like' pattern (supplemented fig.2) distribution (Persic et al, 1997). Moreover, some non tagged scFvs gives a specific localization staining in subcellular compartments such as ER, Golgi, secretory and endocytotic pathways. This is in line with the observation of Paganetti and coworkers (2005) that have shown that a cytoplamic expressed scFv intrabody, raised against the EFRH epitope

of human APP (epitope shared with Aβ), rapidly associates, within ER, with newly synthetized APP that remain associated along the secretory line.

In conclusion, we have observed the expression of anti-Aβ scFvs in mammalian cells. They are mainly soluble and well expressed. Further experiments in other mammalian cell lines and primary cultures are in progress. The expression of the anti-Ab scFv into different subcellular compartment (secretory, mitochondria, nuclear) are also in progress.

7. *In vitro* Characterization of scFvs anti-Aβ IACT-selected

ScFv recombinant proteins (purified from *E.coli*) were tested for binding properties in the following in vitro tests:

1. ELISA using coating with different aggregated forms of synthetic Aβ peptide;
2. ELISA using NeutrAvidin plates (Pierce) with coating of N-term biotinylated Aβ peptides;
3. Immunoprecipitation (IP) of synthetic monomeric or oligomeric Aβ peptide;
4. Immunohystochemistry (IHC) and ImmunoFluorescence (IF) on human AD brain slices;
5. Western blot and Dot Blot analysis of human AD brain extracts enriched in soluble oligomers (experiments still in progress; data not shown).

7.1 ELISA with coating of different aggregated forms of synthetic Aβ peptide

Dahlgren (2002) and Blaine Stine (2003) have described the conditions for Aβ peptide Oligomerization and Fibrillogenesis *in vitro*, as summarized in the following diagram (from Dahlgren et al, 2002).

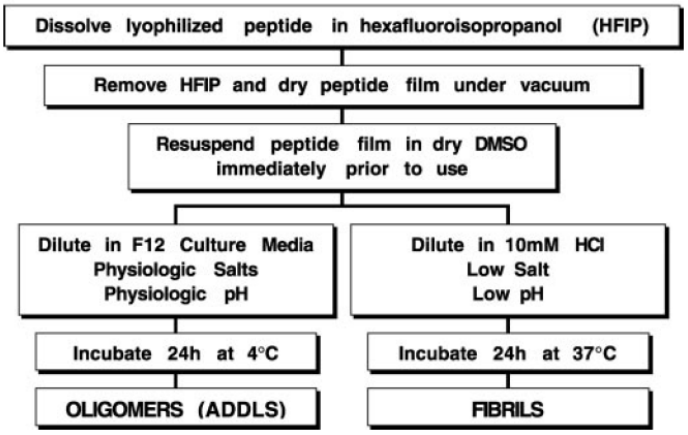

Our collaborator Anita Westlind Daniellson (Stockholm University) kindly provided human and murine synthetic ADDLs. Monomeric and fibrillar Aβ were obtained from synthetic commercial peptide resuspended in DMSO. Different aggregation status of Aβ peptides are confirmed by western blot analysis (fig.1).

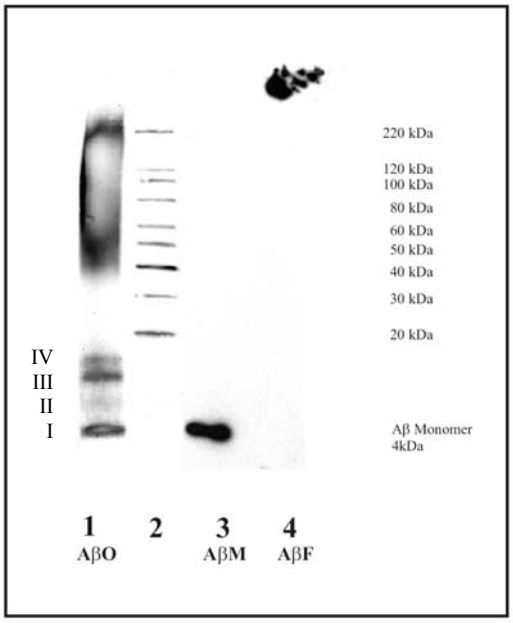

Fig.1 Western blot analysis of different forms of synthetic human Aβ1-42. Aβ oligomers ADDLs (AβO, lane 1), Aβ monomers (AβM, lane 3) and Aβ fibrils (AβF, lane 4) were loaded (1μg/lane equal to ~200pmol of total Aβ42), without heating or boiling samples, in NuPAGE™ 4-12%. WB was performed with MAb antiAβ 4G8. Note that ADDLs (lane 1) consist of small as well as large oligomers, and that large insoluble fibrils (lane 4) remains in the well of the gel. In the lane 1, "I" indicates monomers, "II" dimers, "III" trimers and "IV" tetramers.

The coating of different formats of Aβ peptide in ELISA plates was performed diluting in PBS at the final concentration of 10μg/ml different preparations of Aβ, and incubating overnight at 4°C.

Considering the complex dynamic of Aβ aggregation, we cannot exclude changes in the aggregation status during coating incubation; it is better to define different coating conditions as "mainly monomeric", "mainly oligomeric" and "mainly fibrillar". The most critical point is the maintaining of the monomeric format

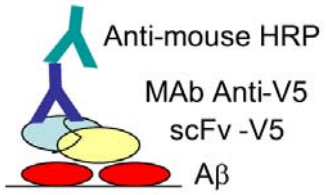

Fig.2 Scheme of the ELISA coating and the antibodies used for the detection.
Synthetic Aβ peptides were coated in solid phase on the ELISA plate, and scFv proteins were used as primary antibodies, as described in the text.

Different formats of Aβ coating were detected using anti-Aβ scFvs selected from naïve and immune SPLINT libraries. Recombinant *E.coli* purified anti-Aβ scFv proteins, have a SV5 tag at the C-terminus of VH region. ScFv-V5 can be detected using MAb or PAb anti-V5. The ELISA signal can be detected with a secondary antibody HRP-conjugated (allowing chromogenic reaction of TMB substrate) (fig.2). ScFvs are used at the concentration of 24μg/ml (equal to 0.8μM). As internal control, the detection of Aβ species was performed using the monoclonal antibody MAb 4G8 (concentration of 1μg/ml, equal to ~7nM) and the sera of the immunized mice (dilution of sera: 1:10000).
Different Aβ species were used in coating at the concentration of 10 μg/ml(fig.3):

1. synthetic human Aβ monomers;
2. synthetic human Aβ fibrils;
3. synthetic human Aβ oligomers (hADDLs);
4. synthetic murine Aβ oligomers (mADDLs);
5. unrelated antigen BSA

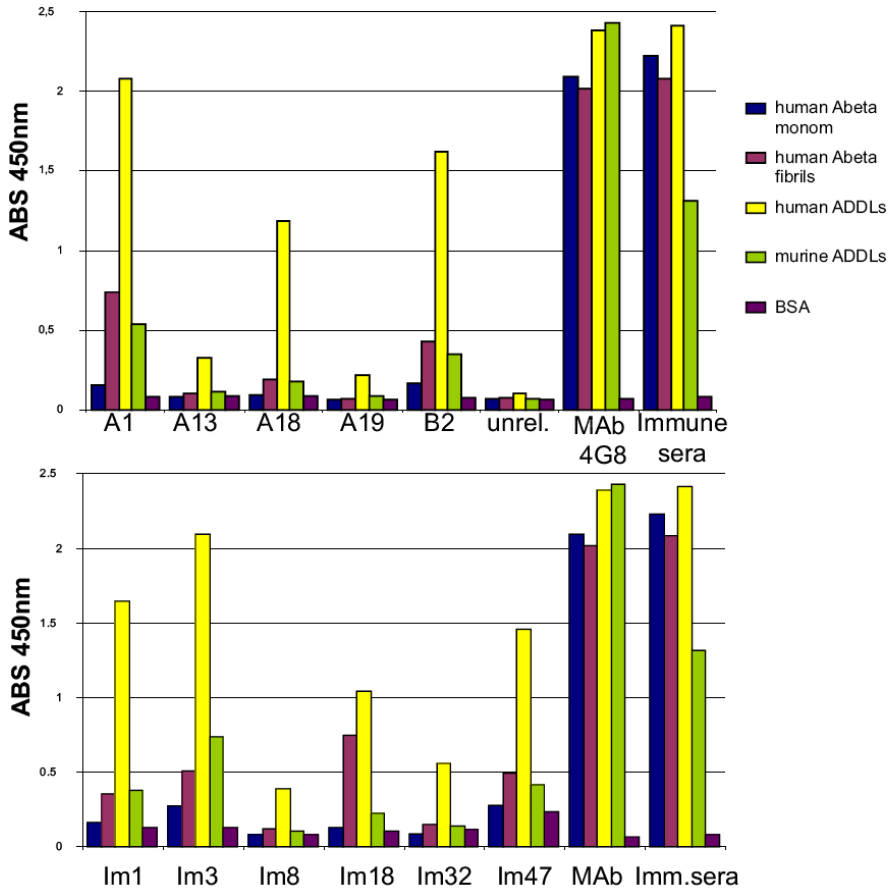

Fig.3 ELISA assay of anti-Aβ scFvs against different aggregated or monomeric forms of synthetic Aβ peptide coated (at the concentration of 10 μg/ml) in solid phase on the plate. The results show, for scFvs, a notable binding against Aβ oligomers in comparison with MAb 4G8 and sera of immunized mice, that do not distinguish between oligomeric, fibrillar and monomeric forms of Aβ. Each point represents the mean (n=3).

The results of ELISA revealed a greater binding specificity of the scFvs selected from SPLINT libraries for human Aβ oligomers (hADDLs). The binding properties of scFvs, in these ELISA conditions, appear significantly different in comparison with the binding specificity of both monoclonal antibody anti-Aβ and of the immunized sera. MAb 4G8 cannot distinguish between different forms of Aβ; PAbs from the immunized mice

discriminate only between human and murine peptides, demonstrating the specificity of immunization against the human antigen (fig.3).

All scFvs anti-Aβ SPLINT-selected, independently from the source of the SPLINT library by which have been selected, show the same binding behavior with the highest specificity against hADDLs. In terms of absolute ELISA O.D. values for hADDLs binding, are described in the following table 1:

Table:1 decreasing scale of scFvs binding to hADDLs, in terms of absolute O.D. values

scFv	***O.D. value*** *(mean±S.E.;n=3)*
Im3	2.10 ± 0.02
A1	2.08 ± 0.03
Im1	1.65 ± 0.02
B2	1.62 ± 0.02
Im47	1.46 ± 0.02
A18	1.19 ± 0.02
Im18	1.04 ± 0.03
Im32	0.56 ± 0.04
Im8	0.39 ± 0.02
A13	0.33 ± 0.02
A19	0.22 ± 0.02
Unrelated αTL	0.09 ± 0.01

ELISA O.D. values of hADDLs binding are significant for all scFvs in comparison with the unrelated scFv (anti Thimosine-β4, derived from the naïve library: Visintin et al., unpublished data) as well as in comparison with the binding values obtained for other Aβ forms.

Each scFv, except for Im3 and Im1, present this decreasing scale of specificity: hADDLs> hAβ fibrils > mADDLs > hAβ monomer (table 2). Generally, the isolated scFvs cannot distinguish between hAβ monomer and an unrelated antigen in coating, as for example BSA; therefore, the binding to Aβ monomer, in these ELISA conditions, is not specific with the exceptions of A1, B2 Im3 and Im47.

Table: 2 Comparative scale for anti-Aβ scFv specificity (Im3 and Im1, shown down): hADDLs > hAβ fibrils > mADDLs > hAβ monomer in terms of absolute O.D. values (mean)

	hAβ42 ADDLs	***hAβ42 Fibrils***	***mAβ42 ADDLs***	***hAβ42 Monomer***
A1	2.08	0.74	0.54	0.16
B2	1.62	0.43	0.35	0.17
Im47	1.46	0.49	0.42	0.27
A18	1.19	0.19	0.18	0.09
Im18	1.04	0.74	0.23	0.13
Im32	0.56	0.15	0.14	0.09
Im8	0.39	0.12	0.11	0.08
A13	0.33	0.10	0.11	0.08
A19	0.22	0.07	0.09	0.07
Unrelated αTL	0.09	0.07	0.07	0.07
MAb 4G8	2.35	2.1	2.4	2.1

	hAβ42 ADDLs	***mAβ42 ADDLs***	***hAβ42 Fibrils***	***hAβ42 Monomer***
Im3	*2.10*	*0.74*	*0.51*	*0.27*
Im1	*1.65*	*0.38*	*0.35*	*0.13*

ELISA specificity for hAβ fibrils and mADDLs binding is comparable for each anti-Aβ except for Im18, that presents significant higher values for human fibrils. ScFvs anti-Aβ, in particular A1, A18, B2, Im1, Im3, Im8, Im32 and Im47, discriminate at least three times better human ADDLs than other aggregated forms of Aβ.

In conclusion, the specificity of the isolated scFvs seems to be not only preferential versus conformational aggregated oligomeric Aβ, but also species-specific versus human Aβ. The ability of our scFvs to distinguish hADDLs from mADDLs is highly relevant: they are very specific, if compared to other conformation specific antibodies, such as the polyclonal anti-oligomer elaborated by Kayed and coworkers (2003) (commercially available and known as A11), that recognize equally well oligomeric-specific epitopes common to different peptides (including Aβ, lysozime, IAPP and prions).

The species-specificity *in vitro* was different from what observed in IACT. In fact, as discussed above in the In Vivo Epitope Mapping (IVEM) characterization, scFvs recognize equally well both human and murine Aβ baits; but in this last case, we have not performed quantitative assays. Therefore, it is likely that the *in vivo* binding could be different from the *in vitro* binding in ELISA condition.

7.2 ELISA with NeutrAvidin plates:

coating with N-term biotinylated Aβ peptides

NeutrAvidin™ protein is a deglycosilated avidin able to bind biotin-labeled molecules, studied generally used to minimize nonspecific adsorption. NeutrAvidin™ plates with high binding capacity (HBC) represent an excellent system to detect small peptides as Aβ. We used N-terminus biotinylated hAβ1-40 and hAβ1-42 peptides. The use of the N-terminal biotinylated Aβ peptides allows to have the conformational structured Aβ more exposed, avoiding non specific interactions with the plastic of ELISA plates.

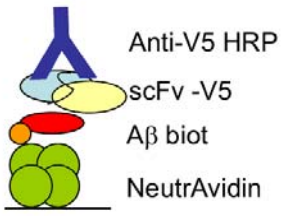

Fig.4 Scheme of the ELISA coating and the antibodies used for the detection, in NeutrAvidin™ plates. *E.coli* purified recombinant anti-Aβ scFv proteins, were used as primary antibodies at different concentrations and detected by an anti-SV5 antibody HRP-conjugated.

NeutrAvidin™ ELISA presents higher sensibility in comparison with standard ELISA. In fact, low concentrations of scFvs (up to 3µg/ml instead of 24µg/ml) as well as of the antigen (down to 0.1µg/ml) give a significant response (figs.5 and 6).

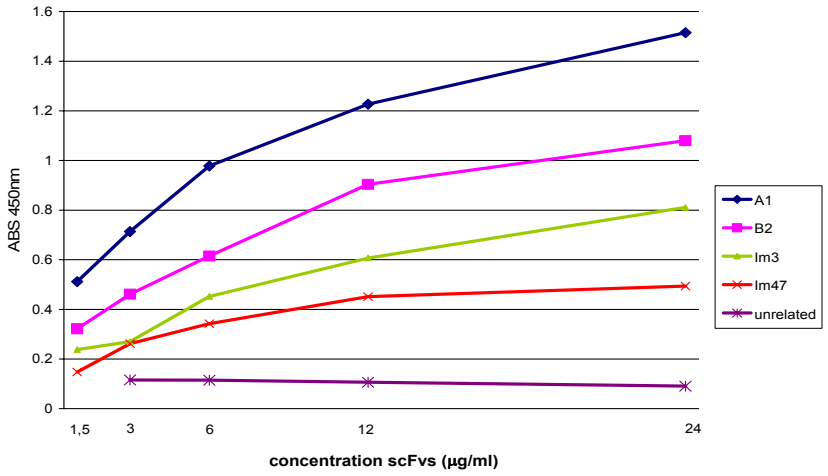

Fig.5 Dose-dependent curves of five different scFvs at five different concentrations. on NeutrAvidin plates were coated with Aβ42-biot (1µg/ml).

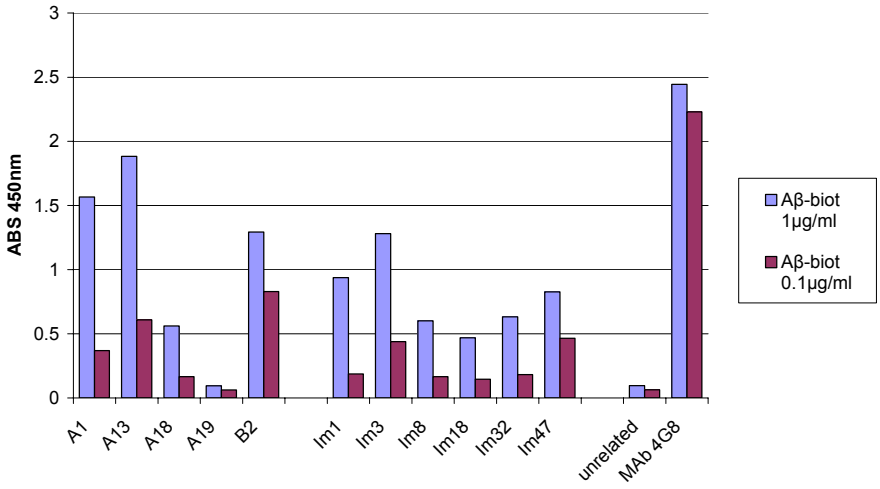

Fig.6 ELISA results: coating with Aβ42-biot (1µg/ml and 0.1µg/ml) onto NeutrAvidin plates (scFvs at saturating concentrations of 25 µg/ml).

The binding capacity of Reacti-Bind™ NeutrAvidin™ HBC plates is of ~60 pmol of D-biotin/well.

The following tables resume the amounts of Aβ-biot peptide, scFvs and MAbs used in our experiments.

Aβ42 biot
(MW 4740.4; 70µl/well)

concentration	pmoles/well
10 µg/ml (2µM)	147
5 µg/ml	73.5
1 µg/ml	14.7
0.1 µg/ml	1.47

scFv
(MW ~30000; 50 µl/well)

concentration	pmoles/well
24 µg/ml (0.8µM)	40
12 µg/ml	20
6 µg/ml	10
3 µg/ml	5
1.5 µg/ml	2.5

MAb anti Aβ
(MW ~150000; 100 µl/well)

concentration	pmoles/well
1 µg/ml (6.7nM)	~0.7

The concentrations of 5µg/ml of Aβ-biot (70µl/well) should potentially saturate all NeutrAvidin binding sites in each well if the highest binding efficiency of biotinylated peptide to NeutrAvidin plates is obtained. We have found that the coating onto NeutrAvidin plates with high and saturating concentrations of Aβ-biot (5-10µg/ml) determines its aggregation in structures recognized by the well established polyclonal

antibody anti-oligomer PAb A11 (Kayed et al., 2003), that was used as a positive anti-oligomer control.

PAb A11 is a conformation-dependent antibody that specifically recognizes soluble Aβ amyloid oligomers and does not recognize low molecular weight monomers or dimers, or mature amyloid fibrils.

As pointed out by Glabe, "this anti-oligomer antibody recognizes soluble oligomers from various amyloids including lysozyme, IAPP, a-synuclein, prion 106–126, polyQ and insulin. Because antibody recognition is independent of the amino acid sequence, the epitope is likely to be a common peptide backbone motif, such as the array of hydrogen bond donors and acceptors at the edge of a β-sheet or a turn motif." (Glabe, 2006)

We found that particular conditions of incubation of Aβ-biot peptide onto NeutrAvidin plates favour its oligomerization. The highest values of O.D., using PAb A11 as primary antibody, are obtained incubating 10μg/ml (2μM) of Aβ-biot peptide at 4°C overnight in F12 phenol red free medium (the same conditions used by Dahlgren and coworkers for the oligomerization of Aβ (100μM) in solution (Dahlgren et al., 2002)). In these conditions (* in fig.7) PAb A11 shows a four-fold discrimination between Aβ-biot coated at 10 μg/ml and Aβ-biot coated at 0.1-1 μg/ml (fig.7).

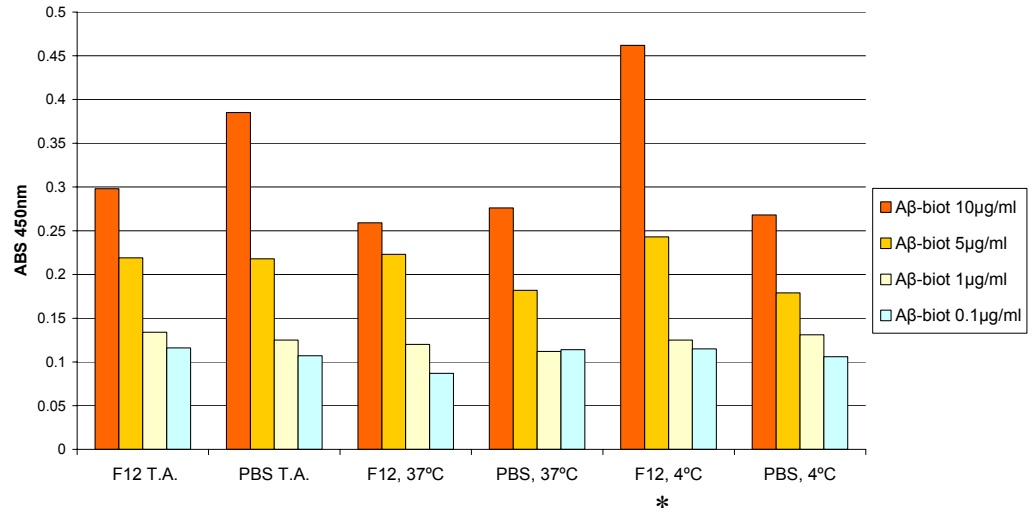

Fig.7 ELISA results: PAb anti-oligomer A11 binding to Aβ42-biot at different conditions of incubation favouring oligomerization onto NeutrAvidin plates.

MAb 4G8 is not able to discriminate between different concentrations of peptide in ELISA (fig.8); under the oligomerization conditions discussed above (but not in normal coating conditions: 1 hour in coating buffer), the concentration of 0.1 µg/ml is partially limiting for the binding of the MAb 4G8. The significant O.D. values observed at 0.1 µg/ml of Aβ (correspondent to 1.5 pmoles/well) with MAb 4G8 could be considered an index of high affinity of the antibody versus the antigen, that is presumably non aggregated at this concentration.

The scFvs anti-Aβ tested in ELISA show a behavior similar to that of PAb A11, which is able to discriminate between Aβ-biot coated at 10 µg/ml and at 1 µg/ml. The sample of scFvs tested was chosen to include two scFvs representative of N-terminal binders (Im3 and B2) and two scFvs representative of C-terminal binders (Im8 and A1) (fig.8).

All scFvs show good affinity versus the human peptide also at concentrations of Aβ coating of 0.1 µg/ml (1.5 pmoles). For some scFvs, (i.e. B2), the high ELISA values at

Aβ peptide coating concentration of 0.1μg/ml could indicate not only a good affinity, but also less specificity for oligomers; in fact these scFvs are able to bind monomer and oligomers.

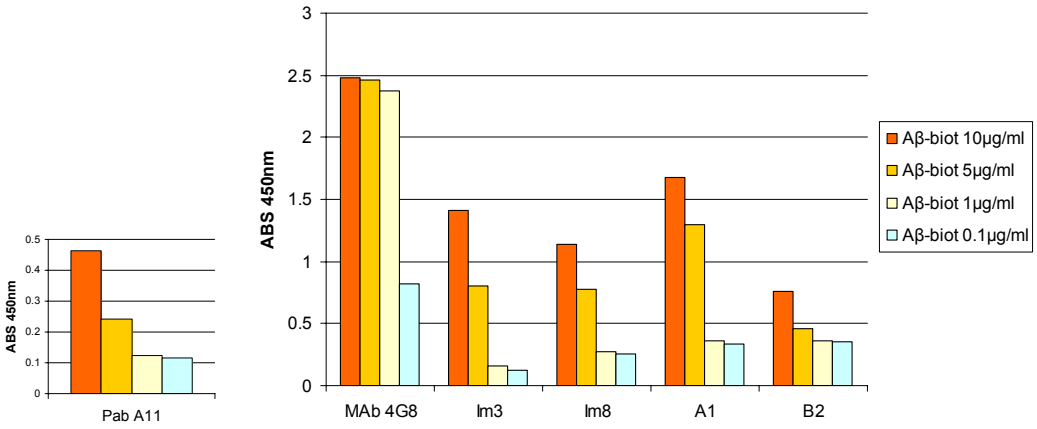

Fig.8 ELISA onto NeutrAvidin plates. Aβ42-biot peptide is coated under conditions of oligomerization. Binding of PAb A11, MAb 4G8 (used at equi-molar concentrations, ~7nM) and four different scFvs anti-Aβ (0.4μM) are shown.

In conclusion, ELISA in NeutrAvidin plates suggest that selected scFvs under study, recognize preferentially the same conformational oligomeric forms recognized by the well characterized anti-oligomer PAb A11.

The use of NeutrAvidin plates, even not in oligomerization conditions, have allowed the conformational structures of Aβ peptide to be recognized by scFvs, uncovering their specific preference for Aβ oligomers to be characterized.

In any event, the behaviour of scFvs in the recognition of Aβ *in vitro*, in comparison to MAbs anti-Aβ 4G8 or 6E10 (antibodies not discriminating between different aggregated and un-aggregated forms of Aβ) is very different.

The ELISA results discussed in the previous section, which showed high specificity of scFv binding to human ADDLs, together with the present results of ELISA in

NeutrAvidin plates, indicate that the recognition of peculiar conformations of Aβ seems to be a crucial property of the SPLINT-selected anti-Aβ scFvs. Probably, the oligomerization of Aβ enriches in the conformational epitopes that are recognized by the selected scFvs under study. Concerning PAb A11, Glabe similarly suggest that "the epitope on the oligomers must be either conformationally distinct or greatly reduced in the fibril structure. In keeping with the latter, the edge of the β-sheet would be expected to be exposed only at the ends of fibrils; thus, the amount of this epitope would decrease as the average length of the fibrils increased." (Glabe, 2004)

ELISA in NeutrAvidin plates performed using biotinylated hAβ40 show that a large-part of scFvs cannot distinguish between Aβ42 and Aβ40. ScFv A19 recognizes two times more specifically Aβ40 than Aβ42 at the concentration of coating of 1μg/ml. Also N-terminal specific scFvs, recognize better Aβ40 than Aβ42 (data not showed), probably because the N-term epitope is better exposed in Aβ40 peptide.

Preliminary experiments of competitive ELISA in NeutrAvidin plates have been performed using hAβ1-16 peptide as a competitor of scFvs binding to hAβ-biot oligomers (fig.9). Aβ16 is not an aggregating peptide and competes significantly with MAb 6E10 (that recognizes the epitope Aβ3-9) for the binding to Aβ-biot in NeutrAvidin plates. Indeed, scFvs anti N-term (B2 and Im3) as well as anti-oligomer PAb A11 do not feel the inhibitory effect of Aβ16 on the binding of Aβ-biot conformational oligomers (fig.9).

These preliminary results suggest that also N-term specific scFvs could recognize specific conformations of Aβ, probably preferential structured in oligomers of Aβ whole peptide (Aβ1-42), confirming the general behaviour of most of the scFvs selected, independently from epitope characterized by IVEM.

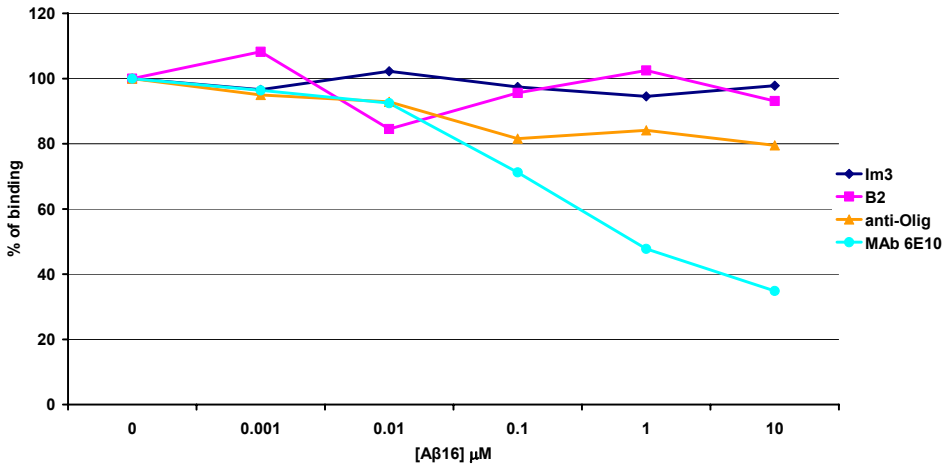

Fig.9 Competitive ELISA: dose-effect of increasing concentrations of Aβ16 competitor peptide to the binding of Aβ-biot oligomers. NeutrAvidin plates are used in this experiment.

7.3 Immunoprecipitation of synthetic antigen

ELISA results show as general characteristic of SPLINT-selected scFvs a preferential binding ability of particular conformations of human Aβ, particularly of oligomeric aggregates.

In order to test the binding and antigen-recognition properties of the anti-Aβ scFvs under solution condition, they were tested for their ability to capture and remove ADDLs or Aβ monomers from solution by immunoprecipitation.

It is likely that solution favours a "natural" conformation of Aβ monomers as well as Aβ oligomers, being both forms of Aβ soluble species (unlike insoluble Aβ fibrils).

Immunoprecipitation (IP) of Aβ monomer as well of Aβ oligomers can show several experimental problems related to critical folding and aggregation properties of this peptide. It is likely that, during the steps of incubation, Aβ changes the aggregation status (for instance the monomers can become oligomers, and oligomers can grow into larger oligomers). Moreover, it was observed also a non-specific binding of Aβ oligomers to protein G beads. The detaching bond antigen from antibody was also a critical step; we have avoided brash conditions (boiling or high salts) in order to reduce changes of the original conformation and in the aggregation status of the peptide.

Nonetheless, we were able to demonstrate that anti-Aβ scFvs bind 'Aβ soluble species' under solution condition.

The general protocol of IP using scFvs (fig.10) provides a preincubation of scFvs and Aβ antigen, in order to allow their complex formation in solution. PAb anti-V5, bound to ProteinG-Sepharose™, provides the capture of scFv-Aβ complex thanks to the binding of

the exposed V5 tag of scFv proteins. The captured complex was finally analyzed by western blot (WB), in semi-denaturing conditions using NuPAGE™ gels (SDS PAGE gels, without boiling samples and in non reducing conditions).

We analyzed two fractions deriving from the last step of the immunoprecipitation protocol: IP pellet and IP supernatant. In the final step of IP, ProteinG-antiV5 beads carrying the captured complex scFv−Aβ, were centrifuged and washed by subsequent centrifugations: the first supernatant was the 'IP supernatant', which is enriched in Aβ not specifically immunoprecipitated, and the final centrifugation pellet was the 'IP pellet', which is enriched in immunoprecipitated Aβ. Subsequently, the two fractions were analyzed by WB, after a gentle detach of Aβ from the IP pellet, as discussed above.

We show results obtained from immunoprecipitation experiments using scFv A1 (C-terminal binder) and scFv B2 (N-terminal binder), which are both good binders of Aβ oligomers in ELISA assays; moreover, as previously shown, scFv B2 can recognize both Aβ oligomers and Aβ monomer in ELISA experiments.

Immunoprecipitation of Aβ monomer in solution by scFv B2

As shown in fig.10, scFv B2 can specifically immuno-precipitate soluble synthetic Aβ42 monomer.

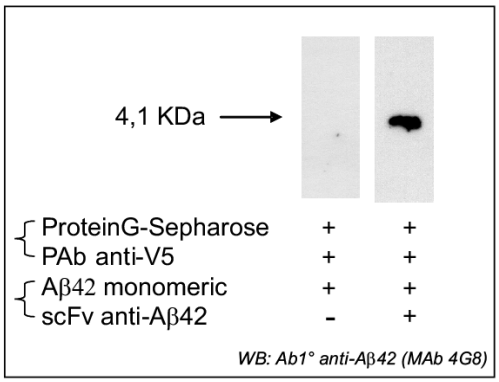

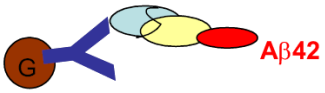

Fig. 10 scFv B2 immunoprecipitates Aβ monomer from solution. ScFv B2 (350pmol) was initially incubated with Aβ monomer (1nmol) and separately PAb anti-V5 (~300pmol) was incubated with ProteinG-Sepharose; the complex B2-Aβ was immunoprecitated by the ProtG-antiV5. IP pellets were loaded, without heating or boiling, in NuPAGE™. WB performed with antiAβ 4G8. Note that the band of 4.1 kDa is present only in the lane of WB loaded with pellet of IP (Aβ+B2).

As shown in fig.11, in the same experiment, the scFv B2 was able to immunoprecipitate both Aβ monomers and Aβ oligomers: the latter are species between 30kDa and 50kDa, probably formed during incubation steps.

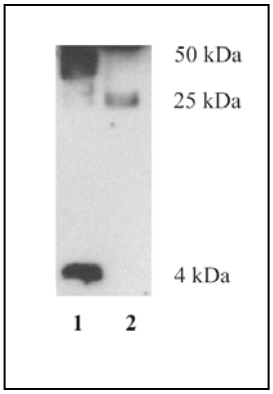

Fig.11 scFv B2 immunoprecipitates Aβ monomer and oligomers from solution. In the lane 1 was loaded IP pellet (B2+Aβ), in the lane 2 IP pellet (Aβ alone). IP pellets were loaded, without heating or boiling, in NuPAGE™. WB performed with antiAβ 4G8.

Immunoprecipitation of Aβ oligomers in solution by scFv B2

As for the immunoprecipitation of 'pre-assembled' Aβ oligomers (ADDLs) by scFvB2, we found that the IP supernatant was significantly depleted in ADDLs of high molecular weight bands (60-180kDa). This is an indirect evidence of ADDLs binding from scFvB2, even if no Aβ bands in the IP pellets could be differentially detected (data not shown). Similarly, Lambert and coworkers (2003), characterizing the specificity of two new antibodies (M93 and M94) raised against Aβ oligomers, tested their ability to remove ADDLs from solution by immunoprecipitation and showed only WB of ADDLs-depleted supernatants and not of ADDLs-enriched IP pellets.

In another experimental trial, changing the incubation binding scheme of ADDLs and B2 scFv protein (as indicated in fig.12) we have obtained a specific enrichment in Aβ immunoreactivity, only in the IP pellet.

We have observed in WB a separation of three Aβ immunoreactive bands (> 190kDa, >100kDa, ~50kDa) (fig.); in this case the IP pellet samples were not boiled, but heated at

70ºC before loading in NuPAGE™. The same IP samples, not boiled and not heated, show a totally different pattern, with immunoreactive enriched species between ~40kDa and ~90kDa (data not shown). Probably, even though the heating procedure changes the aggregation status of the immunoprecipitated ADDLs, it favours their detachment from ProteinG complex, allowing a better detection of the IP enriched fraction.

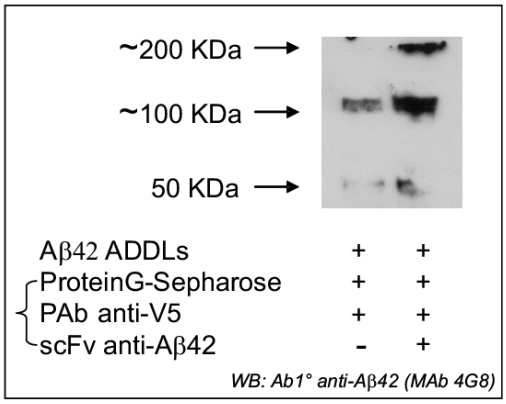

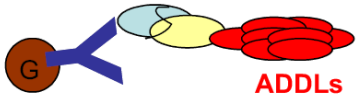

Fig.12 scFv B2 immunoprecipitates ADDLs in solution. scFv B2 (350pmol) was initially incubated with PAb anti-V5 (250pmol) for ~2hrs; the complex B2-PAb antiV5 was then incubated with ProteinG-Sepharose for ~4hrs; finally the ADDLs (100pmol) were immunoprecitated by the whole complex ProtG-antiV5-B2. IP pellets were heated at 70ºC and loaded in NuPAGE. WB performed with antiAβ 4G8.

Immunoprecipitation of Aβ oligomers in solution by scFv A1

According to the first IP protocol [(scFv+ADDLs) + (ProtG-antiV5)], preincubating ADDLs (1000pmol) with scFv A1 (400pmol), we obtained a specific enrichment in Aβ immunoreactivity between 40kDa and 100kDa (without heating of samples). The component of Aβ monomer, normally present in ADDLs preparations, appears in

supernatants but not in pellets, showing that is not immunoprecipitated by scFv A1 (fig.13).

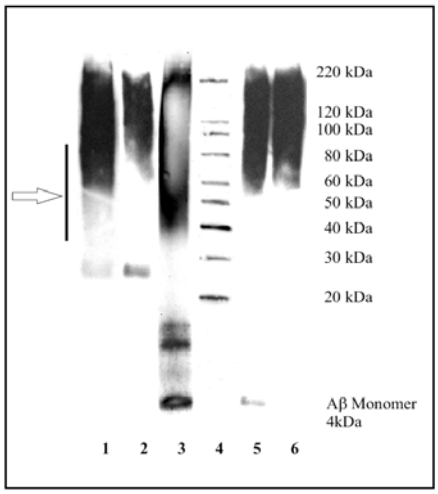

Fig.13 scFv A1 immunoprecipitates ADDLs in solution. ScFv A1 (400pmol) was initially incubated with ADDLs (1nmol) and separately PAb anti-V5 (~300pmol) was incubated with ProteinG-Sepharose; the complex A1-ADDLs was immunoprecitated by the ProtG-antiV5. IP pellets were loaded, without heating or boiling, onto NuPAGE™. WB performed with MAb antiAβ 4G8. Lanes legend: 1) IP pellet (A1+ADDLs); 2) IP pellet (ADDLs alone); 3) input of ADDLs; 4) M.W. markers; 5) supernatant (A1+ADDLs); 6) supernatant (ADDLs alone). The arrow indicates the specific enrichment of 40kDa−100kDa Aβ species in the pellet of IP(ADDLs+A1).

In conclusion, these preliminary results indicates that scFv A1 and B2 are able to bind different soluble species of Aβ peptides, under solution conditions. ScFv B2, respect to scFv A1, results also a good binder of Aβ monomers even if it is preferential binder of Aβ oligomers.

The characterization of the ability of the anti-Aβ SPLINT-selected scFvs, to bind 'Aβ soluble species' in solution could be relevant for different applicative purposes as, for instance, pull-down of conformational critical species from biological samples and *in vivo* therapeutic targeting of pathological Aβ oligomers.

7.4 ImmunoHystoChemistry (IHC) and ImmunoFluorescence (IF) on AD human brains: recognition of in vivo-produced forms of Aβ

The ability to recognize naturally produced and not only synthetic Aβ is a relevant characteristic for anti-Aβ antibodies, both for therapeutic and for diagnostic purposes. For instance, Hock and coworkers (2002, 2003) have demonstrated that in clinical protocols of active immunotherapy in humans, only patients with immune sera highly reactive in vitro versus Amyloid plaques (Tissue Amyloid Plaques Immuno Reactivity assay = TAPIR assay), independently of ELISA titers of anti-Aβ antibodies, show clinical protective effects.

In addition, peculiar pathological conformations of Aβ aggregates can be detected only in biological samples and in tissues. Recently, Lambert and coworkers (2006) similarly to our observations, report that different antibodies produced against the same antigen (synthetic ADDLs) show differential reactivity in human AD brains, against different pathological Aβ assemblies.

In order to verify the peculiarity of the SPLINT selected antibodies, we have tested the tissue immuno-reactivity of some scFvs that were previously characterized in IVEM and ELISA (A1, A13, A18, B2, Im1, Im3, Im8, Im18, Im32 and Im47).

Sections of 40μm were prepared from Temporal Cortex of post-mortem human AD brains (Braak stage V-VI) and control (Braak 0-I).

ScFvs were used as primary antibodies and, as performed in ELISA, detected via a sandwich of antibodies using an intermediate MAb or PAb anti-V5 and after an appropriate secondary for ImmunoHystoChemistry (IHC) or ImmunoFluorescence (IF).

A preliminary set of IHC experiments were performed with scFv A1. It was immediately evident that the scFv staining by this scFv was peculiar, in comparison to classic Amyloid plaques detected by commercial anti-Aβ antibodies as 6E10 or 4G8. In IHC, scFv A1 detect mainly some small cell bodies (probably microglia) and often diffuse halos around them (supplemented figure 3), also without formic acid (90%) pre-treatment of slices. The reactivity is specific if compared with control tissues, which present only tight cellular staining.

ImmunoFluorescence (IF) was essential for colocalisation studies.

To avoid potential stickiness problems, brain slices were preferentially pre-treated with formic acid 90% for antigen retrieval, and treated for autofluorescence reduction after antibodies incubations.

ImmunoFluorescence on AD brains slices showed a specific staining pattern, which is distinct for different scFvs, in comparison to the staining of Aβ deposits obtained with commercial, well established anti-Aβ antibodies. We suggest that different scFvs can detect different Aβ oligomer structural epitopes.

scFv A1 (suppl. fig. 4) shows peculiar cellular reactivity of small cells in plaque-rich areas, and interestingly a partial complementary staining of plaques in comparison to anti-Aβ MAbs 6E10 and 4G8. We postulate that scFvA1 might be specific for the early

stage of amyloid maturation: the supplemented fig. 4A shows that no core staining in the upper plaque can be noted, similarly to the reported case of anti-Aβ globular oligomers detecting a rim around the plaques in AD brains (Barghorn et al., 2005). As observed in IHC, also in IF, scFvA1 often detects pericellular diffuse immunoreactivity (suppl. fig.4B), not detected by classic Abs anti-Aβ; similar pericellular staining is observed by Lambert and coworkers (2006) using their MAbs anti-oligomer. Finally, scFvA1 can specifically recognize blood vessels with Amyloid deposits, especially in plaques rich areas in the brain from one AD patient showing greater signs of Cerebral Amyloid Angiopathy (CAA) (suppl. fig.4C).

ScFv A13 reacts weaker than other scFvs with Aβ deposits in human AD brain slices. A13 detects preferentially some cell bodies (probably of astrocytes) and their pericellular zones in plaques rich areas (suppl. fig.5). It is possible that the fixation/staining conditions do not preserve the epitope recognized by scFv A13.

ScFv A18 (suppl. fig.6) presents a prevalent vascular reactivity in plaque-rich areas; blood vessels are specifically recognized by A18 but not by PAb anti-Aβ42.

ScFv B2 presents mostly strong cellular reactivity, tightly related to plaques (suppl. fig.7A). Similar cellular reactivity corresponding specifically to astrocytes is detected by one of MAbs anti-oligomer developed by Lambert and coworkers. Probably, B2 detect also dystrophic neuritis (suppl. fig.7B). ScFvB2 can detect also specifically blood vessel deposits, near Aβ plaques detected by other Abs (suppl. fig.7C).

ScFv Im8 (suppl. fig.8A-B) detects specific small dotted clusters of mainly pericellular immunoreactive deposits, spatially distinct and separate from small plaque-like depositions (stained with Aβ42 C-terminal specific Ab). This immunoreactive pattern is peculiar of Im8 but not of other scFvs. Im8 shows also secondary cellular and dystrophic-neurites reactivity (suppl. fig.8C).

ScFv Im18 (suppl. fig.9A) shows specific pericellular reactivity near large plaques partially distinct and separate from them. In other fields of slice, Im18 (suppl. fig.9B) similarly to Im32 (suppl. fig.9C) detects cellular reactivity spatially related to Aβ42 plaques.

The immunoreactive pattern of Im47 is similar to that of Im18, with stronger cellular reactivity (probably astrocytes) in smaller plaques zones, and distinct pericellular reactivity near large plaques (suppl. fig.10). Pericellular reactivity of Im47 is often specifically dotted, resembling oligomeric-specific staining of PAb A11 (Kayed et al 2003) in human AD brains (suppl. fig.11) and in 3xTg AD mouse model (Oddo et al 2006).

In the following table we resemble the interesting differential binding properties of scFvs examined in human AD brain slices, in comparison with other characterized properties.

	IVEM Human Aβ 1-10	*ELISA1 Human Aβ1-42 ADDLs*	*ELISA2 Human Aβ1-42 biot*	*IFs Human AD brains*	
A1	-	+++	+++	**P, pC, C, Pa, V**	++
A13	-	+	+++	**C, pC**	+
A18	-	++	+	**V, C**	++
A19	-	+/-	+/-		
B2	+	+++	++	**C, V**	+++
Im1	+	+++	++		
Im3	+	+++	+++		
Im8	-	+	+	**O, pC**	+++
Im18	-	++	++	**C, Pa, pC**	++
Im32	+	+	+	**C**	+
Im47	+	+++	++	**C, O, pC**	+++

P, plaque reactivity; pC, pericellular; Pa, parenchimal; C, cellular; O, oligomeric-like (dotted cluster); V, vascular

ScFvs show different ability to react with Aβ deposits in human AD brain slices (see last column in the table). This diverse staining pattern could derive not only from differential intrinsic properties of recognition of Aβ *in vivo* produced, but also from differential *in vitro* stability of scFvs during the incubation steps. Optimizations of protocols are in progress, as well as experiments of co-localization with other anti-oligomers, unfortunately not all readily available. For scFvs Im1 and Im3, preliminary results are not shown.

The ability of scFv to bind Aβ in AD tissues (extra- or intracellularly) can be qualitatively indicated in a decreasing scale: scFv Im8, B2, Im47, Im18, A18 and A1; noteworthy Im8, which was not very convincing in comparison to other scFvs in ELISA, but results specifically immunoreactive in AD brain slices. Clearly, optimization of the

experimental conditions for individual antibodies might improve the labeling pattern for some of them (this is true for A13, not shown).

Discussion

Pericellular zones (Lacor et al 2004) and cluster deposits, spatially segregated near plaques (Kayed et al 2003) were previously described as targets in AD brains of two different anti-Aβ oligomers (respectively PAb M94 and PAb A11). Recently, also astrocytes have been described clearly stained by NU-6, another MAb anti-Aβ oligomers (Lambert et al 2006). In addition, Barghorn and coworkers (2005) have observed that their PAb anti-Aβ globular oligomers detect a dense rim around the plaques in AD brains, distinctly from thioflavine-S staining.

As above-discussed, our scFvs are peculiarly able to stain similar deposits (intracellular, pericellular and extracellular), and these observations favorably support their oligomeric-specificity. In addition, some of the scFvs are able to react specifically with blood vessels in association with plaques recognized by other anti-Aβ antibodies; vascular reactivity is of interest because it is still unknown if oligomeric forms of Aβ can deposit in blood vessel, and how the perivascular drainage of Aβ oligomers is involved in AD pathogenesis. Other peculiar reactivity of some scFvs giving, for instance, intracellular staining in different cell types or differential dotted pericellular or synaptic-like staining, deserve to be investigate. In conclusion, our scFvs, probably thanks to the *in vivo* selection strategy, allow to detect new interesting conformational oligomeric-specific deposits *in vivo* produced.

8. ScFvs anti-Aβ as neutralizing agents in cellular models of neuronal cell death and of amyloidogenesis

To explore and validate a relevant biological role for the SPLINT-selected anti-Aβ scFvs, we tested them in two different *in vitro* models of externally administered Aβ oligomers (human ADDLs) (points 1 and 2, below) and in a novel cellular model of endogenously produced Aβ and cell death which links neurothrophic deficits and amyloidogenesis (point 3).

Several anti Aβ scFvs were administered *in vitro* as purified recombinant proteins and were tested for the following properties:

1. inhibition of hADDLs-induced toxicity in the SHSY5Y human neuroblastoma cell line;
2. inhibition of hADDLs synaptic binding in rat hippocampal primary cells;
3. block of Aβ aggregation and/or neutralization of Aβ toxic species in neuronal differentiated PC12 cells deprived of serum and NGF (overproducing Aβ peptides and showing their aggregation in ThioflavinT positive structures).

8.1. Model of ADDLs toxicity in SHSY5Y human neuroblastoma cell line

To test the biological activity of scFvs for their possible ability to neutralize the toxic effects of Aβ oligomers, a widely accepted cellular model of Aβ toxicity was exploited: hADDLs externally administered to SHSY5Y human neuroblastoma cells line, following two different protocols of treatment, an acute and a chronic protocol.

The protocol of acute toxicity provides for the administration of 2.5 μM hADDLs (referred to the concentration of total Aβ peptide in the ADDLs preparation) for 16hrs. Instead, the protocol of chronic toxicity provides for the administration of 600nM hADDLs for 46hrs.

The entity of cell death was evaluated by counting the number of apoptotic nuclei (staining with Hoechst 33342) and by the MTT assay (a measure of mitochondrial activity). In our experiments the average of cell viability reduction, measured by MTT assay, comes to 50% in the chronic as well as in the acute protocol. The amount of apoptotic nuclei (mostly pycnotic) is about 20%, consistently with what observed in published reports (Arias et al., 2005).

A biologically relevant anti-Aβ oligomer antibody should, in principle, neutralize the toxicity induced by ADDLs. The anti-oligomer polyclonal antiserum PAb A11 blocks acute toxicity in neuronal differentiated SHSY5Y (Kayed R et al 2003) and protects against chronic toxicity induced by Aβ oligomers in undifferentiated SHSY5Y cells (Ma Q. et al., 2006). Lambert and coworkers (2001, 2006) have described polyclonal and monoclonal antibodies specific for ADDLs, endowed with neutralizing properties.

Testing our scFvs *in vitro* in cellular models was therefore important to establish the experimental conditions for the neutralization of Aβ oligomers cell death or toxicity. Under the established conditions, a number of scFvs demonstrated interesting neutralization properties, and a systematic screen to identify the best lead candidate can therefore be performed.

8.1a. Modulation of hADDLs acute toxicity by administration of scFvs

In order to evaluate the neutralizing ability of scFvs, as inhibitory effects on cell death, a single concentration of 550nM was tested; the protocol provides the coincubation of 2.5μM ADDLs with scFv (or with the 'vehicle' solution, for the negative control) for at least 1h before cell treatment.

The anti-Aβ scFvs tested (scFv A1, A13, Im47) were chosen to be representative of C-terminal and N-terminal binders.

Microscope analysis of nuclei, by *in vivo* staining with Hoechst 33342, allows individuating an altered morphology of nuclei after apoptotic stimuli of ADDLs, in comparison with healthy cells. We focused on the identification and on the count of highly condensed pycnotic nuclei. The quantification has been performed by counting the number of pycnotic nuclei per fields (at least five different fields) of more wells (3-4) for the same experimental point.

We obtained a significant reduction of apoptotic nuclei in the treatment of SHSY5Y cells with scFvs A1, scFv A13 and scFv Im47 (fig.1), in comparison with antibody-untreated control cells and with cells treated with an unrelated scFv (αTL111, anti-Thymosin). Interestingly, the toxicity of hADDLs was almost completely neutralized by scFv A1 and

scFv A13. The results are indicative of a highly specific neutralizing ability of scFvA1 and scFvA13, measured by this test, in the light of the sub-stoichiometric molar ratio scFv:Aβ that is of 1:5 (0.55μM of scFvs and 2.5μM of ADDLs).

These and other scFvs anti-Aβ were tested also by MTT assay, showing a partial protective effect (preliminary results not shown). In the experiments of acute toxicity, the MTT assay, in general, leads to an underestimation of the protective effect of scFvs anti-Aβ, if compared with the quantification of condensed nuclei/field. (approximately 30% less).

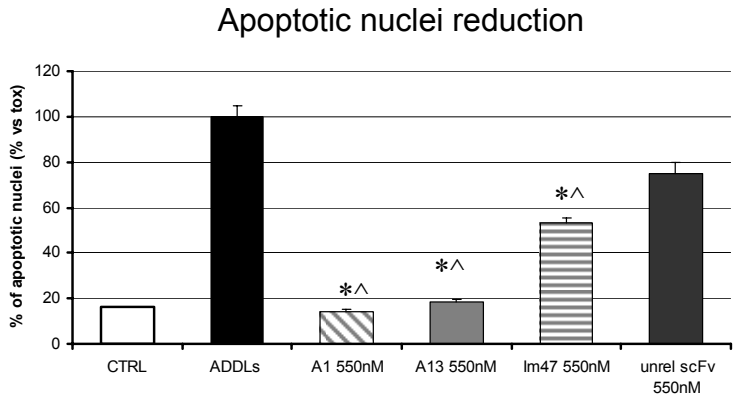

Figure 1. Neutralizing effect of the anti-Aβ scFv A1, scFv A13 and scFv Im47 in acute toxicity protocol, after 16 hrs of apoptosis ADDLs-induced. The values of apoptotic nuclei are expressed as % of apoptotic nuclei in untreated cells (ADDLs treatment, no antibody) versus treated cells (ADDLs treated plus Ab pre-treatment). SHSY5Y cells were exposed to hADDLs (2.5μM), or with hADDLs pre-incubated with anti-Aβ scFvs (550nM) or with the unrelated scFv (anti-Thymosin). All treatments were performed in cell culture medium (D-MEM F12) serum free and without phenol red. Each column represents the mean ± S.E. (bars) of 5 values. * Denotes statistical significance ($p < 0.05$) of apoptotic nuclei values versus ADDLs treatment. ^Denotes statistical significance ($p < 0.05$) of apoptotic nuclei values versus the treatment with the unrelated scFv.

8.1b. Modulation of hADDLs chronic toxicity by administration of scFvs

The effect of anti-Aβ scFvs A1 and A13 on cells survival, in the chronic toxicity protocol, after 46 hrs of hADDLs (600nM) treatment, was studied in the concentration range between 1.5 and 600 nM (1.5nM, 15nM, 150nM, 600nM) (fig.2). The characterization of other anti-Aβ scFvs is in progress.

ScFv were administered to the cell culture 2 hours before hADDLs.

Concerning the amount of protection in terms of rescue of apoptotic nuclei, incubation with scFvs A1 and A13 results in a good neutralization of ADDLs toxicity, because at 1.5nM (with a molar ratio of scFv versus ADDLs of 1:400) they are able to reduce by 60% the number of apoptotic nuclei. Moreover, an unexpected dose-effect behavior was observed. In fact, the reduction of apoptotic nuclei by administration of scFvs A1 and A13 appears to correlate inversely with the scFvs concentration; lowest concentrations of scFvs exhibit a greater protection. The reason for this might be due to an unlikely non specific toxicity of scFvs proteins at higher concentrations for long times (46 hrs), or to the fact that, at higher concentrations, scFvs might lose neutralizing ability, for instance by aggregation.

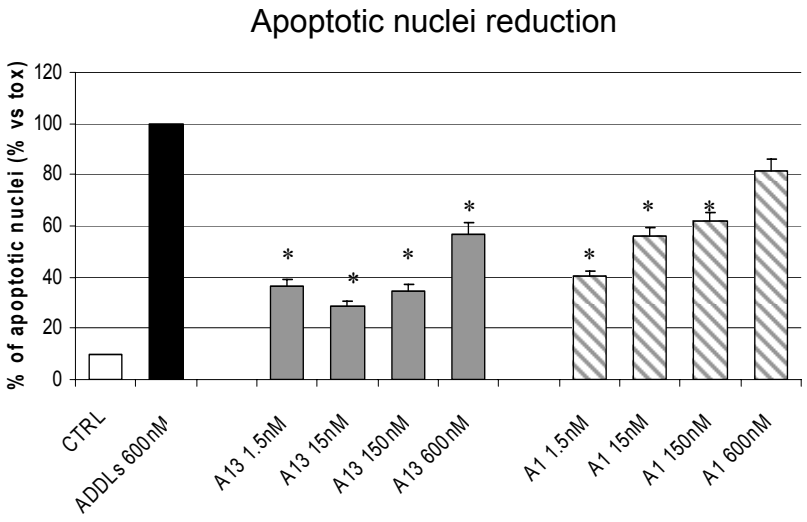

Figure 2. Neutralizing dose-dependent effect of the anti-Aβ scFv A13 and scFv A1 in chronic toxicity protocol, after 46 hrs of ADDLs-induced apoptosis. The values of apoptotic nuclei are expressed as % of apoptotic nuclei in untreated cells (ADDLs treatment, no antibody) versus treated cells (ADDLs treated plus Ab pre-treatment). SHSY5Y cells were treated or not, for 2 hours with four different doses of anti-Aβ scFvs (1.5nM, 15nM, 150nM, 600nM); cells were afterwards exposed to hADDLs (600nM) for 46 hrs. All treatments were performed in cell culture medium (D-MEM F12) serum free and without phenol red. Each column represents the mean ± S.E. (bars) of 5 values. * Denotes statistical significance ($p < 0.05$) of apoptotic nuclei values versus ADDLs treatment.

The protective role of scFvs, as determined by the reduction of apoptotic nuclei, appears to be more significant than that assessed by MTT viability assay (see fig.3). In addition, the neutralizing dose-dependent effect of the anti-Aβ scFv A13 and scFv A1 in the chronic toxicity protocol, as evaluated by MTT assay, showed a different trend in comparison with what observed by the counting of apoptotic nuclei (see fig.3). However, we cannot consider MTT data totally consistent with other experimental observations, probably due to the intrinsic limitations of the MTT assay. In fact, consistently with what recently reported (Hong et al., 2007), we observed that extracellularly applied Aβ oligomers rapidly induce the MTT formazan exocytosis (MTT-FE), with the formation of "needle-like" crystals at the cell surface, whereas, normally, MTT formazan is

accumulated only in the mithocondria of living cells. Thus, using the standard MTT assay procedures, the final quantitative determinations of the solubilized MTT formazan are not completely reliable, as they are flawed by this side-effect specifically induced by exogenous Aβ oligomers.

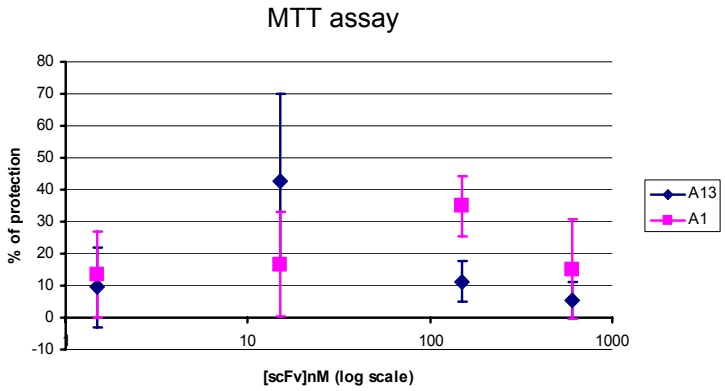

Fig. 3 Dose-dependent neutralizing effect of the anti-Aβ scFv A13 and scFv A1, evaluated by MTT assay, in chronic toxicity protocol, after 46 hrs of ADDLs-induced apoptosis.
SHSY5Y cells were treated or not, for 2 hours with four different doses of anti-Aβ scFvs (1.5nM, 15nM, 150nM, 600nM); cells were afterwards exposed to hADDLs (600nM) for 46 hrs. All treatments were performed in cell culture medium (D-MEM F12) serum free and without phenol red.
The values are expressed as percentage of protection, calculated from the percentage of vitality in different experimental points: % protection = [(scFv+ADDLs) – (ADDLs)] / [(CTRL) – (ADDLs)].
Each point represents the mean ± S.E. (bars) of nine values, from three different experiments. The statistical analysis (one way ANOVA by Student-Newman-Keuls Method) confirms the significance of data in individual experiments ($p<0.05$).

8.1c. Conclusions

Experimental data obtained by administration of scFvs to SHSY5Y cell cultures show that scFvs A1 and A13 are effectively able to modulate ADDLs-induced toxicity, protecting from cell death. The reduction of toxicity is more significant if measured by counting of apoptotic nuclei in acute toxicity. The high anti-apoptotic action of scFvs A1 and A13 at low concentrations in acute toxicity protocol (550nM of scFvs against 2.5μM of ADDLs) is suggesting of a high affinity for hADDLs and of a very specific neutralizing power.

Even more surprising appears the protective role in chronic toxicity protocol: here the administration of as low as 1.5nM of scFvs A1 and A13 results in a significant degree of protection against 600nM of hADDLs.

Recently, in cultured human cortical neuron, different concentration-dependent mechanisms of Aβ oligomers-induced toxicity have been suggested. In fact, 2-10 μM of Aβ oligomers (AβOs) induced rapid and massive neuronal death (with a time lapse that is dose dependent), through a stereotyped succession of cellular changes consistent with the activation of a mitochondrial death apoptotic pathway. At low concentrations (≤1μM) AβOs caused chronic and subtler mitochondrial alterations but minimal cell death (Deshpande et al., 2006).

A recent study, in a protocol of chronic toxicity similar to our experimental conditions (500nM of Aβ oligomers administered for 46 hours to SHSY5Y cells), showed that low concentrations of the anti-oligomer PAb A11 (2ng/ml= ~12.5pM) protect from Aβ oligomers-induced toxicity and prevent the activation of the glycogen synthase kinase-3β (GSK3β) (Ma et al., 2006).

The observations that conformational-specific antibodies can neutralize the AβOs-induced toxicity at concentrations largely sub-stoichiometric (with respect to total Aβ) could suggest for these antibodies shared mechanisms that deserve to be investigated.

We hypothesize that scFvs anti-Aβ target specific conformational epitopes of Aβ, otherwise able to activate, in an unknown way, apoptotic pathways probably both intracellularly and extracellularly.

8.2. Synaptic binding of ADDLs

ADDLs are ligands for particular proteins on neuronal cell surfaces, as demonstrated by experiments in long-term cultures (>21 days) of dissociated rat hippocampal neurons (Lambert et al., 1998). We performed an experimental paradigm, to incubate mature cultures of hippocampal neurons with synthetic or natural ADDLs and then probe with oligomeric-specific antibodies.

ADDLs bind to these neurons with regional specificity, attaching mostly to dendrites and exhibiting a punctate pattern reminiscent of rafts, focal contacts, or synaptic terminals, co-localizing with clusters of PSD-95. Binding occurs within minutes and is localized to the cell surface (being detected without permeabilization of living cells). Hot spots are seen in hippocampal and cortical, but not cerebellar, cultures, a specificity of binding consistent with AD vulnerability (Lambert et al., 1998).

The biological relevance of synaptic binding of ADDLs is today widely accepted because ADDLs are the most synaptotoxic Aβ species and because synaptic dysfunction, occurring early in AD, is considered the best pathological correlate of cognitive decline (Gong et al., 2003; Haass & Selkoe, 2007).

Inhibition of hADDLs synaptic binding by scFvs

The inhibition of ADDLs synaptic binding is therefore a simple, but biologically relevant, experiment to test neutralizing action of antibodies raised against these synaptotoxic Aβ species.

We performed an experimental protocol in which ADDLs, or ADDLs preincubated with scFvs, are administered to primary rat hippocampal neurons. We used 300nM of

hADDLs, preicubated or not with 600nM of scFvs A1 or A13. The extent of ADDLs synaptic binding was evaluated by immunofluorescence using the anti-oligomer PAb A11 and a MAb anti PSD-95 (see supplemented fig.12).

Comparing areas of similar density of PSD-95 positive spots, focusing mainly on dendrites, we performed a qualitative analysis of A11-positive spots density. Quantitative analyses are in progress using MethaMorph and ImageJ (NIH) software.

Our qualitative analysis confirms that synaptic binding can be significantly reduced by prior incubation of ADDLs with scFv A13 and with scFv A1 (see supplemented fig.13).

8.3. Nerve growth factor deprivation causes activation of the amyloidogenic route and release of Aβ in PC_{12} cells: inhibitory effect of scFv A13

As a further evaluation of the protective role of selected scFvs anti-Aβ, we exploited a new cellular model that links neurotrophic deficits and/or deprivation to the activation of an amyloidogenic pathway. This model is based on PC_{12} cells differentiated with NGF.

PC_{12} cells, a clonal cell line derived from rat pheochromocytoma, respond to NGF treatment by undergoing mitotic arrest and differentiation into a neuronal-like phenotype (Greene et al., 1976). These neurons die via an apoptotic mechanism when NGF is withdrawn from the culture (Edwards et al., 1994).

Recently we demonstrated that NGF deprivation causes activation of the amyloidogenic route and release of Aβ peptides in PC_{12} cells (Matrone et al., submitted paper). Moreover, in this cellular model, we demonstrated the causative role of endogenously over-produced and secreted Aβ in triggering apoptosis. In fact, apoptotic death and Aβ production are completely inhibited by β and γ secretase inhibitors, which also favour maintenance of PC_{12} morphology and neuritic network. On the contrary, Aβ production is activated by inhibitors of TrkA, the high affinity receptor of NGF.

These findings indicate that the antiapoptotic action of NGF is tightly linked to the processing of the amyloid precursor protein APP, and suggest that NGF neurotrophic signalling deficits may have direct relevance to the onset of Alzheimer disease, via the activation of aberrant APP processing. Similarly, a previous study, carried out in our laboratory in AD11 transgenic mice, showed that NGF deprivation, via endogenous cerebral expression of NGF-antibodies, induced a neuropathological and behavioural

AD-like phenotype (Capsoni et al., 2000), providing a direct evidence linking reduced NGF signalling and/or activity in the brain to the activation of an amyloidogenic route and Alzheimer neurodegeneration (Capsoni et al., 2002).

ScFv A13 was chosen to evaluate its ability to inhibit cell death in this PC_{12} cell model. Before describing the results obtained, I will describe the properties of this new cellular model.

8.3.1 Cellular model

a. Overproduction of endogenous Aβ peptides

The first experimental observations showed that the progressive death of PC_{12} differentiated cells, when NGF and serum were withdrawn from the culture, was accompanied by a parallel increase of thioflavine (ThT) binding proteins in the medium (*figure1A-B*). Notice that when the extent of ThT binding (*table*) was referred to the corresponding cell death (measured by MTT assay), the ratio (ThT/MTT) changed from a value of 1.0 to a value of 10 after 72 hrs of apoptosis induction (because ThT values increase and MTT values decrease).

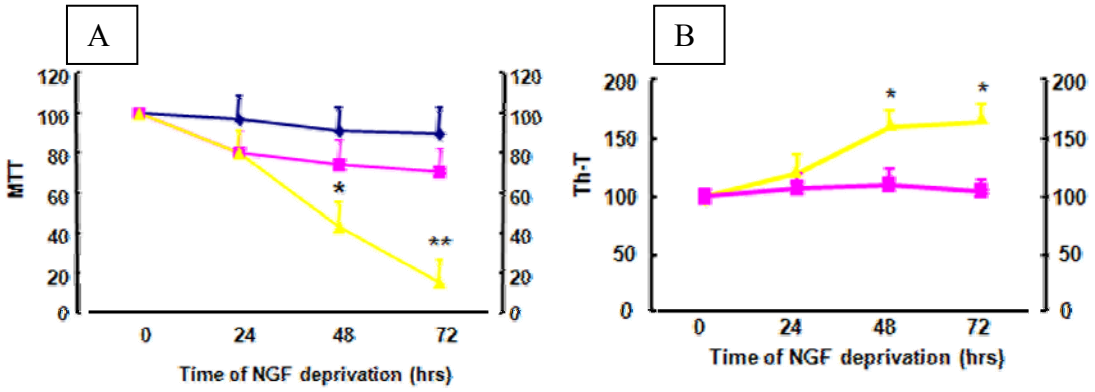

Figure 1*: Panel A* shows the effect of NGF deprivation on PC12 survival evaluated by the MTT procedure. Viability of PC12 incubated in serum and NGF (---♦---), deprived of serum (---■---; *+NGF*) and deprived of serum and NGF (---Δ---;*−NGF*) for *24, 48, or 72 hours* are shown in the figure. The values were expressed as percentage of the values for PC12 control cells (*time 0)*
Panel B reports the values of thioflavine T (ThT) binding proteins in the secreted serum-free medium of PC_{12} differentiated cells (*+NGF*) and in the medium deprived of serum and NGF (*-NGF*) for 24, 48 and 72 hrs (*+NGF,* ---■---; *-NGF,* --Δ---). The corresponding ratio between the values for ThT and MTT assays is represented in the *table below*. The data are expressed as percentage of PC_{12} control cells (*time 0*).
Each point represents the mean ± S.E. (bars) of nine values.
* denotes statistical significance (p <0.05) versus time 0; ** denotes statistical significance (p < 0.001) versus 0 and 24 hrs of apoptosis.

Time (hrs)	**Th-T**		**Th-T/MTT**	
	+NGF	***-NGF***	***+NGF***	***-NGF***
0	100	100	1	1
24	110±7.9	120±12.3	1.25±0.11	1.5±0.12
48	112±10.1	155±17.2*	1,45±0.17	3.5±0.23*
72	109±12.3	160±9.5 *	1.55±0.2	10.6±0.32 **

Thioflavine T (ThT) binds to proteins that undergo a β-sheet transition and cannot, therefore, be taken as a direct measure of Aβ production and its polymeric aggregation. In order to assess the actual presence of Aβ peptide(s) in ThT-positive structures present in the culture medium at different times after NGF withdrawal, cells were harvested and collected, the culture medium was centrifuged and the resulting "fibrillar" pellet was

dissolved in 70% formic acid and Tris 2M and analyzed by Western Blot and ELISA-sandwich assay (*Figure2*).

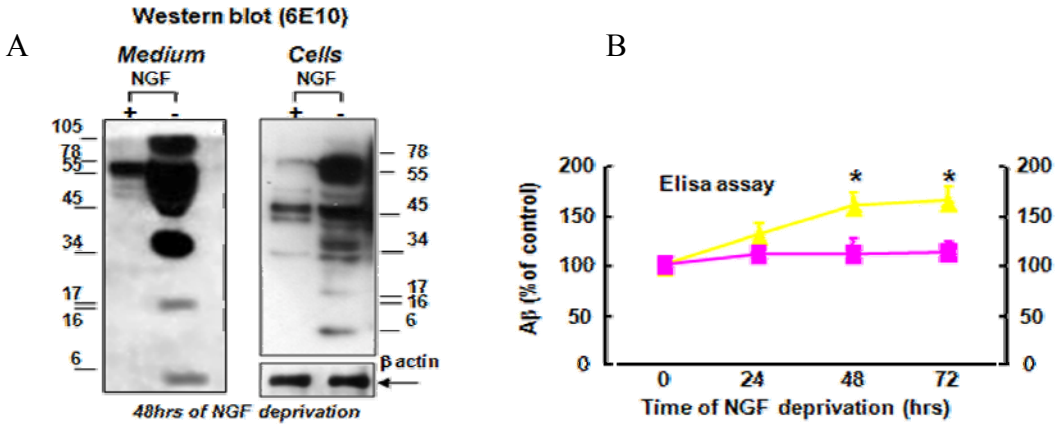

Figure 2*:* **A)** Western blot analysis of $A\beta_{1-42}$ in PC_{12} cells and in the corresponding culture media pellets after 48 hours apoptosis. 10μg of total protein extracts were loaded on Tricine gels and probed with monoclonal anti Aβ antibody (6E10). The data are representative of three distinct experiments.
B) Elisa assay of $A\beta_{1-42}$ amount in pellets derived from culture media of NGF-differentiated PC_{12} deprived of serum or deprived of serum and NGF for 24, 48, 72 hours. The values of $A\beta_{1-42}$ content are referred to total protein amount of each sample and are expressed as percentage of PC_{12} control cells (*time 0*). Each point represents the mean ± S.E. n=4. * denotes statistical significance ($p < 0.05$) versus time 0.

Figure 2A shows a Western Blot analysis of PC_{12} cells and of the corresponding aggregates obtained from culture medium carried out with a monoclonal anti-Aβ antibody (6E10) after 48 hours of apoptosis induction. As it can be seen, NGF withdrawal induces a marked increase of Aβ antibody cross reacting polypeptides of different size in the cells and in the medium (*-NGF*) as compared to the corresponding control samples (*+NGF*). As shown in *figure 2B*, the amount of formic acid soluble aggregated Aβ, as determined by ELISA, closely parallels the amount of ThT binding proteins. PC_{12} cells deprived of serum, but still containing NGF, release a small, constant amount of $A\beta_{1-42}$ in the medium, but when deprived of both serum and NGF, they produced a much larger

amount of Aβ, that peaked at 48 hrs. It is worth noting that also the content of APP protein increases during the same time period of apoptosis induction, indicating that the larger production of Aβ is paralleled by a significant increase of its precursor (*data not shown*). The data reported also demonstrate that these fibrils, containing a large amount of $A\beta_{1-42}$, can be only partially dissolved with a strong detergent such as 10% SDS and need of a treatment with 70% formic acid, generally employed to dissolve senile plaques from AD brains, to be completely solubilised.. In *figure 3A-B* are shown Elisa assay of samples obtained from culture medium of PC_{12} cells for $A\beta_{1-42}$ and $A\beta_{1-40}$. The medium was ultracentrifuged and partially solubilised in 10% SDS. The remaining pellet is totally dissolved in 70% formic acid. $A\beta_{1-40}$ and $A\beta_{1-42}$ peptides are detectable in both the soluble and insoluble fractions, but $A\beta_{1-42}$ amount is higher than $A\beta_{1-40}$. Furthermore, the level of $A\beta_{1-42}$ detected in the insoluble fraction resulted approximately twice than that present in the 10% SDS solution. By contrast, $A\beta_{1-40}$ levels result homogeneously distributed in the different fractions.

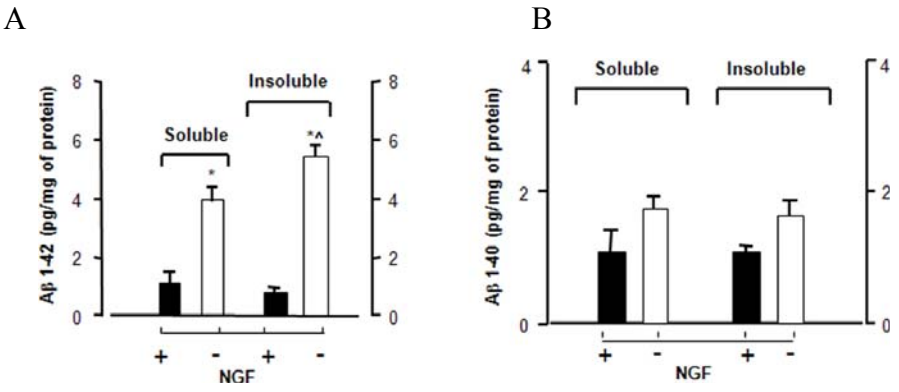

Figure 3. A and **B** Elisa assays of $A\beta_{1-42}$ and $A\beta_{1-40}$, respectively, of pellets derived from culture medium after 48 hrs of apoptosis dissolved with 10% SDS (*soluble*) and subsequently with 70% formic acid (*insoluble*). The values of $A\beta_{1-42}$ and $A\beta_{1-40}$ contents are referred to total protein of each sample and are the average of 3 independent experiments. *denotes statistical significance ($p < 0.05$) of SDS 10% soluble fraction versus *+NGF*; ^denotes statistical significance ($p < 0.05$) of SDS 10% insoluble fraction versus the corresponding SDS 10% soluble fraction.

Finally, the analysis of SDS 10% insoluble fraction by MALDI-TOF analysis (*data not shown*) completely validate the presence of $A\beta_{1-42}$ in the medium of PC_{12} cells after NGF deprivation.

b. Modulation of Aβ over-production

Aβ peptides derive from APP precursor by its cleavage by beta and gamma secretases. In our model, as shown in *figure 4*, inhibitors of β and γ secretases largely block not only the increase of thioflavine binding proteins but, very significantly, also PC_{12} cell death, underlining the tight correlation between NGF deprivation, pathological APP processing and cell death of PC_{12} cells. γ and β-secretase inhibitors, separately added, are able to exert a strong but partial inhibition, while, together, they fully restore cell viability and reduce fibril production to control levels. Moreover, the overall morphology and neuritic network of PC_{12} cells is maintained when β and γ secretase inhibitors are added in the serum free medium deprived of NGF (*data not shown*).

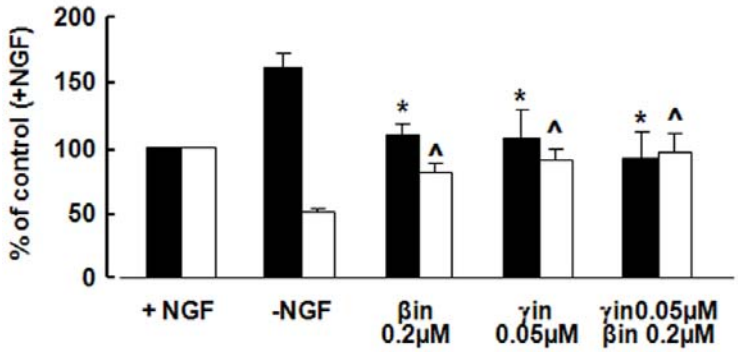

Figure 4. Effect of γ and β secretase inhibitors on PC_{12}cell survival and ThT release, evaluated by MTT and ThT assay in NGF-differentiated PC_{12} cells after 48 hrs of NGF withdrawal. The values of MTT (*white bars*) and ThT (*black bars*) are expressed as % of control cells. PC_{12} differentiated cells deprived of serum (*+NGF*) and serum and NGF *(-NGF*) were exposed to γ and β secretase inhibitors. All the values are expressed as percentage of control cells (*+NGF*). Each column represents the mean ± S.E. (bars) of 6 values. * Denotes statistical significance ($p < 0.05$) of ThT values versus *–NGF*. ^Denotes statistical significance ($p < 0.05$) of MTT values versus *–NGF*.

In order to start dissecting the involvement of NGF signalling, through the NGF tyrosine kinase TrkA receptor in the Aβ production and in cell death, both parameters were assessed after incubation with a Trk-A inhibitor, K252-a (Berg et al., 1993). As shown in *figure 2C*, after 2 hrs of incubation, 100 nM K252-a induce 60% of cell death and the additional incubation with NGF (50ng/ml) fails to revert this effect, confirming a significant inhibition of Trk-A receptor signalling. Moreover, after 2 hrs of incubation with K252-a, the extent of thioflavine binding structures increases by 50%, a value identical to that observed in PC_{12} cells undergoing apoptosis after NGF withdrawal. Finally, the combined treatment with β and γ secretase inhibitors, totally blocks cell death and thioflavine binding production, further indicating that the NGF-high affinity receptor is involved in controlling APP processing and Aβ production.

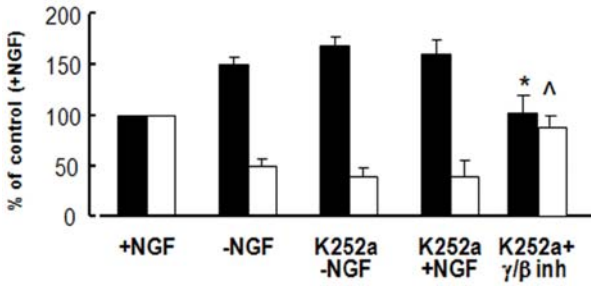

Figure 5. Effect of 100 nM K-252a on cell viability and ThT binding and the effect of γ and β secretase inhibitors on the proapoptotic action of K-252a. After 2 hrs of incubation with K-252a, cells were washed three times and re-exposed to NGF 50ng/ml for 48 hrs in some samples and to γ and β secretase inhibitors for 48 hrs. All the values were expressed as percentage of control values (*+NGF*) and represents the mean ± S.E. (bars) of 5 values. * Denotes statistical significance ($p < 0.05$) of ThT assay versus K-252a –NGF (black bars) and ^denotes statistical significance ($p<0.05$) of MTT assay versus K-252a –NGF (white bars).

c. Conclusions

The studies here reported demonstrate that apoptosis following NGF withdrawal is accompanied by activation of an amyloidogenic route with overproduction and release of Aβ and its aggregation into thioflavineT-positive structures.

The free and organized overproduced Aβ structures can be quantified and are easily detectable by the thioflavine binding procedure. ELISA as well as Western blot assays demonstrate that these polymers contain large amounts of Aβ in a ratio relatively comparable to that observed by the thioflavine measure.

The finding that inhibition of the Aβ production by a combined treatment with β and γ secretase specific inhibitors is accompanied by a parallel inhibition of apoptosis, further underlines the tight correlation between NGF withdrawal and APP processing with Aβ formation. This conclusion is also supported by the finding that treatment with a TrK-A inhibitor, K-252a, causes a marked reduction of cell survival and an increase of Aβ production that is fully counteracted by a combined treatment with the two secretase inhibitors. Previous studies have shown that cortical or cerebellar granule neurons undergoing apoptosis produce Aβ peptides (LeBlanc, 1995; Romano et al, 2003) and the latter affect healthy neurons thus generating a sort of autocrine toxic loop (Marques et al., 2003). The present study further demonstrates that this toxic loop may also be operative in PC_{12} differentiated cells, and provides evidence for a direct causal link between NGF withdrawal, APP abnormal processing and Aβ toxicity, as suggested by the antiapoptotic action of γ and β secretase inhibitors and of the anti-Aβ antibodies.

8.3.2 Antibodies treatments: the protective role of scFv A13

In order to assess whether the Aβ peptides, and in particular their particular conformation or oligomeric aggregation, produced after NGF removal, play a role in the cell death process, NGF-deprived PC_{12} cells were treated with scFv A13 and with MAb 4G8 as a reference.

The well established MAb 4G8, recognizes the linear epitope aa18-22 of Aβ, regardless of its quaternary state (monomeric, oligomeric or fibrillar); scFv A13, as discussed above, similarly to the other SPLINT-selected scFvs anti-Aβ, recognizes a conformational epitope (C-terminal), preferentially exposed in Aβ oligomeric aggregates. In addition, in the previously described cellular bioassays (ADDLs-induced toxicity in SHSY5Y cells, and synaptic binding of ADDLs in hippocampal primary cultures), scFv A13 resulted one of the best candidates among the panel of scFvs anti-Aβ tested.

The effect of the anti-Aβ scFv A13 on cells survival and ThT "release" after 48 hrs of NGF deprivation was studied in the concentration range between 1 and 2 nM (*Figure 6*) (concentrations established so that the molar ratio of scFv versus total Aβ (measured by ELISA assay) was between 1:5 and 1:3).

scFv A13, at 1.5 nM, almost totally rescues the cells from apoptotic death, and inhibits Th-T "release", in comparison with similar concentrations of an unrelated scFv (anti-thymosin αTL111).

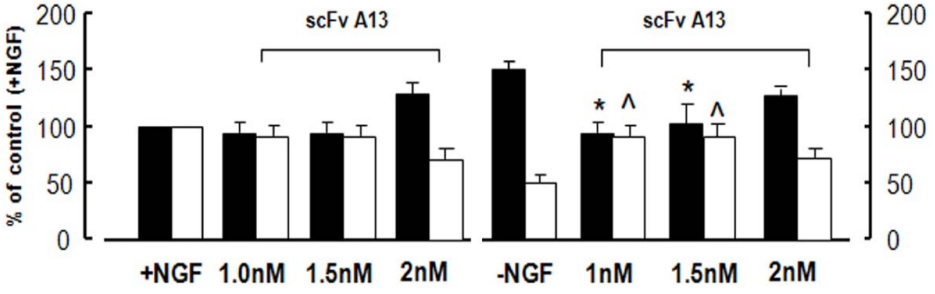

Figure 6. Effect of scFv A13 on PC_{12} cells deprived for 48hrs of serum and NGF evaluated by the MTT (*white bars*) and ThT (*black bars*) procedure, in the dose range from 1 to 2 nM. The values were expressed as percentage of the corresponding PC_{12} control cells (*+NGF)*
Each point represents the mean ± S.E. (bars) of nine values. *denotes statistical significance ($p < 0.05$) versus ThT values versus *-NGF*; ^ denotes statistical significance ($p < 0.05$) versus MTT values versus *-NGF* .

Both anti-Aβ antibodies scFv A13 and MAb 4G8 largely inhibit both fibril production and PC_{12} cell death (*figure 7*). It is noteworthy that the conformationally selective antibody scFv A13 is protective at concentrations (1nM) lower than those at which MAb 4G8 is effective (6.7 nM).

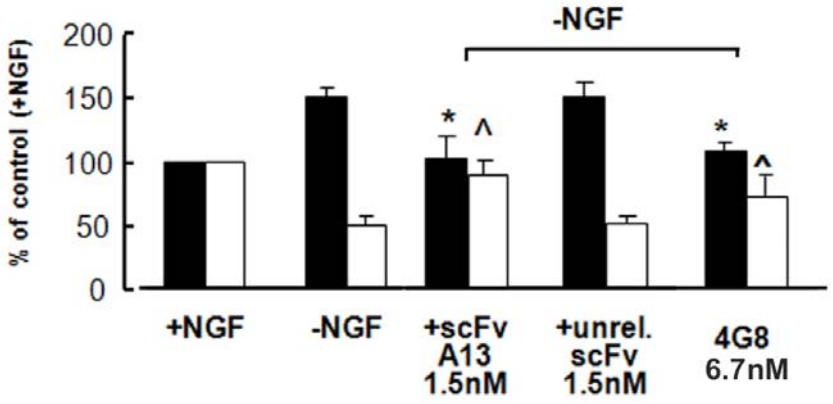

Figure 7. Inhibitory effect of the anti Aβ scFv A13 recombinant antibody and of the anti-Aβ MAb 4G8 on cell viability and Aβ production in NGF-differentiated PC_{12} cells after 48 hrs of apoptosis. The values of MTT (*white bars*) and ThT (*black bars*) are expressed as % of control cells. PC_{12} differentiated cells deprived of serum and NGF *(-NGF*) were exposed to scFv A13 (1.5nM) or to an unrelated scFv (anti-Thymosin) (1.5nM) or to MAb 4G8 (6.7nM). All the values are expressed as percentage of control cells (*+NGF*). Each column represents the mean ± S.E. (bars) of 6 values. * Denotes statistical significance ($p < 0.05$) of ThT values versus *–NGF*. ^Denotes statistical significance ($p < 0.05$) versus of MTT values versus*–NGF*.

The reduction of Aβ production after the treatment with this antibody became more evident by Western Blot and Elisa assay (*figure 8A-B*). Western Blot (*figure 8A*) shows that the treatment with scFv A13 induces a marked decrease of Aβ-antibody cross-reacting polypeptides in the medium of NGF-deprived cells (*−NGF*, after 48 hours of NGF withdrawal) as compared to the corresponding control samples (*+NGF*). We observed a significant reduction of Aβ-immunoreactivity at 30-60 kDa; moreover, the medium of A13-treated cells (*−NGF*) does not show more the bands higher than 60 kDa and lower than 30 kDa, included the faint band at 4kDa (probable Aβ monomer).

Similarly, ELISA assay (*figure 8B*), used to measure the amounts of Aβ1-42 in pellets derived from culture media (SDS soluble and insoluble), shows that scFv A13 determines a total reduction of Aβ1-42 in NGF-deprived cells (from ~8pg/mg of total proteins, down to ~1.5pg/mg of total proteins) at the levels of control cells (+NGF).

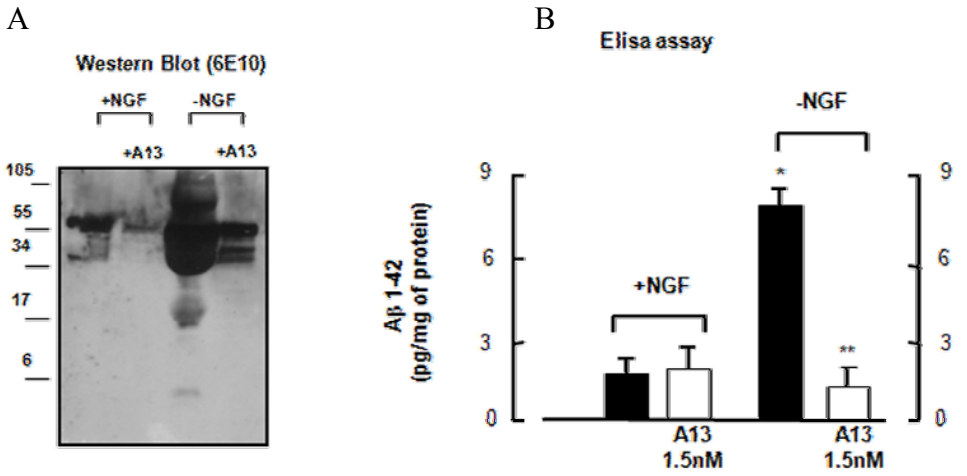

Figure 8: A) Western blot analysis for Aβ in the culture medium of PC_{12} control cells and after 48 hours apoptosis exposed or not to scFv A13 antibody (1.5nM). 10 μg of total protein extracts were loaded on Tricine gels and probed with monoclonal anti Aβ antibody (6E10). The data are representative of three distinct experiments.
B) ELISA assay of $Aβ_{1-42}$ amount in pellets derived from culture media of NGF differentiated PC_{12} deprived of serum or deprived of serum and NGF for 48 hours and treated with or without scFv A13 antibody (1.5nM). The values of $Aβ_{1-42}$ content are referred to total protein amount of each sample and are expressed as percentage of PC_{12} control cells (*+NGF*). Each point represents the mean ± S.E. n=3. * denotes statistical significance ($p < 0.05$) versus *+NGF,* **denotes statistical significance ($p < 0.001$) versus *-NGF*.

The complete rescue from apoptosis and the overall reduction of Aβ species and Th-T positive structures, after 48 hours of NGF deprivation, can suggest for scFv A13 some mechanisms of neuroprotection. ScFv A13 can probably recognize Aβ and/or early Aβ oligomers, avoiding their superior aggregation and/or neutralizing them as activators, via an autocrine toxic loop, of an amyloidogenic route that can trigger apoptosis through the overproduction and aggregation of Aβ peptides.

The scFv A13 is protective at concentrations (1nM) lower than those at which MAb 4G8 is effective (6.7nM): one hypothesis could be that scFv A13 neutralizes early, low concentrated but conformationally critic Aβ species only partially recognized by MAb 4G8, in the medium of NGF-deprived cells. We could hypothesize also a preferential intracellular internalization of scFv A13, in the light of a new mechanism of action recently suggested for anti-Aβ antibodies (Tampellini et al., 2007).

Investigating the mechanism of action of scFv A13, can help the discovery of a new link between reduced NGF signalling and/or activity, and the activation of an amyloidogenic route.

DISCUSSION

1. Anti-Aβ scFvs: SPLINT libraries as a good source of unique recombinant antibodies against a relevant antigen in AD pathology

Targeting Aβ pathological species, in particular Aβ oligomers, is one of the primary hot-topics of actual research in AD and antibodies represent elective tools to target, with different purposes, this relevant antigen.

Here, we discussed the novel generation of a panel of 18 recombinant anti-Aβ antibodies, in the format of single chain fragments (scFvs), using the novel approach of Intracellular Antibody Capture Technology (IACT) developed in our laboratory (Visintin et al, 1999, 2002, 2004). Anti-Aβ scFvs were selected from recently derived libraries, Single Pot Libraries of INTrabodies (SPLINT) (Visintin et al., 2004a), that are repertoires of recombinant scFvs engineered by amplifications and assemblies of VH and VL genes of immunoglobulins of different source. In these libraries, each scFv clone derives from a random VH-VL pairing of natural VH and VL immunoglobulin regions.

Two different SPLINT libraries were used in this work:

- a naïve library derived from a non-immunized source of natural VH and VL mouse regions genes (Visintin et al, 2004a); this library, of complexity of ~10^7 different scFv clones, was constructed and kindly provided by Dr Visintin, (LayLineGenomics, Trieste);
- an immune library derived from a source of natural V genes from spleen lymphocytes of mice immunized with human Aβ42 (Meli et al, 2005, 2006). The construction of this immune library, of complexity of ~10^6 different scFv clones, was here described for the first time.

Antibody libraries can be engineered in vitro, displaying a complexity comparable to that of the natural immune system of mammals, so that theoretically their repertoire is complete and every imaginable antibody may be derived. In general, the larger the library, the higher the chance is to isolate specific antibodies with good binding characteristics (in terms of affinity) (Perelson & Oster, 1979; Griffiths et al., 1994). It has been shown that libraries containing about 10^7 independent clones are sufficient to yield antibodies to proteins with affinities in the low micromolar range (similar to those obtained in a primary immune response in vivo), while larger antibody libraries of 10^9 – 10^{10} clones yielded specific antibodies with affinities in the nanomolar range (similar to those obtained after a secondary immune response) (Griffiths et al., 1994; Vaughan et al., 1996; Sheets et al., 1998).

As discussed, the immune library, even though smaller by a factor of 10 in comparison with the naïve library (10^6 versus 10^7), has been a good source of specific scFv antiAβ because of the immunization enrichment.

In addition, regarding the SPLINT libraries, as discussed by Visintin and coworkers (2004a), the real diversity of the library could be higher than the number of yeast transformants (10^6), which provides the nominal "cellular" diversity: this peculiarity could be achieved by yeast cells that, after transformation, can express more than one scFv. The final diversity may or may not result after further recombination events and after segregation of different scFvs in daughter cells. This latter event, could easily contribute to an increase of the real diversity by a factor ≥10 leading therefore, under the selective pressure of IACT, to the selective isolation of antigen-specific scFv fragments.

Even though we have not yet performed affinity measurements for anti-Aβ scFvs, we know from previous studies in our group that affinities of other scFvs selected from naïve SPLINT libraries are in the range of nM.

The naïve library is an un-biased source of scFvs and results an excellent source of antibodies against a wide panel of different antigens tested (Visintin et al, 2004a) and also, as demonstrated in this thesis, against Aβ42. The specificity of preferential epitope (N-terminal) recognized by scFvs selected from the immune library suggests that Aβ immunization could be a good strategy to improve, in a biased way, a library of recombinant scFvs against this antigen.

Sequence analysis confirms the high similarities between scFvs selected from the Immune library, suggesting a selective enrichment of VL and VH natural regions amplified from lymphocytes of active-immunized mice, resembling a real mechanism of oligoclonal response of the immune system to the Aβ antigen. A single functional consensus sequence that might represent a fingerprint of the CDR sequences against Aβ has not been identified. In any case, this work provides the first systematic sequence data on the antibodies generated against Aβ.

It is noteworthy that, even though scFvs anti-Aβ have been selected as stable intracellular binders, they maintain the ability to bind Aβ species *in vitro* in different conditions, from all the *in vitro* tests incubations to the cell cultures treatments, suggesting a significant stability and solubility. Even though we have not yet performed chemico-physical and thermodynamic stability characterization of the anti-Aβ scFvs proteins, high stability and

solubility are characteristics improved by the conditions of intracellular expression and selection employed with the IACT technology.

In all of the *in vitro* characterizations of the scFv binding ability, we have not verified a distinctive advantage for scFvs selected from the immune library in comparison to scFvs deriving from the naïve library, even with two 'naïve' scFvs (A1 and A13) showing interesting biological properties in cellular bioassays.

The biological relevance of scFvs have been demonstrated *in vitro* by experiments using them as recombinant proteins externally administered, in different cellular models.

Results show a good ability of scFvs A13 and A1 to reduce significantly the synaptic binding of synthetic ADDLs to the neuritic processes of hippocampal neurons. ScFvs A1 and A13 (at very low concentrations 1.5nM) are also able to reduce cell death ADDLs-induced in SHSY5Y cells.

ScFv A13, in a cellular model (PC12 neuronal differentiated cells) of endogenous overproduction, secretion and aggregation of Aβ after NGF deprivation, protects PC12 cells from neuronal apoptosis and significantly reduces Aβ42 and the ThT positive structures accumulation in the medium. ScFv A13 have been used ~10 fold less concentrated than the "gold-standard" MAb 4G8 (Matrone et al, submitted paper). The molecular mechanisms of action of this neuroprotective activity of A13 are under investigation, but probably scFv A13 acts as blocker of early "malicious" Aβ oligomers, significantly reducing their toxicity but also reducing their further aggregation in large ThT positive fibrils.

In conclusion, we have described the isolation and characterization both *in vitro* and *in vivo* of a large panel of oligomeric-specific anti-Aβ scFvs, taking advantage of the

IACT/SPLINT technology. The ability to recognize *in vivo* produced Aβ species and also to neutralize them is directly related to the selection strategy (IACT), that enriches in selective binders of *in vivo* (in the yeast cytoplasm) folded and probably aggregated Aβ bait.

2. Conformation specificity of anti-Aβ SPLINT-selected scFvs

Different results obtained with several experimental approaches suggest that anti-Aβ scFvs selected from SPLINT libraries show conformation specificity and preferential binding ability versus Aβ oligomers.

The *in vivo* data obtained from SPLINT scFvs selection in yeast, in particular the IVEM (in vivo epitope mapping) results, suggested also a reliable conformational hypothesis in order to explain the lack of recognized epitopes in the central part of Aβ peptide. The conformational hypothesis is consistently supported by strictly related studies in yeast, as below discussed.

The results from the first ELISA assay, performed with different Aβ species directly coated in solid phase, showed that SPLINT-selected scFvs were specifically able to recognize human Aβ42 oligomers 3-5 fold better than humanAβ42 fibrils, and up to 10-20 fold better than human Aβ42 monomers.

Subsequently, the more sensitive NeutrAvidin ELISA assay showed that scFvs anti-Aβ recognizes conformational structural epitopes probably more exposed in Aβ42 oligomers;

Aβ oligomers in this assay were also recognized by the well established PAb A11 anti-oligomer antibody (Kayed et al., 2003).

Immunoprecipitation results showed that the two anti-Aβ scFvs (A1 and B2) can differentially bind Aβ42 soluble species under solution conditions which could favour the native folding conformations of Aβ monomers and oligomers.

The data obtained by the recognition of *in vivo* produced Aβ, in human AD brains, suggested also a specificity of anti-Aβ scFvs for Aβ deposits, in line with previous experimental reports of other anti-oligomer antibodies tissue-immunoreactivity. Moreover, in AD brains the ability of different scFvs to recognize various immunoreactive structures (cells, pericellular, intracellular and extracellular deposits, blood vessels) and to show distinct labeling patterns, suggested a peculiarity of each scFv, in spite of their common ability to recognize Aβ antigen in biochemical assays *in vitro*. This interesting ability of SPLINT-selected anti-Aβ scFvs could be strictly linked to the peculiarity not only of Aβ itself as misfolded antigen, but also of the complex 'scenario' in the pathological tissues. In fact, it is known that Aβ, *in vivo* can interact with a variety of cofactors including metals, glycosaminoglycans, glycoproteins such as serum amyloid P and apolipoprotein E, and constituents of basement membranes such as perlecan, laminin, and agrin (Alexandrescu, 2005). These "pathological chaperones" have effects that range from mediating the rate of amyloid fibril formation to increasing the stability of amyloid deposits, and may contribute to the different "immunoreactivity properties" of Aβ deposits in human brains (and in general of Aβ aggregates in biological samples). Because of in the literature are not yet available complete data on the Aβ

oligomeric immunoreactivity in human and animal tissues, scFvs anti-Aβ SPLINT-selected could be a relevant tool to characterize this interesting aspect of AD pathology.

It is likely that the presence of 'chaperones' bound to Aβ in biological samples (as brain extracts) could preserve particular conformations of Aβ immunoreactive species when analyzed by Immunoblot procedures. As observed in the preliminary DotBlot and WesternBlot analysis, some scFvs SPLINT-selected show weak reactivity versus Aβ species in these assays. In particular, scFvs can recognize only natural Aβ oligomers (from AD brain extracts) but not synthetic Aβ preparations well recognized in other *in vitro* assays. Consistently with experimental observations of others (Kayed et al., 2003), it is likely that immunoblot (IB) procedures do not preserve native conformations of Aβ oligomers, especially if synthetic, even if they are considered SDS stable species. Changes in the native conformation of Aβ oligomers in IB analysis could compromise the detection ability of conformational specific antibodies as observed with the well established polyclonal anti-oligomer PAb A11 (Kayed et al., 2003), and with the SPLINT selected scFvs.

In the above-discussed cellular bioassays it is likely that the neuroprotective actions of scFvs A1 and A13 are related to their ability to target pathological assembled species, through the recognition of specific conformational epitopes.

ScFv A1 and A13 are significantly able to neutralize the toxicity induced by externally administered ADDLs. We have observed that scFvs A1 and A13, used at concentrations largely sub-stoichiometric (with respect to the concentrations of total Aβ), similarly to the conformational-specific polyclonal antibody PAb A11 (Ma et al. 2006), could be able to

neutralize the Aβ oligomers-induced toxicity, suggesting for these antibodies shared mechanisms.

In addition, it is likely that, in the above-described model of amyloidogenesis in PC12 cells, the ability of scFv A13 to block Aβ aggregation and cell death could be related to the specific targeting of spontaneously misfolded and early endogenously produced Aβ peptide.

3. IACT selection from SPLINT libraries: might Aβ-bait determine conformation specificity of selected scFvs?

The success of the selection campaign in isolating a large number of scFv fragments with biased specificity for Aβ oligomers was largely unanticipated. The high proportion of conformation-specific anti-Aβ isolated leads to postulate that the Aβ bait itself might be the basis for the high enrichment of anti-Aβ oligomers in the selected panel of scFv. If so, how could the Aβ bait have influenced and biased the downstream antibody selection process?

3.1 Experimental reports supporting Aβ folding and aggregation in yeast cells

Different studies have demonstrated that Aβ bait and Aβ prey can interact in two hybrid system (Hughes 1998). It has been demonstrated also that this ability to interact is related to crucial residues (Festy et al 2001) related to the structure of Aβ. So, it has been supposed that Aβ can aggregate with specifically structured scaffold in yeast two hybrid

system. Moreover, aggregation for prion endogenous proteins and for other aggregating protein ectopically expressed (synuclein, huntigtin) has been very well demonstrated in yeast cell cytoplasm and mediated by specific chaperone proteins. Recently also the modulation of Aβ oligomerization in yeast cytoplasm have been related to the activity of chaperone proteins (Bagriantsev and Liebman, 2006)

3.1a Beta-amyloid in two-hybrid system

Two-hybrid system as a model to study the interaction of β-amyloid peptide monomers was explored for the first time by Hughes and coworkers (Hughes et al., 1996). Afterwards, several interactors of Aβ were successfully found through two-hybrid system (Yan et al., 1997; Hughes et al., 1998). Moreover, Festy and coworkers (2001) showed that Aβ-Aβ interactions in two-hybrid can be disrupted by several mutations in the Aβ sequence.

All these studies were preparatory to our approach of IACT selection, providing the rationale feasibility basis for the aim of using the Aβ bait to select for anti-Aβ oligomeric-specific antibodies. The results of planned experiments were successful beyond expectations. At the same time, they supported the hypotheses of a conformational structure of the Aβ bait.

The first finding that mutations in Aβ sequence (F_{19} F_{20} > T_{19} T_{20}) compromise Aβ-Aβ interactions (Hughes et al. 1996) were consistent with *in vitro* observations made by others: in fact, previously reported data showed that a well preserved hydrophobic core around aminoacids 17–24 was important for the formation of β-sheet structure and amyloid properties (Hilbich et al., 1992).

Interestingly, Festy and coworkers (2001) designed by molecular modeling and tested by the two-hybrid approach, series of mutations spread all over the sequence of Aβ1-42 and changing the distribution of hydrophobicity and/or the spatial hindrance. By molecular design consistently with experimental models, the sequence of the amyloid peptide can be split into four clusters, two hydrophilic (1-16 and 22-28) and two hydrophobic (17-21 and 29-42). Screening of mutations demonstrated that the C-domain (residues 29-40 (42)), the median domain (residues 17-22) and the N-domain (1-16) are all crucial for interaction. This demonstrated that almost all fragments of the amyloid peptide except an intermediate loop (residues 23-28) are important for the native interaction. The native fold of Aβ could be stabilized in Aβ–Aβ complexes. It is likely that the secondary structure of Aβ (probably β-sheet) showing a high susceptibility to mutations, should have a low stability; thus, the formation of tertiary structures (Aβ-Aβ complexes) could be strongly favored.

These data supported a conformational hypothesis of Aβ *in vivo*, in the two-hybrid format in the yeast nucleus, even though Aβ is the C-terminal fragment of the larger fusion protein LexA-Aβ bait.

3.1b Beta-amyloid oligomerization in yeast cells

Recently, Bagriantsev and Liebman (2006) described a new yeast model system focused on the initial stages of Aβ42 oligomerization, not related to the two-hybrid system. They exploited as reporter protein, the yeast translational termination factor Sup35p; this is also a protein that can form self-propagating infectious amyloid aggregates, arising

spontaneously in the cell, and manifest a prion phenotype referred to as [*PSI+*] (Glover et al., 1997). The N-terminal part of Sup35p is responsible for the aggregation, and was substituted by Aβ42 from the authors in the functional fusion protein AβMRF, that maintain the C-terminal RF (release factor) functional domain, performing translation termination. The easily scored activity of Sup35p's MRF domain was impaired in AβMRF fusions because the Aβ42 causes the fusion to form SDSstable low-n oligomers (dimers, trimers, tetramers), similarly to the wild type Sup35p. Using this model system, they found that oligomerization of the fusion protein is stimulated by millimolar concentrations of the yeast prion curing agent guanidine. Surprisingly, deletion of the chaperone Hsp104 (a known target for guanidine) inhibited oligomerization of the fusion protein. Furthermore, they demonstrated that Hsp104 interacts with the Aβ42-fusion protein and appears to protect it from disaggregation and degradation.

This experimental approach gives three relevant considerations:

- Aβ42-fusion proteins can oligomerize in the yeast cytoplasm;
- the chaperone machinery of yeast cell can participate also in the oligomerization process of Aβ42-MRF;
- oligomerization of Aβ42-MRF can be chemically modulated (by guanidine) exactly as for yeast ‘natural’ prions.

These general conclusions from an experimental system, distinct from, but related to the IACT system, used in this thesis, provide an additional framework to interpret and

discuss the success of our approach in generating a high proportion of anti-Aβ oligomers scFvs antibody fragments.

3.2 Beta-Amyloid in IACT system

On the basis of the experimental reports discussed before, regarding the use of Aβ bait in two hybrid system and the oligomerization of Aβ in yeast cells, it is likely that also in IACT system, Aβ42 bait is conformationally structured and/or oligomeric.

Regarding the mechanisms of oligomerization we can postulate two hypotheses not mutually exclusive:

- a mechanism of Aβ oligomerization favoured by Aβ itself and/or chaperone-mediated in the yeast cytoplasm and/or nucleus;
- a mechanism of Aβ oligomerization favoured in the L40 yeast nucleus by the multiple LexA binding operators, hypothesizing interactions between adjacent LexA-Aβ fusion proteins.

3.2a Is Aβ bait conformationally structured?

In IACT system, similarly to the above described two hybrid systems, Aβ is expressed as a C-terminal fusion of LexA DNA binding domain.

On the basis of "In Vivo Epitope Mapping" (IVEM) results, we suggested that, for conformational reasons, some epitopes of the Aβ bait are not easily accessible. Consequently, during the SPLINT selection of anti-Aβ scFvs, there is an enrichment of epitope-specific scFvs for the C-terminus and the N-terminus of Aβ42, epitopes that should be more exposed. In particular, the N-terminus is preferentially recognized by

scFvs selected from the immune library, a biased repertoire of recombinant antibodies enriched in N-terminal binders. It is likely that the central part (a.a. 10-28) of the Aβ bait used in the IACT system could be "hidden", and difficultly recognized by the SPLINT-selected scFvs. These observations could be indirect evidences for the Aβ folding in yeast nucleus.

By the IVEM approach, we studied the interactions of scFvs selected against Aβ42, with other Aβ baits (both human and murine) that are deletion mutants of the whole Aβ: Aβ40, Aβ28, Aβ17, Aβ10.

Essentially, a large part of scFvs selected against Aβ42 from the naïve SPLINT library and a smaller part of scFvs selected against Aβ42 from the SPLINT immune library, can recognize only Aβ42 or Aβ40. We called these scFvs "C-terminal-specific" but they could potentially recognize conformational epitopes not displayed by the shorter deletion mutants of Aβ. On the contrary, scFvs recognizing Aβ10, recognize the N-terminal epitope in all the deletion mutants of Aβ baits.

Several structural models suggest that the N-terminus of Aβ, especially the region 1-10, is unstructured (Petkova et al., 2002). On the other hand, the N-terminal part of Aβ seems to play a role in the aggregation of Aβ42 peptides (also reported in the above-mentioned two hybrid system (Festy al al., 2001)) and a recent experimental report showed that, by using antibodies raised against Aβ1-15, the N-terminus of Aβ plays a conformation-specific role in the preferential recognition of Aβ42 oligomers and fibrils, but not of Aβ42 monomers (Moretto et al., 2007). The ELISA results discussed in this thesis confirmed that the conformation-specificity versus Aβ oligomers is a common behaviour of anti-Aβ scFvs SPLINT-selected, not related to the epitope-specificity. On the basis of

these results, it is likely that the fusion with LexA favours structural conformations of the N-terminus of Aβ.

Finally, the scFvs described in this thesis were originally selected against the human Aβ42 bait; however, they cannot distinguish between human and murine baits *in vivo* (by IVEM), in spite of the *in vitro* ELISA results that showed their ability to discriminate significantly from human and murine ADDLs. This could indicate that the folding *in vivo* is different from the folding *in vitro*, as well as the exposure of particular conformational epitopes.

3.2b Aβ bait oligomerization

The oligomerization of Aβ-bait in yeast is a fascinating hypothesis that could explain the specificity and the preferential binding of IACT-selected anti-Aβ scFvs to Aβ oligomers, obtained in different *in vitro* assays. In the opposite scenario, in absence of bait aggregation, scFvs could be selected against structural epitopes (see above) that *in vitro* could be favourably exposed in oligomeric assemblies.

Some data, discussed above, support the Aβ bait oligomerization hypothesis:

- Aβ fusion proteins can oligomerize in the yeast cytoplasm (Bagriantsev, 2006);
- Aβ bait and Aβ prey can interact *in vivo* in the yeast nucleus (Hughes et al., 1996; Festy et al., 2001).

In addition, we have obtained one preliminary experimental evidence in favour of the Aβ42 bait oligomerization. Protein extracts from L40 yeast expressing the Aβ42 bait, analyzed by Western Blot in NuPAGE show a laddered pattern of immunoreactive species positive to the anti-Aβ MAb 4G8. As indicated in the figure 1 the pattern could be in accordance with the dimerization (band at 58 kDa) or the multimerization of the LexA-Aβ bait (fig.1)

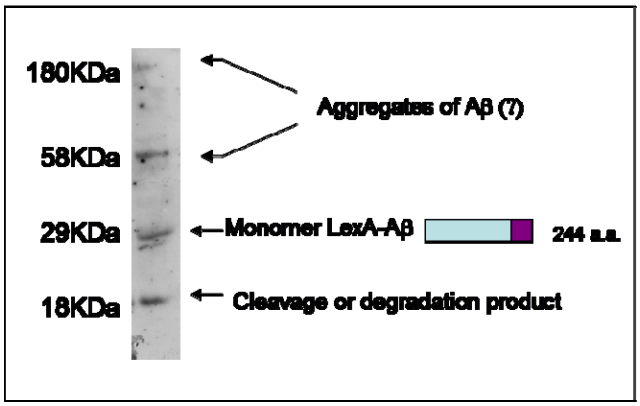

Fig.1 Western Blot analysis of protein extracts from L40yeast expressing the LexA-Aβ42 bait, analyzed by in NuPAGE: samples not reduced and not boiled. Note not only the monomeric form of the fusion protein but also the dimeric form and other specific high molecular weight aggregates, that are probably oligomers. WB: anti-Aβ MAb 4G8

As discussed above, two general hypotheses, probably not mutually exclusive, can explain the mechanisms triggering Aβ42 bait oligomerization: i) a mechanism favoured by Aβ itself and/or chaperone-mediated in the yeast cytoplasm and/or nucleus; ii) a mechanism favoured by the multiple LexA binding operators, in the L40 yeast nucleus.

Regarding the first hypothesis, in yeast cell, Aβ-Aβ interaction could happen both in the cytoplasm and/or in the nucleus.

If LexA-Aβ oligomers are assembled in the cytoplasm, the nuclear pores could act as a 'filters' for high molecular weight aggregates, when the fusion proteins are translocated into the nucleus.

However, we cannot exclude that Aβ oligomers *in vivo* produced in the yeast nucleus and/or cytoplasm could be also assembled with yeast endogenous proteins and with cleavage products of LexA-Aβ bait (normally, LexA repressor undergoes a self-cleavage reaction (Luo et al., 2001)).

The second general hypothesis could suggest that Aβ-Aβ interactions are favored by LexA operators in the L40 yeast nucleus.

LexA protein as binder of DNA operator box is a dimer, as well as observed for other regulative proteins in different operator systems (Mohana-Borges et al, 2000). The structure of LexA dimer could be *per se* not sufficiently explanatory of the dimerization of Aβ, for structural reasons related to the molecular distances of the two C-terminals in models of LexA dimers (Aβ is a C-terminal fusion of LexA). However, we may hypothesize that Aβ fusions of different, but adjacent, dimers of LexA could interact and aggregate. Reporter genes in L40 are under control of multiple LexA binding operators (4LexA operator control His3, 8LexA operator control LacZ), and interactions between adjacent LexA might be possible (see fig.2).

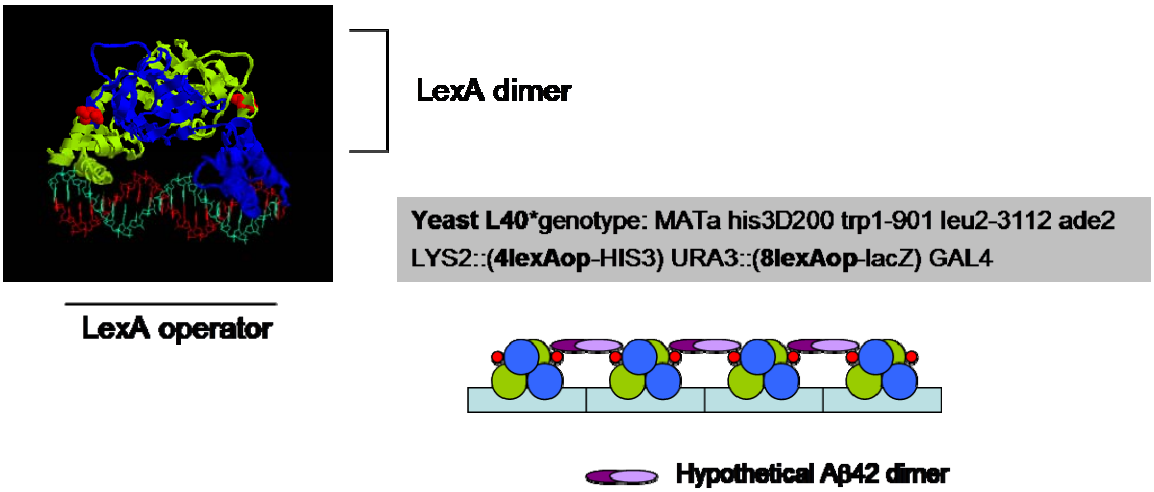

Fig.2 Model of LexA dimer bound to DNA operator (lexAop) (top left), and 'linear' model of oligomerization in the yeast nucleus (bottom right).
In the grey box: genotype of L40 yeast strain; in bold the different LexAop, functioning as upstream activation sequence (UAS) of the repoter genes (HIS3 and lacZ).

The formation of oligomers of Aβ bait fusion proteins *in vivo*, is a fascinating hypothesis supporting a direct role of the bait in biasing the selection of conformationally oligomeric specific scFvs from naïve and immune SPLINT libraries. Different scFvs could interact with specific pattern of Aβ oligomeric baits, binding their different epitopes in the nucleus or in the cytoplasm, and determining different phenotypic IACT selections.

Several experimental data are in accordance with Aβ oligomerization:

1. Some observations supporting the conformation structure of Aβ bait are in agreement with Aβ oligomerization, as preferential epitope recognition by scFvs. It is likely that the N-terminus and the C-terminus of Aβ are more exposed in the oligomeric forms of Aβ baits;
2. Oligomeric conformations of the Aβ42 bait could determine in the IACT system a difficult assembly of functional transcription machinery. As commented in the IVEM section, β-structured and probably aggregated Aβ, interacting with the C-

terminal specific scFvs, could interfere with the assembly of functional transcription machinery. On the contrary, the N-terminal specific scFvs, interacting with epitopes of Aβ baits not showing steric hindrance problems, could favour activation of reporter genes and give healthy phenotype in yeast cells;

3. Finally, in IACT-based SPLINT selections using Aβ-bait, the observed differential activation of the two reporter gene systems HIS3 and lacZ can be explained by another mechanism. The Aβ bait could show a different degree of oligomerization onto the two multi-binding sites operators that control the reporter genes (4 LexA operators for HIS3 gene and 8 LexA operators for LacZ gene, respectively), determining differential interaction and reporter gene activation. For instance, the scFv Im8 shows high specificity for the HIS3 reporter gene activation assay but shows a weak activation of the lacZ gene. A large number of scFvs show a similar behaviour in the secondary screening. Normally, in IACT screenings, these clones are excluded because HIS3 reporter gene is leaky in comparison to LacZ, but the case of Aβ bait could be particular in the light of the above-mentioned hypothesis.

In conclusion, the preliminary results of Aβ42 bait yeast extracts and the experimental observations obtained from IACT screenings of the SPLINT selected anti-Aβ scFvs, together with the experimental reports of other authors in related yeast systems (Hughes et al., 1996; Festy et al., 2001; Bagriantsev, 2006) support the hypothesis of Aβ bait oligomerization in yeast using the IACT system.

The conformation of Aβ bait and its probable oligomeric nature *in vivo* (in yeast) might determine the unique characteristic of the selection strategy used for the isolation of scFvs under study. Therefore, the IACT strategy appears to be particularly suitable for the selection of oligomeric specific anti-Aβ antibodies, as demonstrated by the *a priori* unexpected large number of conformation-specific scFvs SPLINT-selected.

4. Future perspectives

Conformation specific scFvs anti-Aβ, developed in the experimental work described in this PhD thesis, show relevant features to several kinds of *in vitro* cell biology studies as well as to the *in vivo* therapeutic use.

In the present state of knowledge we propose to exploit our unique experimental tool and strategy (intrabodies) to gain a better understanding of basic Aβ oligomerization in AD pathogenesis and, on this basis, to develop novel therapeutic approaches.

1) The use of anti-Aβ scFvs as new tool of study: intrabodies

The intracellular expression of antibodies for spatio-temporal interference with pathological protein function has been pioneered and developed by our group (Cattaneo & Biocca, 1997, Visintin et al, 1999, 2002).

Using the selected anti-Aβ scFvs, we propose a fine and precise dissection of the intracellular formation and trafficking of Aβ, in particular of Aβ oligomers, exploiting also the engineering of scFvs intrabodies for synaptic targeting and neurosecretion.

In these studies, scFvs can act as specific functional knock-out tools, both intracellularly and extracellularly, if secreted. The effects of this functional knock-out, especially if oligomeric-specific, could be evaluated at different levels:

• modulation of neuronal survival;

• modulation of synaptic activity and plasticity;

• modulation of gene expression and protein synthesis/modifications of specific targets synaptic

2) The use of scFvs as new "therapeutics" in animal models.

We propose different routes for the pharmacological delivery of scFvs anti-Aβ to central nervous system.

The first is the passive immunization through peripheral or intranasal administration of scFvs purified proteins. The latter could be supported by the positive experience in our group obtained with the nasal delivery of NGF in the CNS of AD11 mice (Capsoni et al, 2002; De Rosa et al, 2005).

The second is represented by the exploitation (especially by intranasal administration) of new systems of delivery, using viral vectors or engineered cells secreting the anti-Aβ scFvs; these systems can deliver quantifiable amounts of scFv protein directly to central nervous system (CNS), modulating synaptotoxicity of Aβ oligomers.

REFERENCES

Agadjanyan, M. G., Ghochikyan, A., Petrushina, I., Vasilevko, V., Movsesyan, N., Mkrtichyan, M., Saing, T., and Cribbs, D. H. (2005). Prototype Alzheimer's disease vaccine using the immunodominant B cell epitope from beta-amyloid and promiscuous T cell epitope pan HLA DR-binding peptide. J Immunol *174*, 1580-1586.

Alexandrescu, A. T. (2005). Amyloid accomplices and enforcers. Protein Sci *14*, 1-12.

Antzutkin, O. N. (2004). Amyloidosis of Alzheimer's Abeta peptides: solid-state nuclear magnetic resonance, electron paramagnetic resonance, transmission electron microscopy, scanning transmission electron microscopy and atomic force microscopy studies. Magn Reson Chem *42*, 231-246.

Bacskai, B. J., Kajdasz, S. T., McLellan, M. E., Games, D., Seubert, P., Schenk, D., and Hyman, B. T. (2002). Non-Fc-mediated mechanisms are involved in clearance of amyloid-beta in vivo by immunotherapy. J Neurosci *22*, 7873-7878.

Bagriantsev, S., and Liebman, S. (2006). Modulation of Abeta42 low-n oligomerization using a novel yeast reporter system. BMC Biol *4*, 32.

Balbach, J. J., Petkova, A. T., Oyler, N. A., Antzutkin, O. N., Gordon, D. J., Meredith, S. C., and Tycko, R. (2002). Supramolecular structure in full-length Alzheimer's beta-amyloid fibrils: evidence for a parallel beta-sheet organization from solid-state nuclear magnetic resonance. Biophys J *83*, 1205-1216.

Bard, F., Cannon, C., Barbour, R., Burke, R. L., Games, D., Grajeda, H., Guido, T., Hu, K., Huang, J., Johnson-Wood, K.*, et al.* (2000). Peripherally administered antibodies against amyloid beta-peptide enter the central nervous system and reduce pathology in a mouse model of Alzheimer disease. Nat Med *6*, 916-919.

Barghorn, S., Nimmrich, V., Striebinger, A., Krantz, C., Keller, P., Janson, B., Bahr, M., Schmidt, M., Bitner, R. S., Harlan, J.*, et al.* (2005). Globular amyloid beta-peptide oligomer - a homogenous and stable neuropathological protein in Alzheimer's disease. J Neurochem *95*, 834-847.

Berg, M.M., Stenberg, D.W., Parada, L.F.; Chao, M.V. (1992) K-252a inhibits nerve growth factor-induced trk proto-oncogene tyrosine phosporilation and kinase activity. J Biol Chem. *267*(1):13-6

Biocca, S., and Cattaneo, A. (1995). Intracellular immunization: antibody targeting to subcellular compartments. Trends Cell Biol *5*, 248-252.

Bird, R. E., Hardman, K. D., Jacobson, J. W., Johnson, S., Kaufman, B. M., Lee, S. M., Lee, T., Pope, S. H., Riordan, G. S., and Whitlow, M. (1988). Single-chain antigen-binding proteins. Science *242*, 423-426.

Buxbaum, J. D., Thinakaran, G., Koliatsos, V., O'Callahan, J., Slunt, H. H., Price, D. L., and Sisodia, S. S. (1998). Alzheimer amyloid protein precursor in the rat hippocampus: transport and processing through the perforant path. J Neurosci *18*, 9629-9637.

Capsoni, S., Giannotta, S., and Cattaneo, A. (2002). Beta-amyloid plaques in a model for sporadic Alzheimer's disease based on transgenic anti-nerve growth factor antibodies. Mol Cell Neurosci *21*, 15-28.

Capsoni, S., Giannotta, S., and Cattaneo, A. (2002b). Nerve growth factor and galantamine ameliorate early signs of neurodegeneration in anti-nerve growth factor mice. Proc Natl Acad Sci U S A *99*, 12432-12437.

Capsoni, S., Ugolini, G., Comparini, A., Ruberti, F., Berardi, N., and Cattaneo, A. (2000). Alzheimer-like neurodegeneration in aged antinerve growth factor transgenic mice. Proc Natl Acad Sci U S A *97*, 6826-6831.

Cattaneo, A., and Biocca, S. (1999). The selection of intracellular antibodies. Trends Biotechnol *17*, 115-121.

Cattaneo, A. & Biocca, S. (1997) Intracellular Antibodies: Development and Applications (Springer, New York).

Chao, M. V., and Hempstead, B. L. (1995). p75 and Trk: a two-receptor system. Trends Neurosci *18*, 321-326.

Cirrito, J. R., Yamada, K. A., Finn, M. B., Sloviter, R. S., Bales, K. R., May, P. C., Schoepp, D. D., Paul, S. M., Mennerick, S., and Holtzman, D. M. (2005). Synaptic activity regulates interstitial fluid amyloid-beta levels in vivo. Neuron *48*, 913-922.

Cribbs, D. H., Ghochikyan, A., Vasilevko, V., Tran, M., Petrushina, I., Sadzikava, N., Babikyan, D., Kesslak, P., Kieber-Emmons, T., Cotman, C. W., and Agadjanyan, M. G. (2003). Adjuvant-dependent modulation of Th1 and Th2 responses to immunization with beta-amyloid. Int Immunol *15*, 505-514.

D'Andrea, M. R., Nagele, R. G., Wang, H. Y., Peterson, P. A., and Lee, D. H. (2001). Evidence that neurones accumulating amyloid can undergo lysis to form amyloid plaques in Alzheimer's disease. Histopathology *38*, 120-134.

Dahlgren, K. N., Manelli, A. M., Stine, W. B., Jr., Baker, L. K., Krafft, G. A., and LaDu, M. J. (2002). Oligomeric and fibrillar species of amyloid-beta peptides differentially affect neuronal viability. J Biol Chem *277*, 32046-32053.

De Felice, F. G., Velasco, P. T., Lambert, M. P., Viola, K., Fernandez, S. J., Ferreira, S. T., and Klein, W. L. (2007). Abeta oligomers induce neuronal oxidative stress through an N-methyl-D-aspartate receptor-dependent mechanism that is blocked by the Alzheimer drug memantine. J Biol Chem *282*, 11590-11601.

De Rosa, R., Garcia, A. A., Braschi, C., Capsoni, S., Maffei, L., Berardi, N., and Cattaneo, A. (2005). Intranasal administration of nerve growth factor (NGF) rescues recognition memory deficits in AD11 anti-NGF transgenic mice. Proc Natl Acad Sci U S A *102*, 3811-3816.

DeMattos, R. B., Bales, K. R., Cummins, D. J., Dodart, J. C., Paul, S. M., and Holtzman, D. M. (2001). Peripheral anti-A beta antibody alters CNS and plasma A beta clearance and decreases brain A beta burden in a mouse model of Alzheimer's disease. Proc Natl Acad Sci U S A *98*, 8850-8855.

DeMattos, R. B., Bales, K. R., Parsadanian, M., O'Dell, M. A., Foss, E. M., Paul, S. M., and Holtzman, D. M. (2002). Plaque-associated disruption of CSF and plasma amyloid-beta (Abeta) equilibrium in a mouse model of Alzheimer's disease. J Neurochem *81*, 229-236.

Deshpande, A., Mina, E., Glabe, C., and Busciglio, J. (2006). Different conformations of amyloid beta induce neurotoxicity by distinct mechanisms in human cortical neurons. J Neurosci *26*, 6011-6018.

Dodart, J. C., Bales, K. R., Gannon, K. S., Greene, S. J., DeMattos, R. B., Mathis, C., DeLong, C. A., Wu, S., Wu, X., Holtzman, D. M., and Paul, S. M. (2002). Immunization reverses memory deficits without reducing brain Abeta burden in Alzheimer's disease model. Nat Neurosci *5*, 452-457.

Edwards, S.N., Tolkovsky, A.M. (1994) Characterization of apoptosis in cultured rat sympathetic neurons after nerve growth factor withdrawal. J Cell Biol *124*:537-546

Ferreira, A., Caceres, A., and Kosik, K. S. (1993). Intraneuronal compartments of the amyloid precursor protein. J Neurosci *13*, 3112-3123.

Ferrer, I., Boada Rovira, M., Sanchez Guerra, M. L., Rey, M. J., and Costa-Jussa, F. (2004). Neuropathology and pathogenesis of encephalitis following amyloid-beta immunization in Alzheimer's disease. Brain Pathol *14*, 11-20.

Festy, F., Lins, L., Peranzi, G., Octave, J. N., Brasseur, R., and Thomas, A. (2001). Is aggregation of beta-amyloid peptides a mis-functioning of a current interaction process? Biochim Biophys Acta *1546*, 356-364.

Fields, S., and Song, O. (1989). A novel genetic system to detect protein-protein interactions. Nature *340*, 245-246.

Frenkel, D., Balass, M., Katchalski-Katzir, E., and Solomon, B. (1999). High affinity binding of
monoclonal antibodies to the sequential epitope EFRH of beta-amyloid peptide is essential for modulation of fibrillar aggregation. J Neuroimmunol *95*, 136-142.

Frenkel, D., Balass, M., and Solomon, B. (1998). N-terminal EFRH sequence of Alzheimer's beta-amyloid peptide represents the epitope of its anti-aggregating antibodies. J Neuroimmunol *88*, 85-90.

Frenkel, D., Solomon, B., and Benhar, I. (2000). Modulation of Alzheimer's beta-amyloid neurotoxicity by site-directed single-chain antibody. J Neuroimmunol *106*, 23-31.

Fukuchi, K., Tahara, K., Kim, H. D., Maxwell, J. A., Lewis, T. L., Accavitti-Loper, M. A., Kim, H., Ponnazhagan, S., and Lalonde, R. (2006). Anti-Abeta single-chain antibody delivery via adeno-associated virus for treatment of Alzheimer's disease. Neurobiol Dis *23*, 502-511.

Fung, J., Frost, D., Chakrabartty, A., and McLaurin, J. (2004). Interaction of human and mouse Abeta peptides. J Neurochem *91*, 1398-1403.

Gilman, S., Koller, M., Black, R. S., Jenkins, L., Griffith, S. G., Fox, N. C., Eisner, L., Kirby, L., Rovira, M. B., Forette, F., and Orgogozo, J. M. (2005). Clinical effects of Abeta immunization (AN1792) in patients with AD in an interrupted trial. Neurology *64*, 1553-1562.

Glabe, C. G. (2004). Conformation-dependent antibodies target diseases of protein misfolding. Trends Biochem Sci *29*, 542-547.

Glabe, C. G., and Kayed, R. (2006). Common structure and toxic function of amyloid oligomers implies a common mechanism of pathogenesis. Neurology *66*, S74-78.

Glenner, G. G., and Wong, C. W. (1984). Alzheimer's disease: initial report of the purification and characterization of a novel cerebrovascular amyloid protein. Biochem Biophys Res Commun *120*, 885-890.

Glenner, G. G., Wong, C. W., Quaranta, V., and Eanes, E. D. (1984). The amyloid deposits in Alzheimer's disease: their nature and pathogenesis. Appl Pathol *2*, 357-369.

Glover, J. R., Kowal, A. S., Schirmer, E. C., Patino, M. M., Liu, J. J., and Lindquist, S. (1997). Self-seeded fibers formed by Sup35, the protein determinant of [PSI+], a heritable prion-like factor of S. cerevisiae. Cell *89*, 811-819.

Gong, Y., Chang, L., Viola, K. L., Lacor, P. N., Lambert, M. P., Finch, C. E., Krafft, G. A., and Klein, W. L. (2003). Alzheimer's disease-affected brain: presence of oligomeric A beta ligands (ADDLs) suggests a molecular basis for reversible memory loss. Proc Natl Acad Sci U S A *100*, 10417-10422.

Gouras, G. K., Tsai, J., Naslund, J., Vincent, B., Edgar, M., Checler, F., Greenfield, J. P., Haroutunian, V., Buxbaum, J. D., Xu, H., *et al.* (2000). Intraneuronal Abeta42 accumulation in human brain. Am J Pathol *156*, 15-20.

Greene, L.A., Tischler, A.S. (1976) Establishment of a noradrenergic clonal line of rat adrenal pheochromocytoma cells which respond to nerve growth factor. Proc Natl Acad Sci *73*:2424-2428

Griffiths, A. D., Williams, S. C., Hartley, O., Tomlinson, I. M., Waterhouse, P., Crosby, W. L., Kontermann, R. E., Jones, P. T., Low, N. M., Allison, T. J., and et al. (1994). Isolation of high affinity human antibodies directly from large synthetic repertoires. Embo J *13*, 3245-3260.

Haass, C., and Selkoe, D. J. (2007). Soluble protein oligomers in neurodegeneration: lessons from the Alzheimer's amyloid beta-peptide. Nat Rev Mol Cell Biol *8*, 101-112.

Hardy, J., and Selkoe, D. J. (2002). The amyloid hypothesis of Alzheimer's disease: progress and problems on the road to therapeutics. Science *297*, 353-356.

Hardy, J. A., and Higgins, G. A. (1992). Alzheimer's disease: the amyloid cascade hypothesis. Science *256*, 184-185.

Hilbich, C., Kisters-Woike, B., Reed, J., Masters, C. L., and Beyreuther, K. (1992). Substitutions of hydrophobic amino acids reduce the amyloidogenicity of Alzheimer's disease beta A4 peptides. J Mol Biol *228*, 460-473.

Hock, C., Konietzko, U., Papassotiropoulos, A., Wollmer, A., Streffer, J., von Rotz, R. C., Davey, G., Moritz, E., and Nitsch, R. M. (2002). Generation of antibodies specific for beta-amyloid by vaccination of patients with Alzheimer disease. Nat Med *8*, 1270-1275.

Hock, C., Konietzko, U., Streffer, J. R., Tracy, J., Signorell, A., Muller-Tillmanns, B., Lemke, U., Henke, K., Moritz, E., Garcia, E., *et al.* (2003). Antibodies against beta-amyloid slow cognitive decline in Alzheimer's disease. Neuron *38*, 547-554.

Hong, H. S., Maezawa, I., Yao, N., Xu, B., Diaz-Avalos, R., Rana, S., Hua, D. H., Cheng, R. H., Lam, K. S., and Jin, L. W. (2007). Combining the rapid MTT formazan exocytosis assay and the MC65 protection assay led to the discovery of carbazole analogs as small molecule inhibitors of Abeta oligomer-induced cytotoxicity. Brain Res *1130*, 223-234.

Hoogenboom, H. R., Marks, J. D., Griffiths, A. D., and Winter, G. (1992). Building antibodies from their genes. Immunol Rev *130*, 41-68.

Hoogenboom, H. R., and Winter, G. (1992). By-passing immunisation. Human antibodies from synthetic repertoires of germline VH gene segments rearranged in vitro. J Mol Biol *227*, 381-388.

Hsiao, K., Chapman, P., Nilsen, S., Eckman, C., Harigaya, Y., Younkin, S., Yang, F., and Cole, G. (1996). Correlative memory deficits, Abeta elevation, and amyloid plaques in transgenic mice. Science *274*, 99-102.

Hudson, P. J., and Souriau, C. (2001). Recombinant antibodies for cancer diagnosis and therapy. Expert Opin Biol Ther *1*, 845-855.

Hughes, S. R., Goyal, S., Sun, J. E., Gonzalez-DeWhitt, P., Fortes, M. A., Riedel, N. G., and Sahasrabudhe, S. R. (1996). Two-hybrid system as a model to study the interaction of beta-amyloid peptide monomers. Proc Natl Acad Sci U S A *93*, 2065-2070.

Hughes, S. R., Khorkova, O., Goyal, S., Knaeblein, J., Heroux, J., Riedel, N. G., and Sahasrabudhe, S. (1998). Alpha2-macroglobulin associates with beta-amyloid peptide and prevents fibril formation. Proc Natl Acad Sci U S A *95*, 3275-3280.

Kamenetz, F., Tomita, T., Hsieh, H., Seabrook, G., Borchelt, D., Iwatsubo, T., Sisodia, S., and Malinow, R. (2003). APP processing and synaptic function. Neuron *37*, 925-937.

Kayed, R., Head, E., Thompson, J. L., McIntire, T. M., Milton, S. C., Cotman, C. W., and Glabe, C. G. (2003). Common structure of soluble amyloid oligomers implies common mechanism of pathogenesis. Science *300*, 486-489.

Klyubin, I., Walsh, D. M., Lemere, C. A., Cullen, W. K., Shankar, G. M., Betts, V., Spooner, E. T., Jiang, L., Anwyl, R., Selkoe, D. J., and Rowan, M. J. (2005). Amyloid beta protein immunotherapy neutralizes Abeta oligomers that disrupt synaptic plasticity in vivo. Nat Med *11*, 556-561.

Koo, E. H., Sisodia, S. S., Archer, D. R., Martin, L. J., Weidemann, A., Beyreuther, K., Fischer, P., Masters, C. L., and Price, D. L. (1990). Precursor of amyloid protein in Alzheimer disease undergoes fast anterograde axonal transport. Proc Natl Acad Sci U S A *87*, 1561-1565.

Lacor, P. N., Buniel, M. C., Chang, L., Fernandez, S. J., Gong, Y., Viola, K. L., Lambert, M. P., Velasco, P. T., Bigio, E. H., Finch, C. E.*, et al.* (2004). Synaptic targeting by Alzheimer's-related amyloid beta oligomers. J Neurosci *24*, 10191-10200.

Lacor, P. N., Buniel, M. C., Furlow, P. W., Clemente, A. S., Velasco, P. T., Wood, M., Viola, K. L., and Klein, W. L. (2007). Abeta oligomer-induced aberrations in synapse composition, shape, and density provide a molecular basis for loss of connectivity in Alzheimer's disease. J Neurosci *27*, 796-807.

Lambert, M. P., Velasco, P. T., Chang, L., Viola, K. L., Fernandez, S., Lacor, P. N., Khuon, D., Gong, Y., Bigio, E. H., Shaw, P.*, et al.* (2007). Monoclonal antibodies that target pathological assemblies of Abeta. J Neurochem *100*, 23-35.

Lazarov, O., Lee, M., Peterson, D. A., and Sisodia, S. S. (2002). Evidence that synaptically released beta-amyloid accumulates as extracellular deposits in the hippocampus of transgenic mice. J Neurosci *22*, 9785-9793.

LeBlanc A. (1995) Increased production of 4kDa Amyloid β peptide in serum deprived human primary neuron cultures: possible involvement of apoptosis. J Neurosc *15*: 7837-7846.

Lee, E. B., Zhang, B., Liu, K., Greenbaum, E. A., Doms, R. W., Trojanowski, J. Q., and Lee, V. M. (2005). BACE overexpression alters the subcellular processing of APP and inhibits Abeta deposition in vivo. J Cell Biol *168*, 291-302.

Lemere, C. A., Beierschmitt, A., Iglesias, M., Spooner, E. T., Bloom, J. K., Leverone, J. F., Zheng, J. B., Seabrook, T. J., Louard, D., Li, D.*, et al.* (2004). Alzheimer's disease abeta vaccine reduces central nervous system abeta levels in a non-human primate, the Caribbean vervet. Am J Pathol *165*, 283-297.

Lemere, C. A., Maron, R., Spooner, E. T., Grenfell, T. J., Mori, C., Desai, R., Hancock, W. W., Weiner, H. L., and Selkoe, D. J. (2000). Nasal A beta treatment induces anti-A beta antibody production and decreases cerebral amyloid burden in PD-APP mice. Ann N Y Acad Sci *920*, 328-331.

Lesne, S., Koh, M. T., Kotilinek, L., Kayed, R., Glabe, C. G., Yang, A., Gallagher, M., and Ashe, K. H. (2006). A specific amyloid-beta protein assembly in the brain impairs memory. Nature *440*, 352-357.

Levites, Y., Jansen, K., Smithson, L. A., Dakin, R., Holloway, V. M., Das, P., and Golde, T. E. (2006). Intracranial adeno-associated virus-mediated delivery of anti-pan amyloid beta, amyloid beta40, and amyloid beta42 single-chain variable fragments attenuates plaque pathology in amyloid precursor protein mice. J Neurosci *26*, 11923-11928.

Linke, R. P., Tischendorf, F. W., Zucker-Franklin, D., and Franklin, E. C. (1973a). The formation of amyloid-like fibrils in vitro from Bence Jones Proteins of the VlambdaI subclass. J Immunol *111*, 24-26.

Linke, R. P., Zucker-Franklin, D., and Franklin, E. D. (1973b). Morphologic, chemical, and immunologic studies of amyloid-like fibrils formed from Bence Jones Proteins by proteolysis. J Immunol *111*, 10-23.

Liu, R., Yuan, B., Emadi, S., Zameer, A., Schulz, P., McAllister, C., Lyubchenko, Y., Goud, G., and Sierks, M. R. (2004b). Single chain variable fragments against beta-amyloid (Abeta) can inhibit Abeta aggregation and prevent abeta-induced neurotoxicity. Biochemistry *43*, 6959-6967.

Lobato, M. N., and Rabbitts, T. H. (2003). Intracellular antibodies and challenges facing their use as therapeutic agents. Trends Mol Med *9*, 390-396.

Luo, Y., Pfuetzner, R. A., Mosimann, S., Paetzel, M., Frey, E. A., Cherney, M., Kim, B., Little, J. W., and Strynadka, N. C. (2001b). Crystal structure of LexA: a conformational switch for regulation of self-cleavage. Cell *106*, 585-594.

Ma, Q. L., Lim, G. P., Harris-White, M. E., Yang, F., Ambegaokar, S. S., Ubeda, O. J., Glabe, C. G., Teter, B., Frautschy, S. A., and Cole, G. M. (2006). Antibodies against beta-amyloid reduce Abeta oligomers, glycogen synthase kinase-3beta activation and tau phosphorylation in vivo and in vitro. J Neurosci Res *83*, 374-384.

Maier, M., Seabrook, T. J., Lazo, N. D., Jiang, L., Das, P., Janus, C., and Lemere, C. A. (2006). Short amyloid-beta (Abeta) immunogens reduce cerebral Abeta load and learning deficits in an Alzheimer's disease mouse model in the absence of an Abeta-specific cellular immune response. J Neurosci *26*, 4717-4728.

Manoutcharian, K., Acero, G., Munguia, M. E., Becerril, B., Massieu, L., Govezensky, T., Ortiz, E., Marks, J. D., Cao, C., Ugen, K., and Gevorkian, G. (2004). Human single chain Fv antibodies and a complementarity determining region-derived peptide binding to amyloid-beta 1-42. Neurobiol Dis *17*, 114-121.

Manoutcharian, K., Acero, G., Munguia, M. E., Montero, J. A., Govezensky, T., Cao, C., Ugen, K., and Gevorkian, G. (2003). Amyloid-beta peptide-specific single chain Fv antibodies isolated from an immune phage display library. J Neuroimmunol *145*, 12-17.

Marques C. et al. (2003) Neurotoxic mechanism caused by the Alzheimer's disease-linked swedish amyloid precursor protein mutation. J Biol Chem *279*: 28294-28302

Masliah, E., Hansen, L., Adame, A., Crews, L., Bard, F., Lee, C., Seubert, P., Games, D., Kirby, L., and Schenk, D. (2005). Abeta vaccination effects on plaque pathology in the absence of encephalitis in Alzheimer disease. Neurology *64*, 129-131.

Masliah, E., Mallory, M., Alford, M., DeTeresa, R., Hansen, L. A., McKeel, D. W., Jr., and Morris, J. C. (2001). Altered expression of synaptic proteins occurs early during progression of Alzheimer's disease. Neurology *56*, 127-129.

Masters, C. L., Simms, G., Weinman, N. A., Multhaup, G., McDonald, B. L., and Beyreuther, K. (1985). Amyloid plaque core protein in Alzheimer disease and Down syndrome. Proc Natl Acad Sci U S A *82*, 4245-4249.

Mastrangelo, I. A., Ahmed, M., Sato, T., Liu, W., Wang, C., Hough, P., and Smith, S. O. (2006). High-resolution atomic force microscopy of soluble Abeta42 oligomers. J Mol Biol *358*, 106-119.

Mattson, M. P. (2004). Pathways towards and away from Alzheimer's disease. Nature *430*, 631-639.

McLaurin, J., Cecal, R., Kierstead, M. E., Tian, X., Phinney, A. L., Manea, M., French, J. E., Lambermon, M. H., Darabie, A. A., Brown, M. E*., et al.* (2002). Therapeutically effective antibodies against amyloid-beta peptide target amyloid-beta residues 4-10 and inhibit cytotoxicity and fibrillogenesis. Nat Med *8*, 1263-1269.

Meli G, Visintin M, Cannistraci I. et al. (2005) *Society for Neuroscience* Abstract No. 325.8

Meli G., Visintin M., Cannistraci I., Avossa D., Westlind-Danielsson A., Cattaneo A. (2006) Intracellularly selected recombinant antibodies targeting beta-amyloid oligomers *Alzheimer's & Dementia: The Journal of The Alzheimer's Association 2* (3): S612.

Mohana-Borges, R., Pacheco, A. B., Sousa, F. J., Foguel, D., Almeida, D. F., and Silva, J. L. (2000). LexA repressor forms stable dimers in solution. The role of specific dna in tightening protein-protein interactions. J Biol Chem *275*, 4708-4712.

Monsonego, A., Maron, R., Zota, V., Selkoe, D. J., and Weiner, H. L. (2001). Immune hyporesponsiveness to amyloid beta-peptide in amyloid precursor protein transgenic mice: implications for the pathogenesis and treatment of Alzheimer's disease. Proc Natl Acad Sci U S A *98*, 10273-10278.

Mosmann, T. (1983) Rapid colorimetric assay for cellular growth and survival: application to proliferation and cytotoxicity assays. J Immunol Methods *65*(1-2):55-63

Moretto, N., Bolchi, A., Rivetti, C., Imbimbo, B. P., Villetti, G., Pietrini, V., Polonelli, L., Del Signore, S., Smith, K. M., Ferrante, R. J., and Ottonello, S. (2007). Conformation-sensitive antibodies against alzheimer amyloid-beta by immunization with a thioredoxin-constrained B-cell epitope peptide. J Biol Chem *282*, 11436-11445.

Morgan D. (2006) Immunotherapy for Alzheimer's disease. J Alzheimers Dis. *9*, 425-32.

Nicoll, J. A., Wilkinson, D., Holmes, C., Steart, P., Markham, H., and Weller, R. O. (2003). Neuropathology of human Alzheimer disease after immunization with amyloid-beta peptide: a case report. Nat Med *9*, 448-452.

O'Nuallain, B., and Wetzel, R. (2002). Conformational Abs recognizing a generic amyloid fibril epitope. Proc Natl Acad Sci U S A *99*, 1485-1490.

Oddo, S., Billings, L., Kesslak, J. P., Cribbs, D. H., and LaFerla, F. M. (2004). Abeta immunotherapy leads to clearance of early, but not late, hyperphosphorylated tau aggregates via the proteasome. Neuron *43*, 321-332.

Oddo, S., Caccamo, A., Shepherd, J. D., Murphy, M. P., Golde, T. E., Kayed, R., Metherate, R., Mattson, M. P., Akbari, Y., and LaFerla, F. M. (2003). Triple-transgenic model of Alzheimer's disease with plaques and tangles: intracellular Abeta and synaptic dysfunction. Neuron *39*, 409-421.

Oddo, S., Caccamo, A., Smith, I. F., Green, K. N., and LaFerla, F. M. (2006a). A dynamic relationship between intracellular and extracellular pools of Abeta. Am J Pathol *168*, 184-194.

Oddo, S., Caccamo, A., Tran, L., Lambert, M. P., Glabe, C. G., Klein, W. L., and LaFerla, F. M. (2006b). Temporal profile of amyloid-beta (Abeta) oligomerization in an in vivo model of Alzheimer disease. A link between Abeta and tau pathology. J Biol Chem *281*, 1599-1604.

Orlandi, R., Figini, M., Tomassetti, A., Canevari, S., and Colnaghi, M. I. (1992). Characterization of a mouse-human chimeric antibody to a cancer-associated antigen. Int J Cancer *52*, 588-593.

Paganetti, P., Calanca, V., Galli, C., Stefani, M., and Molinari, M. (2005). beta-site specific intrabodies to decrease and prevent generation of Alzheimer's Abeta peptide. J Cell Biol *168*, 863-868.

Perelson, A. S., and Oster, G. F. (1979). Theoretical studies of clonal selection: minimal antibody repertoire size and reliability of self-non-self discrimination. J Theor Biol *81*, 645-670.

Persic, L., Righi, M., Roberts, A., Hoogenboom, H. R., Cattaneo, A., and Bradbury, A. (1997). Targeting vectors for intracellular immunisation. Gene *187*, 1-8.

Persic, L., Roberts, A., Wilton, J., Cattaneo, A., Bradbury, A., and Hoogenboom, H. R. (1997b). An integrated vector system for the eukaryotic expression of antibodies or their fragments after selection from phage display libraries. Gene *187*, 9-18.

Petkova, A. T., Ishii, Y., Balbach, J. J., Antzutkin, O. N., Leapman, R. D., Delaglio, F., and Tycko, R. (2002). A structural model for Alzheimer's beta -amyloid fibrils based on experimental constraints from solid state NMR. Proc Natl Acad Sci U S A *99*, 16742-16747.

Piccioli, P., Di Luzio, A., Amann, R., Schuligoi, R., Surani, M. A., Donnerer, J., and Cattaneo, A. (1995). Neuroantibodies: ectopic expression of a recombinant anti-substance P antibody in the central nervous system of transgenic mice. Neuron *15*, 373-384.

Proba, K., Worn, A., Honegger, A., and Pluckthun, A. (1998). Antibody scFv fragments without disulfide bonds made by molecular evolution. J Mol Biol *275*, 245-253.

Romano, A. et al. (2003) Neuronal fibrillogenesis: amyloid fibrils from primary neuronal cultures impair long-term memory in the crab Chasmagnathus. Behav Brain Res *147*(1-2):73-82

Roßner, S., Ueberham, U., Schliebs, R., Perez-Polo, J. R., and Bigl, V. (1998). The regulation of amyloid precursor protein metabolism by cholinergic mechanisms and neurotrophin receptor signaling. Prog Neurobiol *56*, 541-569.

Sblattero, D., and Bradbury, A. (2000). Exploiting recombination in single bacteria to make large phage antibody libraries. Nat Biotechnol *18*, 75-80.

Schenk, D., Barbour, R., Dunn, W., Gordon, G., Grajeda, H., Guido, T., Hu, K., Huang, J., Johnson-Wood, K., Khan, K.*, et al.* (1999). Immunization with amyloid-beta attenuates Alzheimer-disease-like pathology in the PDAPP mouse. Nature *400*, 173-177.

Schenk, D., Hagen, M., and Seubert, P. (2004). Current progress in beta-amyloid immunotherapy. Curr Opin Immunol *16*, 599-606.

Seabrook, T. J., Thomas, K., Jiang, L., Bloom, J., Spooner, E., Maier, M., Bitan, G., and Lemere, C. A. (2007). Dendrimeric Abeta1-15 is an effective immunogen in wildtype and APP-tg mice. Neurobiol Aging *28*, 813-823.

Selkoe, D. J. (1991). The molecular pathology of Alzheimer's disease. Neuron *6*, 487-498.

Selkoe, D. J. (2001). Alzheimer's disease: genes, proteins, and therapy. Physiol Rev *81*, 741-766.

Selkoe, D. J. (2004). Cell biology of protein misfolding: the examples of Alzheimer's and Parkinson's diseases. Nat Cell Biol *6*, 1054-1061.

Shankar, G. M., Bloodgood, B. L., Townsend, M., Walsh, D. M., Selkoe, D. J., and Sabatini, B. L. (2007). Natural oligomers of the Alzheimer amyloid-beta protein induce reversible synapse loss by modulating an NMDA-type glutamate receptor-dependent signaling pathway. J Neurosci *27*, 2866-2875.

Sheets, M. D., Amersdorfer, P., Finnern, R., Sargent, P., Lindquist, E., Schier, R., Hemingsen, G., Wong, C., Gerhart, J. C., and Marks, J. D. (1998). Efficient construction of a large nonimmune phage antibody library: the production of high-affinity human single-chain antibodies to protein antigens. Proc Natl Acad Sci U S A *95*, 6157-6162.

Sheng, J. G., Bora, S. H., Xu, G., Borchelt, D. R., Price, D. L., and Koliatsos, V. E. (2003). Lipopolysaccharide-induced-neuroinflammation increases intracellular accumulation of amyloid precursor protein and amyloid beta peptide in APPswe transgenic mice. Neurobiol Dis *14*, 133-145.

Sheng, J. G., Price, D. L., and Koliatsos, V. E. (2002). Disruption of corticocortical connections ameliorates amyloid burden in terminal fields in a transgenic model of Abeta amyloidosis. J Neurosci *22*, 9794-9799.

Singer, O., Marr, R. A., Rockenstein, E., Crews, L., Coufal, N. G., Gage, F. H., Verma, I. M., and Masliah, E. (2005). Targeting BACE1 with siRNAs ameliorates Alzheimer disease neuropathology in a transgenic model. Nat Neurosci *8*, 1343-1349.

Solomon, B., Koppel, R., Frankel, D., and Hanan-Aharon, E. (1997). Disaggregation of Alzheimer beta-amyloid by site-directed mAb. Proc Natl Acad Sci U S A *94*, 4109-4112.

Solomon, B., Koppel, R., Hanan, E., and Katzav, T. (1996). Monoclonal antibodies inhibit in vitro fibrillar aggregation of the Alzheimer beta-amyloid peptide. Proc Natl Acad Sci U S A *93*, 452-455.

Soto, C., Estrada, L., and Castilla, J. (2006a). Amyloids, prions and the inherent infectious nature of misfolded protein aggregates. Trends Biochem Sci *31*, 150-155.

Stine, W. B., Jr., Dahlgren, K. N., Krafft, G. A., and LaDu, M. J. (2003). In vitro characterization of conditions for amyloid-beta peptide oligomerization and fibrillogenesis. J Biol Chem *278*, 11612-11622.

Takahashi, R. H., Almeida, C. G., Kearney, P. F., Yu, F., Lin, M. T., Milner, T. A., and Gouras, G. K. (2004). Oligomerization of Alzheimer's beta-amyloid within processes and synapses of cultured neurons and brain. J Neurosci *24*, 3592-3599.

Tampellini, D., Magrane, J., Takahashi, R. H., Li, F., Lin, M. T., Almeida, C. G., and Gouras, G. K. (2007). Internalized antibodies to the Abeta domain of APP reduce neuronal Abeta and protect against synaptic alterations. J Biol Chem. (Papers in Press published on May 1, 2007 as doi:10.1074/jbc.M700373200)

Town, T., Tan, J., Sansone, N., Obregon, D., Klein, T., and Mullan, M. (2001). Characterization of murine immunoglobulin G antibodies against human amyloid-beta1-42. Neurosci Lett *307*, 101-104.

Townsend, M., Shankar, G. M., Mehta, T., Walsh, D. M., and Selkoe, D. J. (2006). Effects of secreted oligomers of amyloid beta-protein on hippocampal synaptic plasticity: a potent role for trimers. J Physiol *572*, 477-492.

Tse, E., Lobato, M. N., Forster, A., Tanaka, T., Chung, G. T., and Rabbitts, T. H. (2002). Intracellular antibody capture technology: application to selection of intracellular antibodies recognising the BCR-ABL oncogenic protein. J Mol Biol *317*, 85-94.

Vaughan, H. A., Loveland, B. E., and Sandrin, M. S. (1994). Gal alpha(1,3)Gal is the major xenoepitope expressed on pig endothelial cells recognized by naturally occurring cytotoxic human antibodies. Transplantation *58*, 879-882.

Visintin, M., Meli, G. A., Cannistraci, I., and Cattaneo, A. (2004a). Intracellular antibodies for proteomics. J Immunol Methods *290*, 135-153.

Visintin, M., Quondam, M., and Cattaneo, A. (2004b). The intracellular antibody capture technology: towards the high-throughput selection of functional intracellular antibodies for target validation. Methods *34*, 200-214.

Visintin, M., Settanni, G., Maritan, A., Graziosi, S., Marks, J. D., and Cattaneo, A. (2002). The intracellular antibody capture technology (IACT): towards a consensus sequence for intracellular antibodies. J Mol Biol *317*, 73-83.

Visintin, M., Cattaneo, A. (2001) Selecting intracellular antibodies using the two-hybrid system, in: R. Kontermann, S. Dubel (Eds.), Antibody Engineering, vol. 1, Springer Lab Manual, Springer, Heidelberg, Germany, p. 790

Visintin, M., Tse, E., Axelson, H., Rabbitts, T. H., and Cattaneo, A. (1999). Selection of antibodies for intracellular function using a two-hybrid in vivo system. Proc Natl Acad Sci U S A *96*, 11723-11728.

Walker, L. C., Levine, H., 3rd, Mattson, M. P., and Jucker, M. (2006). Inducible proteopathies. Trends Neurosci *29*, 438-443.

Wall, N. R., and Shi, Y. (2003). Small RNA: can RNA interference be exploited for therapy? Lancet *362*, 1401-1403.

Walsh, D. M., Klyubin, I., Fadeeva, J. V., Cullen, W. K., Anwyl, R., Wolfe, M. S., Rowan, M. J., and Selkoe, D. J. (2002). Naturally secreted oligomers of amyloid beta protein potently inhibit hippocampal long-term potentiation in vivo. Nature *416*, 535-539.

Weiner, H. L., Lemere, C. A., Maron, R., Spooner, E. T., Grenfell, T. J., Mori, C., Issazadeh, S., Hancock, W. W., and Selkoe, D. J. (2000). Nasal administration of amyloid-beta peptide decreases cerebral amyloid burden in a mouse model of Alzheimer's disease. Ann Neurol *48*, 567-579.

Wilcock, D. M., DiCarlo, G., Henderson, D., Jackson, J., Clarke, K., Ugen, K. E., Gordon, M. N., and Morgan, D. (2003). Intracranially administered anti-Abeta antibodies reduce beta-amyloid deposition by mechanisms both independent of and associated with microglial activation. J Neurosci *23*, 3745-3751.

Winter, G., Griffiths, A. D., Hawkins, R. E., and Hoogenboom, H. R. (1994). Making antibodies by phage display technology. Annu Rev Immunol *12*, 433-455.

Winter, G., and Milstein, C. (1991). Man-made antibodies. Nature *349*, 293-299.

Yan, S. D., Fu, J., Soto, C., Chen, X., Zhu, H., Al-Mohanna, F., Collison, K., Zhu, A., Stern, E., Saido, T.*, et al.* (1997). An intracellular protein that binds amyloid-beta peptide and mediates neurotoxicity in Alzheimer's disease. Nature *389*, 689-695.

Yau, K. Y., Lee, H., and Hall, J. C. (2003). Emerging trends in the synthesis and improvement of hapten-specific recombinant antibodies. Biotechnol Adv *21*, 599-637.

Supplemented figures

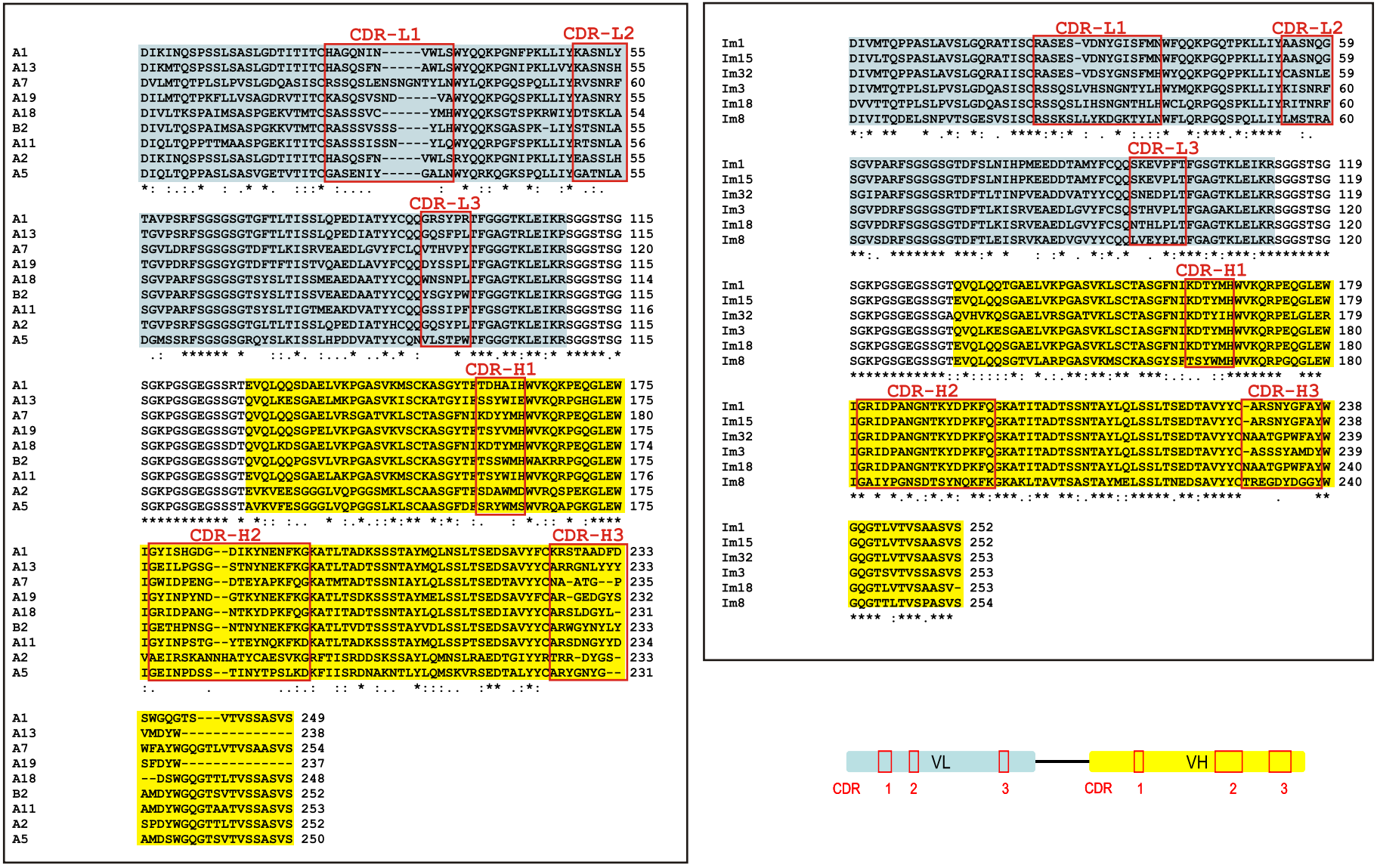

Supplemented figure1. CLUSTAL W multiple alignment of 6 scFvs immune and 9 scFvs naïve; variable regions VL and VH are highlighted in blue and yellow respectively, CDRs are boxed in red.

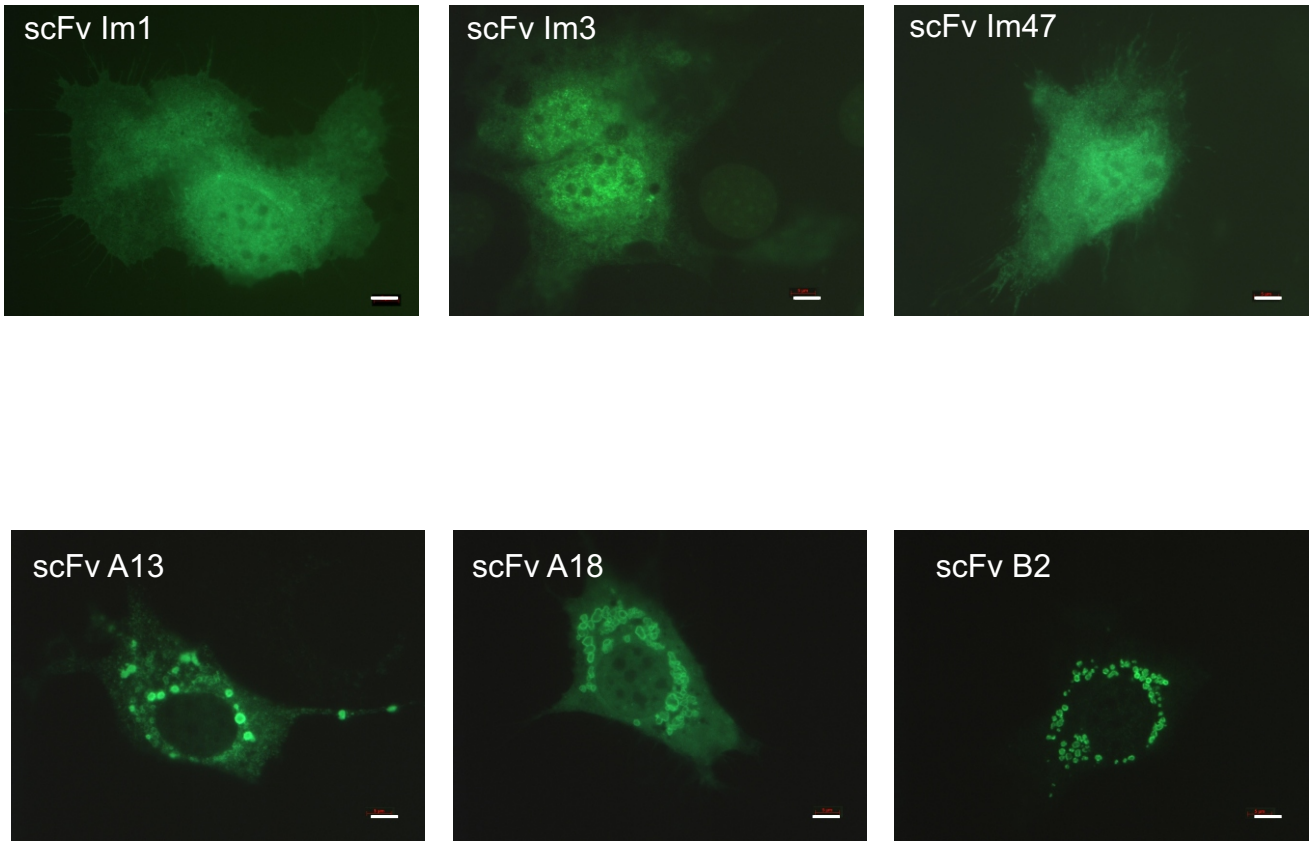

Supplemented figure2.

Immunofluorescence microscopy of the anti-A scFv fragments transiently transfected in 3T3 cells. scFvs cloned in the vector scFv-excytoV5 were expressed in the cell cytoplasm. Cells were reacted with the anti-V5 tag monoclonal antibody, followed by incubation with an anti-mouse AlexaFluor488.

Some scFvs, such as Im1, Im47, Im3 show a diffuse expected intracellular staining, typical of soluble cytoplasmic proteins, but others (A13, A18, B2) display the accumulation of the intracellular scFv in a puntiform or 'donut-like' pattern distribution.

Scale bar 5 m.

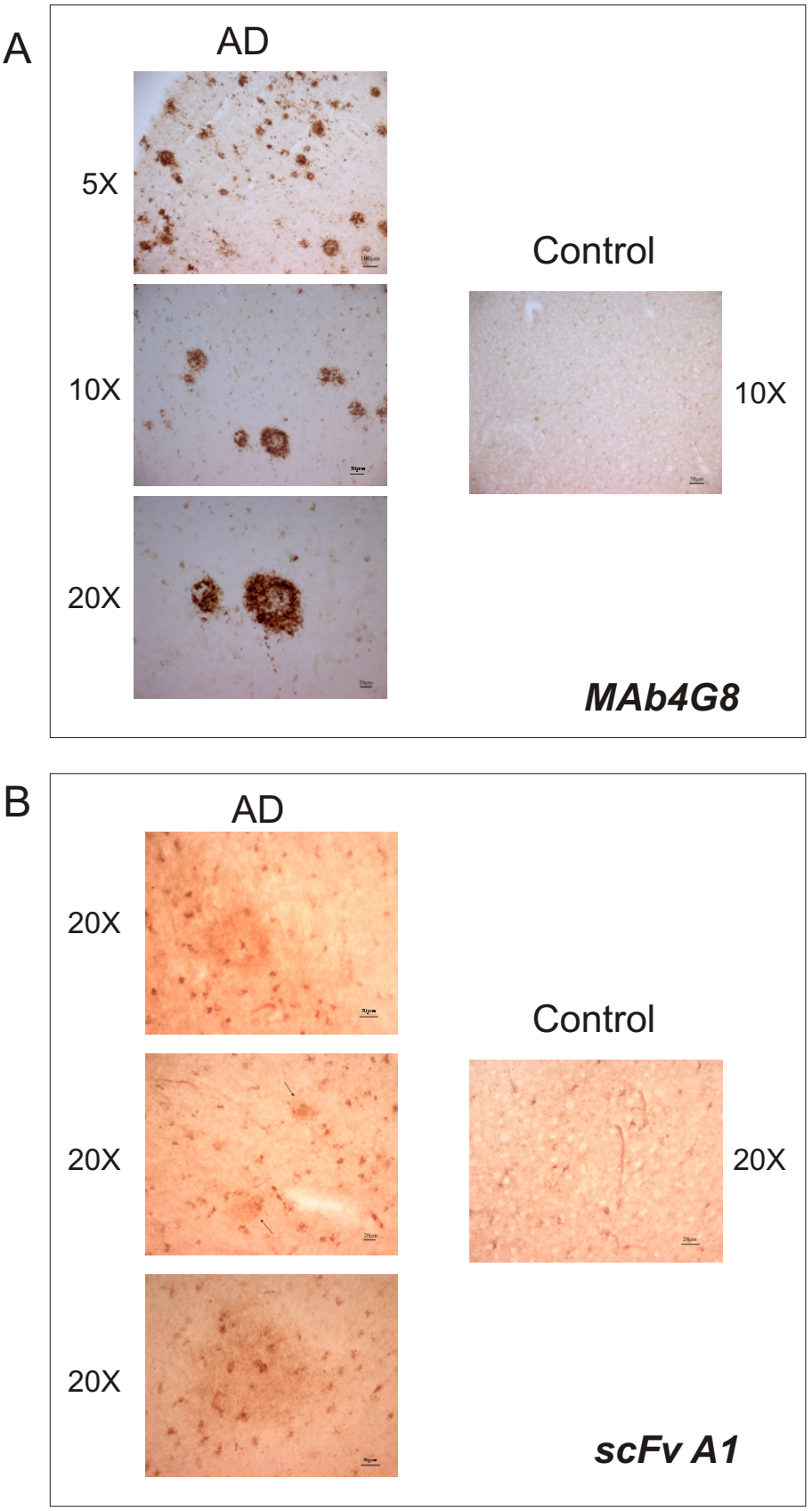

Supplemented figure 3. Immunohystochemistry of temporal cortex sections (40 m) prepared from severe Alzheimer's (Braak V-VI) and control (Braak 0-I) brains; the anti-A scFvA1 and mAb 4G8 were used as primary antibodies. Sections were not pre-treated with formic acid.
ScFvA1 shows high cellular reactivity (panel B); pericellular and extracellular deposits detected by scFvA1 (panel B) are different from A plaques detected by mAb 4G8 (panel A). The diffuse staining of scFvA1 could suggest a recognition of soluble non-fibrillar A oligomers.
Scale bar 20 m in magnifications 20x, 50 m in magnif. 10x, 100 m in magnif. 5x.

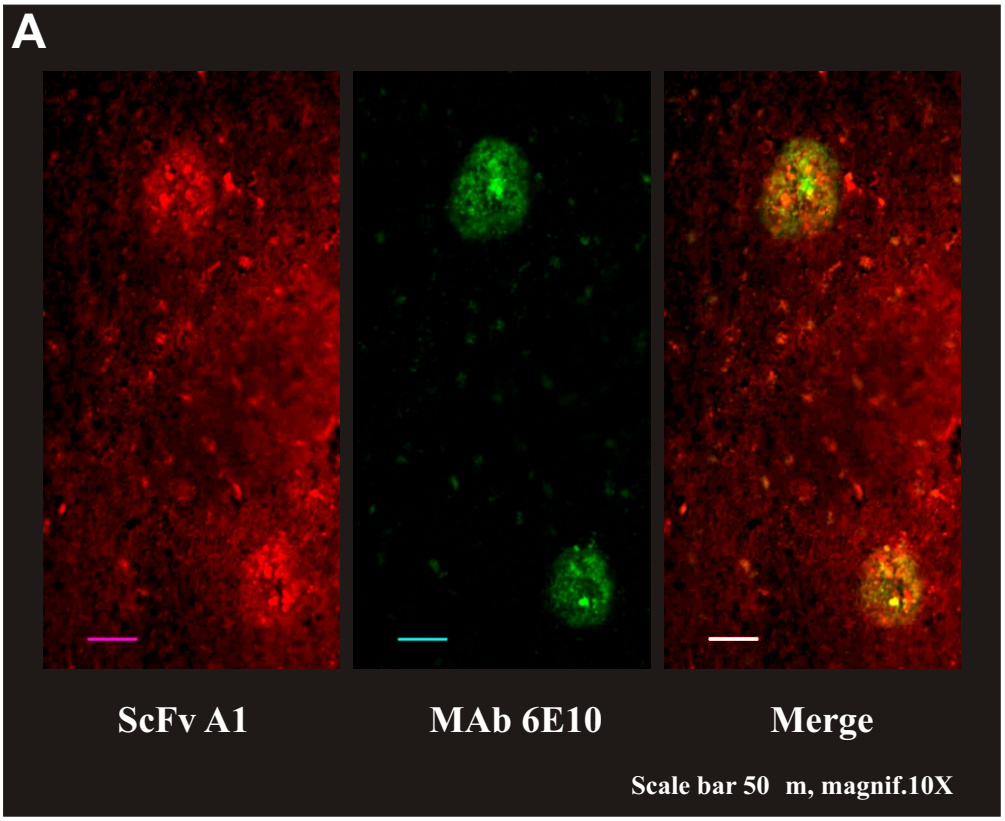

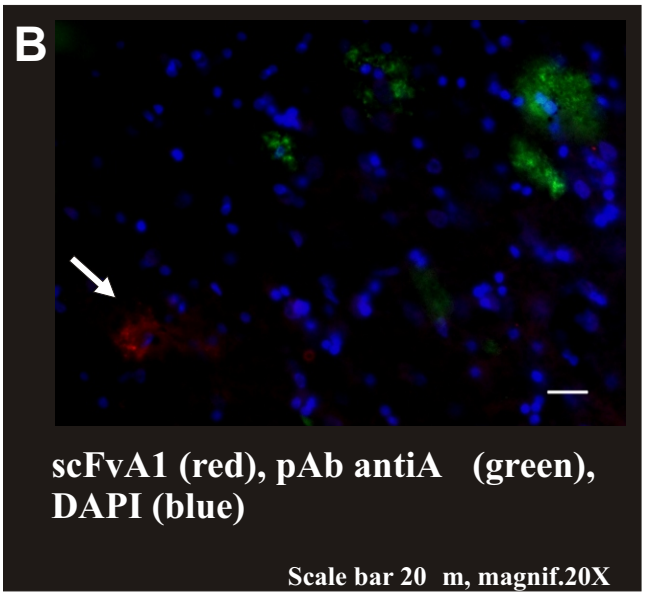

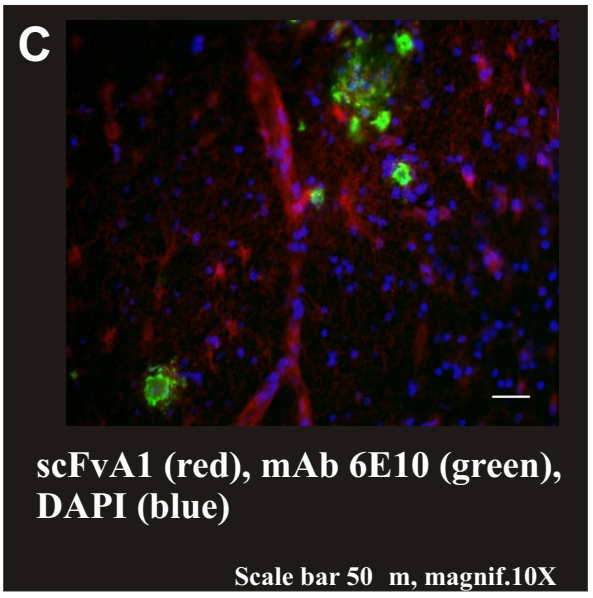

Supplemented figure 4. Immunofluorescence of temporal cortex sections (40 m) prepared from severe Alzheimer's (Braak V-VI) brains; the anti-A scFvA1, mAb 6E10 and pAb anti-A were used as primary antibodies. Sections were pre-treated with formic acid (90%).

Panel A. scFv A1 shows intense cellular reactivity in plaque-rich areas, and interestingly a partial complementary staining of plaques in comparison to anti-A MAbs 6E10. We postulate that scFvA1 might be specific for the early stage of amyloid maturation: the figure shows no core staining of scFvA1 in the upper plaque.

Panel B. scFvA1 often detects pericellular diffuse immunoreactivity (indicated by the arrow), not detected by classic Abs anti-A .

Panel C. scFvA1 can specifically recognize blood vessels with Amyloid deposits, especially in plaques rich areas in the brain from one AD patient showing greater signs of Cerebral Amyloid Angiopathy (CAA).

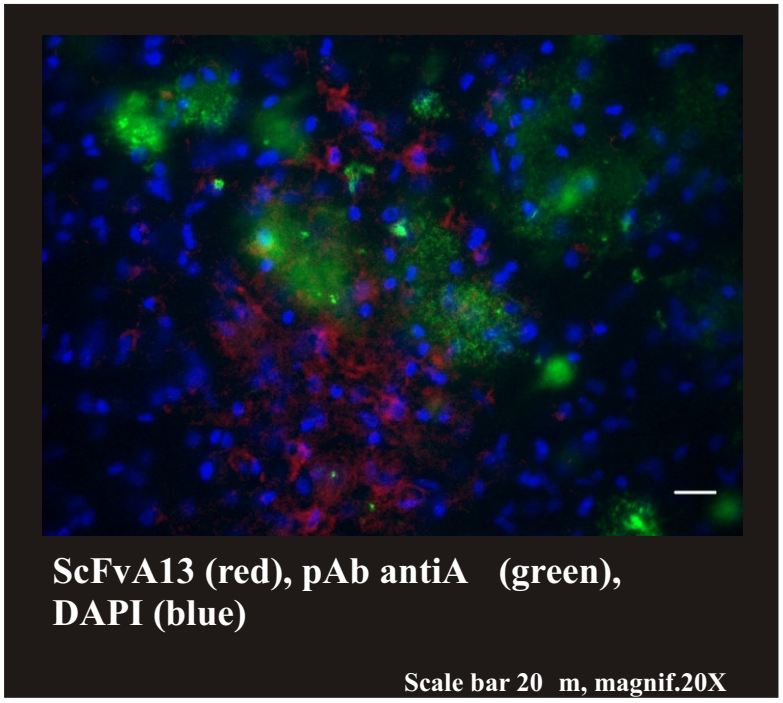

Supplemented Figure 5. Prevalent cellular reactivity of scFvA13 in plaques rich areas of temporal cortex sections (40 m) prepared from human AD brains.

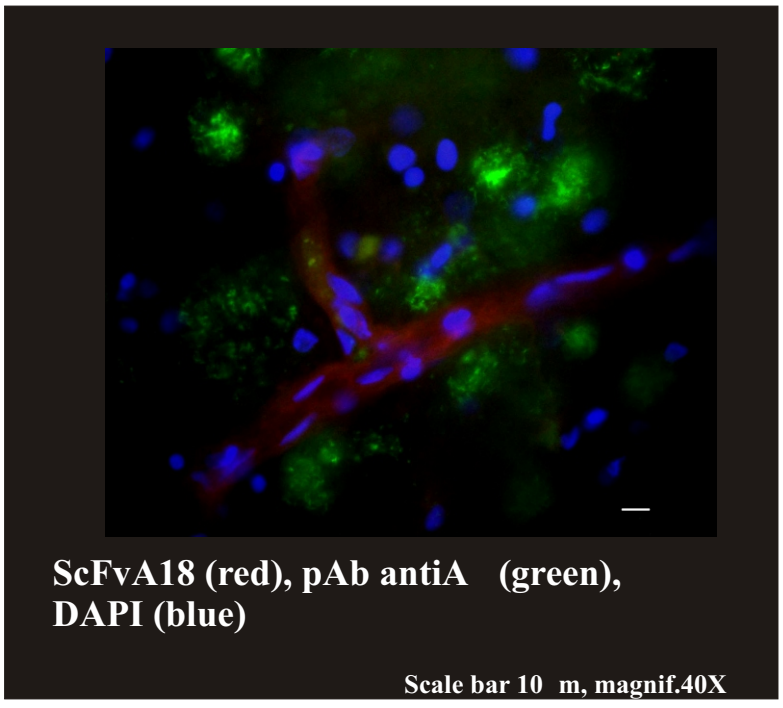

Supplemented Figure 6. Specific vascular reactivity of scFvA18 in plaques rich areas of temporal cortex sections (40 m) prepared from human AD brains.

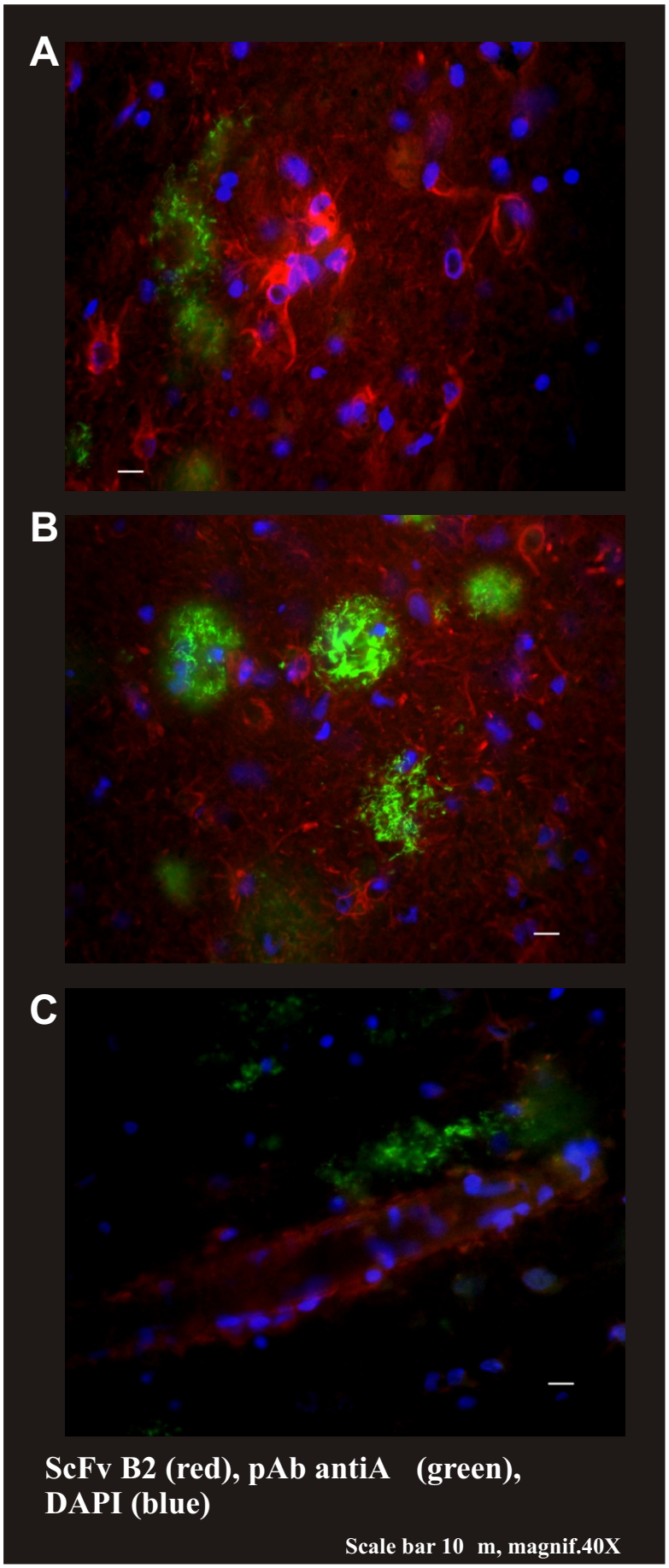

Supplemented figure 7. ScFv B2 presents mostly strong cellular reactivity (similar to astrocytes), tightly related to plaques (panel A). Probably, B2 detect also dystrophic neurites (panel B). ScFvB2 can detect also specifically blood vessel deposits, near A plaques detected by other Abs (panel C). Temporal cortex sections (40 m) prepared from human AD brains.

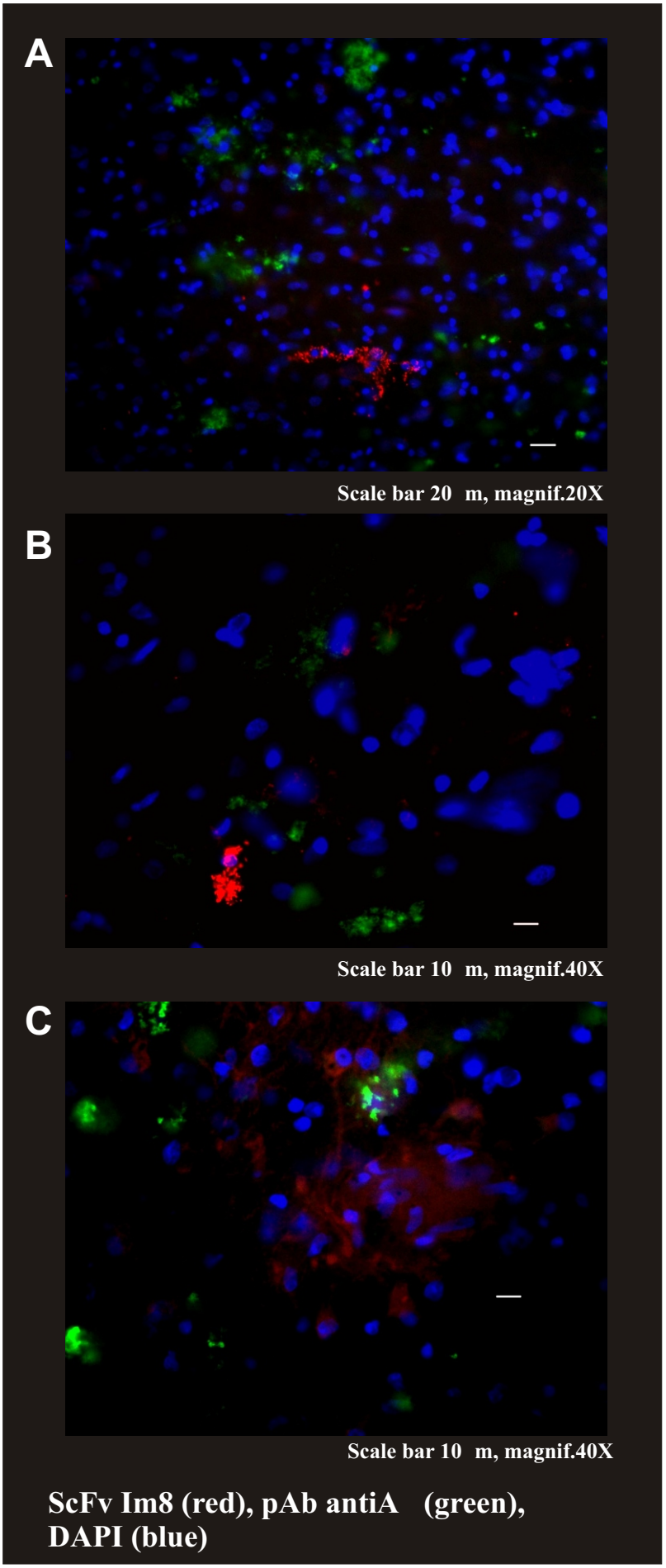

Supplemented figure 8. ScFv Im8 (panel A and B) detects specific small dotted clusters of mainly pericellular immunoreactive deposits, spatially distinct and separate from small plaque-like depositions (stained with A 42 C-terminal specific pAb). Im8 shows also secondary cellular and dystrophic neurites reactivity (panel C). Temporal cortex sections (40 m) prepared from human AD brains.

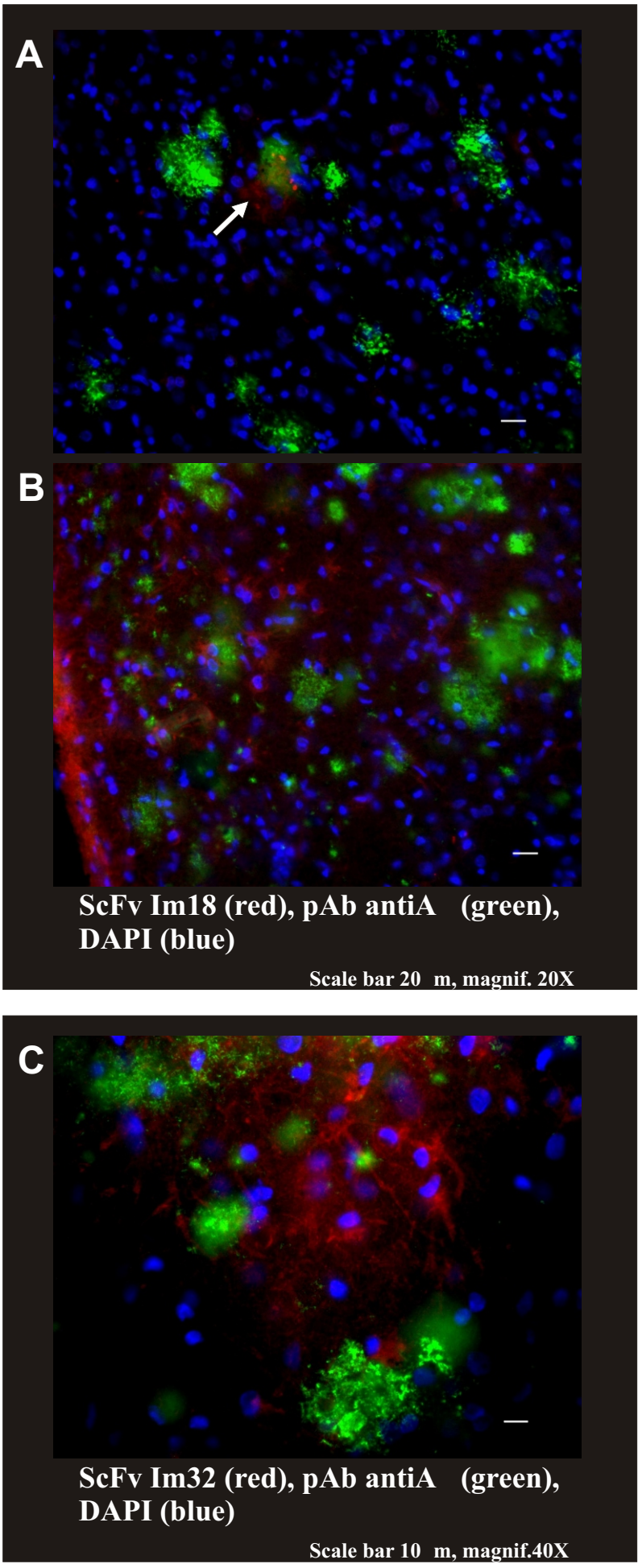

Supplemented figure 9. ScFv Im18 (panel A) shows specific pericellular reactivity near large plaques partially distinct and separate from them. In other fields of slice, Im18 (panel B) similarly to Im32 (panel C) detects cellular reactivity spatially related to A plaques. Temporal cortex sections (40 m) prepared from human AD brains.

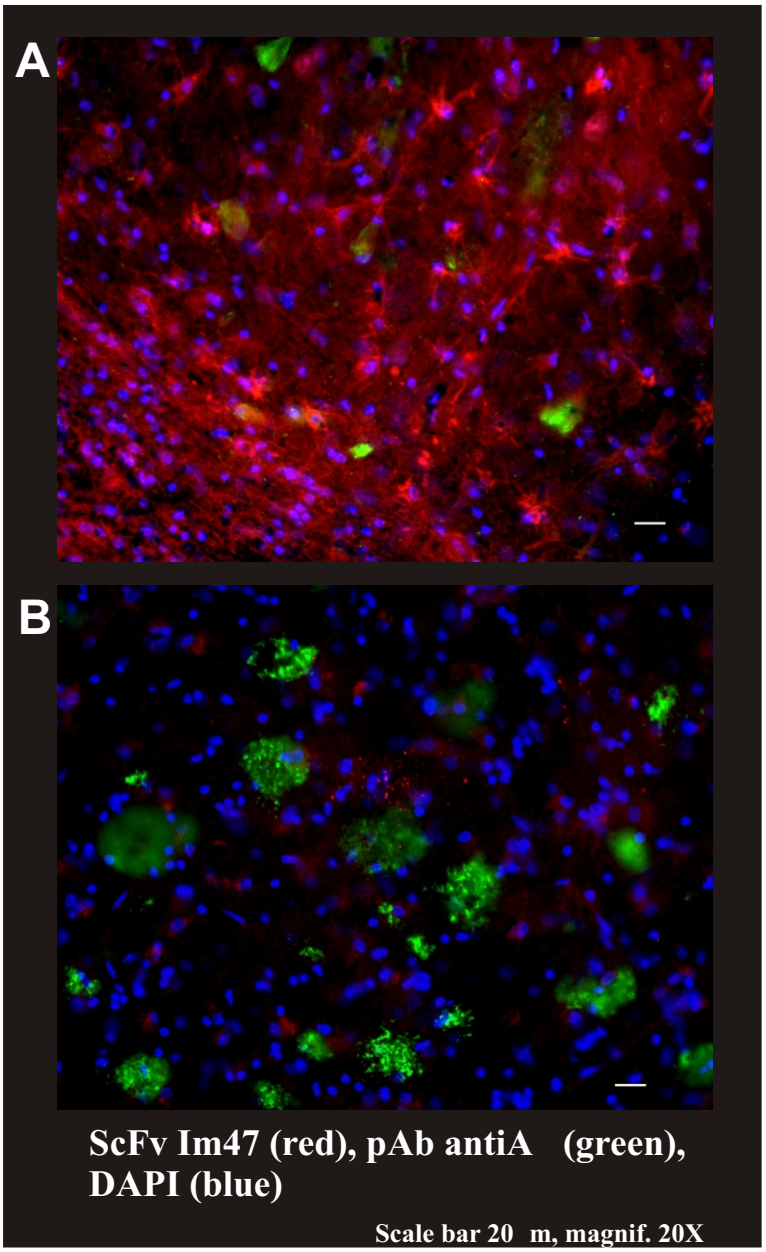

Supplemented figure 10. The immunoreactive pattern of Im47 shows stronger cellular reactivity (probably astrocytes) in smaller plaques zones (panel A), and distinct pericellular reactivity near large plaques (panel B). Pericellular reactivity of Im47 is often specifically dotted, resembling oligomeric-specific staining of pAb A11 (see below suppl. Fig.11). Temporal cortex sections (40 m) prepared from human AD brains.

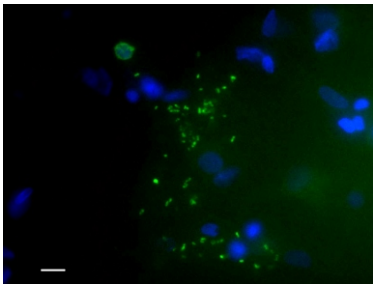

Supplemented figure 11. Pericellular reactivity of the oligomeric-specific pAb A11 (Kayed et al., 2003). Counter-staining of nuclei with DAPI. Temporal cortex sections (40 m) prepared from human AD brains. Scale bar 10 m, magnification 40X.

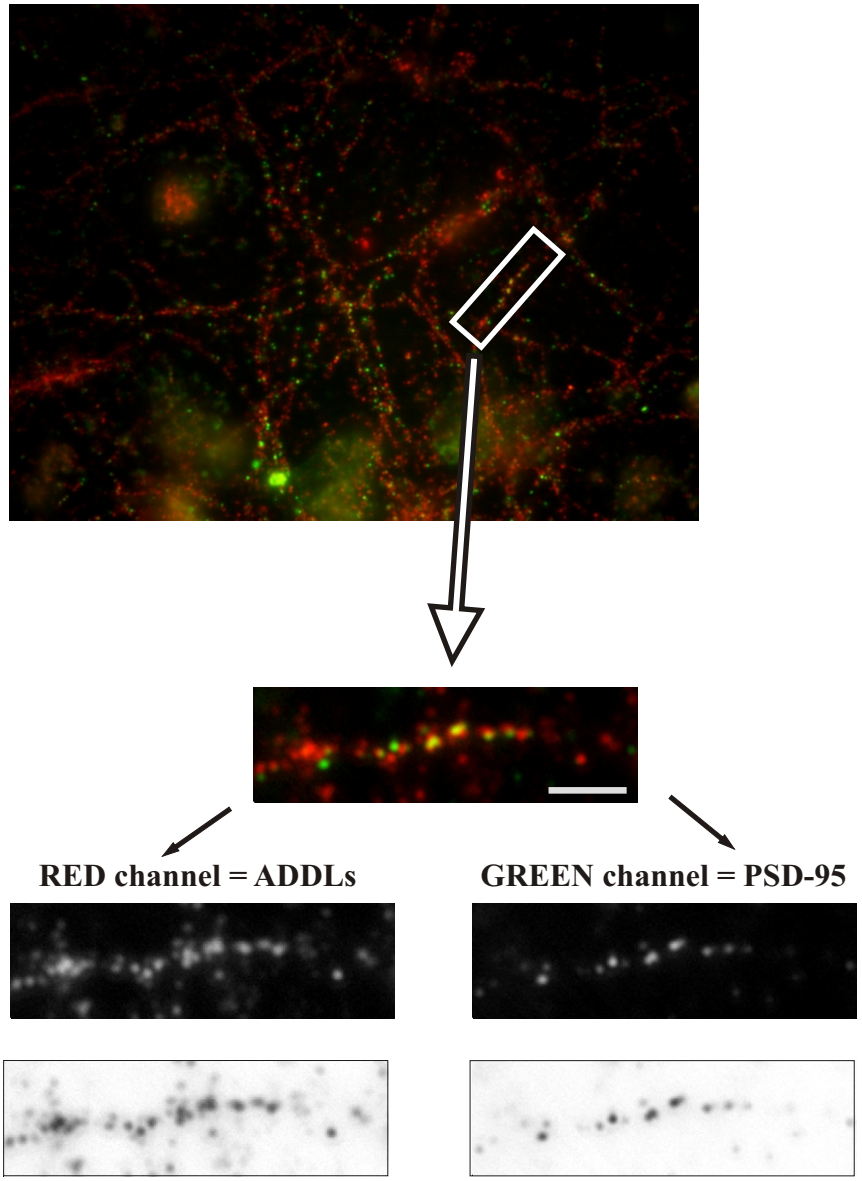

Supplemented figure 12. Synthetic ADDLs bind neurons with punctate specificity.
Primary rat hippocampal neurons treated with ADDLs (300nM) were double immunolabeled for ADDLs (red), using the anti-oligomer PAb A11, and for PSD-95 (green) using a mAb anti-PSD95. Dendritic clusters of ADDL-immunoreactive puncta colocalized partially with PSD-95. Comparing areas of similar density of PSD-95 positive spots, focusing mainly on dendrites, we performed a qualitative analysis of A11-positive spots density.
Scale bar 5 m.

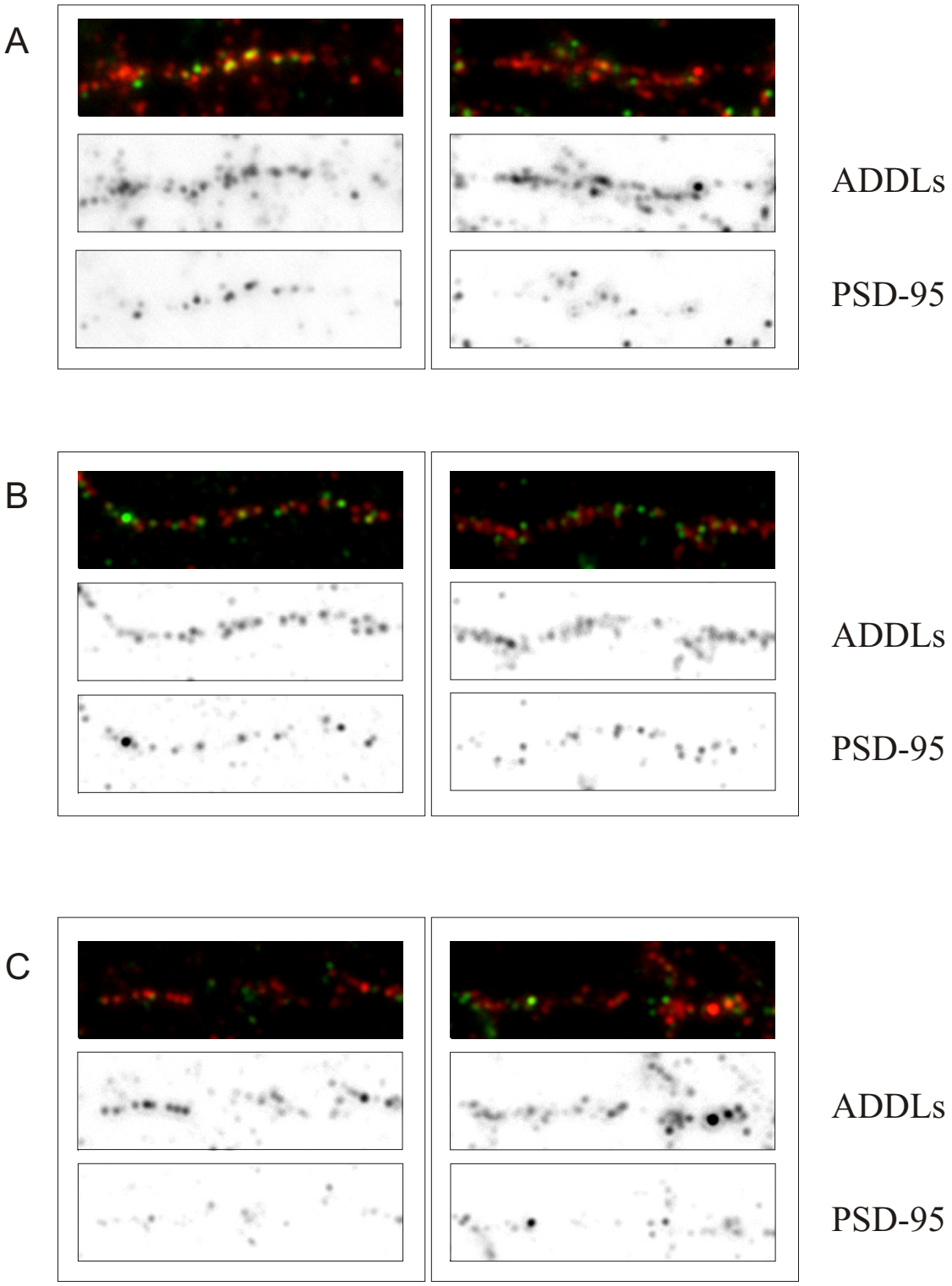

Supplemented figure 13. ADDLs synaptic binding can be modulated by the SPLINT-selected anti-A scFvs A1 and A13.

300nM of ADDLs alone (panel A), or preincubated with 600nM of anti-A scFvs (panel B and C), were administered to primary rat hyppocampal neurons.

Our qualitative analysis confirms that ADDLs synaptic binding (punctate pattern showed in the middle boxes of the panels A, B and C) can be significantly reduced by the pre-incubation with scFv A1 (panel B) or with scFv A13 (panel C).

Two representative fields per treatment are showed. The double immunolabeling for ADDLs (red) and for PSD-95 (green) was obtained using respectively the anti-oligomer PAb A11 and a mAb anti-PSD95.

Ringraziamenti

Durante lo svolgimento della presente tesi di Ph.D. ho avuto modo di interagire con una moltitudine di colleghi, ricercatori e docenti (che sarà difficile ringraziare singolarmente), sia nei primi tre anni presso i laboratori di Neurobiologia Molecolare e presso il laboratorio Bellavista della SISSA (Trieste), che nel corso del quarto anno presso il laboratorio di Neurotrofine e Neurodegenerazione dell'European Brain Research Institute (EBRI), Fondazione Rita Levi-Montalcini, di Roma.

Ringrazio il mio supervisor Prof. Antonino Cattaneo per avermi dato la possibilità di sviluppare come tesi sperimentale di Ph.D., presso i laboratori SISSA ed EBRI, un così interessante e stimolante progetto di frontiera tra Biotecnologie e Neuroscienze. Ringrazio altresì Antonino per il continuo supporto scientifico nella discussione critica dei dati sperimentali e nella stesura della presente dissertazione scritta.

Desidero ringraziare il mio co-supervisor Dott.ssa Michela Visintin (Lay Line Genomics, Trieste) per la costante supervisione e per le stimolanti discussioni negli sviluppi sperimentali del progetto, nell'ambito della selezione degli anticorpi in lievito, della costruzione della library immune e della caratterizzazione biochimica degli anticorpi ricombinanti selezionati. Esprimo la mia gratitudine a Michela anche per il suo concreto contributo sperimentale nella sintesi e purificazione citoplasmatica degli anticorpi e per il suo contributo nella revisione del testo della tesi.

Ringrazio Isabella Cannistraci (Lay Line Genomics, Trieste) per il suo fondamentale supporto tecnico negli esperimenti svolti a Trieste, per la sua continua disponibilità, nonché per il suo proverbiale buonumore nelle situazioni difficili.

Desidero inoltre ringraziare Daniela Avossa (SISSA) per il fondamentale supporto negli esperimenti di immunoistochimica, Sonia Covaceuszach (Lay Line Genomics, Trieste) per le analisi cromatografiche di gel filtrazione, Marco Stebel (Università di Trieste) per le immunizzazioni dei topi, Carmela Matrone (CNR-CERC, Roma) per la caratterizzazione del modello cellulare di amiloidogenesi in PC12, Maria Teresa Ciotti (CNR-CERC, Roma) per le colture primarie di cellule ippocampali, Federica Ferrero e Jessica Franzot (SISSA) per il servizio di sequenziamento di DNA, Teresa Melchionna (Lay Line Genomics, Trieste) e Francesca Paoletti (EBRI), "ex-colleghe" alla SISSA, per la loro disponibilità in svariate situazioni e per gli stimolanti confronti sperimentali.

Ringrazio Francesca Paoletti, Cecilia Tiveron e Raffaella Scardigli, attuali colleghe presso l'EBRI, per il loro supporto morale, linguistico e pratico nella stesura della tesi. Desidero ringraziare anche Simona Capsoni (Lay Line Genomics, Roma) per il suo aiuto in diverse circostanze.

Ringrazio infine tutti i colleghi della SISSA e dell'EBRI, nonché i componenti della segreteria della SISSA, particolarmente Amanda Colombo e Riccardo Iancer, sempre disposti ad aiutarmi anche a distanza.

Vorrei esprimere la mia gratitudine verso tutte le suddette persone anche da un punto di vista umano, in particolare ad Antonino per la sua costante disponibilità, a Michela, Isabella e Teresa per gli anni passati a Trieste, e a tutti gli attuali colleghi dell'EBRI di Roma.